Novel Palladium(II) Complexes Belonging to a Family of Potential Catalytic Precursors.

by

Gavin Blewett

THESIS

Presented in fulfillment of the requirements for the degree of

MASTER

of

SCIENCE

in the

FACULTY OF SCIENCE

at the

UNIVERSITY OF STELLENBOSCH

SUPERVISOR : Prof. H.G. Raubenheimer

Co-promoter : Dr R Brüll

MARCH 2001

Declaration

I, the undersigned, hereby declare that the work contained in this thesis is my own original work and that I have not previously in its entirety or in part submitted it at any university for a degree.

Signature : _____

Date _____8/2/2001_____

Summary

This study comprises the preparation and characterization of various novel organometallic complexes of palladium(II) which contain symmetric and unsymmetric (heteroatom-containing) ß-dicarbonyl-type ligands, η^3-heteroallyl ligands and η^3-coordinated trimethylsilyl-containing ligands.

With the ultimate objective of preparing potential catalytic precursors similar to known catalytic precursors which exhibit hemilabile activity, the main goals of this study were the following: -

- Investigate the coordination mode of the aforementioned ligand-types to the palladium of the starting compound, trans-[Pd(C$_6$H$_5$)Cl{P(C$_6$H$_5$)$_3$}$_2$] (**1**), by physical measurements.
- Carry out single crystal structure determinations where possible.
- Investigate the influence of the properties of the ligands on the stability of the prepared complexes.
- Investigate the existence of hemilability (if any) in the prepared complex.

The deprotonated symmetric and unsymmetric ß-dicarbonyl-type ligands readily bind to the palladium of the starting compound in a bidentate fashion through the oxygens by displacing a triphenylphosphine group and producing easily removable sodium chloride. These complexes show that a negative charge can be accommodated in a delocalized fashion by the $-S=O$ and $-P=O$ groups of these acac$^-$-type ligands in a similar manner to the carbonyl groups of acetylacetonate. However, no evidence of hemilabile activity was found in this series of complexes.

In a similar fashion, the deprotonated η^3-heteroallyl ligands, L = [Ph$_2$PS$_2^-$], [PhCO$_2^-$], [PhC{NSi(CH$_3$)$_3$}$_2^-$], [(Ph)$_2$P{NSi(CH$_3$)$_3$}$_2^-$], were linked to palladium in the same starting complex, in η^3-fashion by triphenylphosphine substitution. No evidence of hemilabilty was evident in this series of complexes, but when L = [Ph$_2$PS$_2^-$], an exchange of the coordinated triphenylphosphine group with the free triphenylphosphine group was observed in the reaction mixture.

Finally, the preparation, isolation and spectroscopic characterization of several η^3-allyl palladium(II) complexes with ligands of the type R-TeCH$_2$CH$_2$COOCH$_3$, (R = isopropyl, *t*-butyl ,ethyl) were attempted with the compound bis-(η^3-allyl)-di-μ-iodo-dipalladium(II), [η^3-(CH$_2$CHCH$_2$)$_2$Pd$_2$I$_2$], which had also now been crystallographically characterized. Chelate formation by Te^O coordination seemed possible by halide precipitation with silver tetrafluoroborate. Unfortunately the resulting compounds were too unstable to be isolated in the pure form for characterization.

Opsomming

Die studie behels die bereiding en karakterisering van verskeie nuwe palladium(II) organometaalkomplekse met inbegrip van simmetriese en onsimmetriese (heteroatoom bevattende) β-dikarboniel-tipe ligande, η^3-heteroalliel ligande en η^3-gekoordineerde trimetielsiliel bevattende ligande.

Met die beoogde einddoel die bereiding van potensiele katalitiese voorgangers soortgelyk aan bekende katalitiese voorgangers met hemilabiele aktiviteit, sluit die hoof mikpunte van die studie die volgende in: -

- 'n Ondersoek na koordinasie-wyse van die bogenoemde ligand tipes aan die palladium van die uitgangstof, $trans$-[Pd(C$_6$H$_5$)Cl{P(C$_6$H$_5$)$_3$}$_2$] (**1**), met behulp van fisiese bepalings.

- Enkel kristal struktuur bepalings waar moontlike.

- 'n Ondersoek na die invloed van die einskappe van die ligande op die stabilitiet van die komplekse.

- 'n Ondersoek na die bestaan van hemilabiele aktiwiteit (indien enige) in die voorbereide complekse.

Die gedeprotoneerde simmetriese en onsimmetriese β-dikarboniel-tipe ligande het geredelik, bidentaat deur middel van die suurstowwe gebind aan die palladium van die uitgangstof deur die verplasing van die trifenielfosfien group en die vorming van verweiderbare natriumchloried. Hierdie komplekse dui aan dat 'n negatiewe lading wel geakkommodeer kan word deur delokalisasie by die –S=O- en –P=O-groepe van hierdie acac⁻-tipe ligande, soortgelyk aan die karbonielgroep van asetielasetonaat. Geen hemilabiliteit is waargeneem in hierdie reeks komplekse nie.

Die gedeprotoneerde η^3-heteroalliel ligande, L = [Ph$_2$PS$_2$⁻], [PhCO$_2$⁻], [PhC{NSi(CH$_3$)$_3$}$_2$⁻], [(Ph)$_2$P{NSi(CH$_3$)$_3$}$_2$⁻], is op 'n soortgelyke wyse η^3-gekoppel aan palladium van dieselfde uitgangstof met trifenielfosfien verplasing. Geen hemilabiliteit is waargeneem in hierdie reeks komplekse nie,

maar wanneer L = [Ph$_2$PS$_2^-$], is 'n uitruiling van 'n gekoordineerde trifenielfosfien met 'n vrye trifenielfosfien in die reaksiemengsel waargeneem.

Die bereiding, isolasie en spektroskopiese karakterisering van η^3-alliel palladium(II) komplekse met ligande van die tipe R-TeCH$_2$CH$_2$COOCH$_3$, (R = isopropiel, t-butiel ,etiel) is gepoog met die uitgangstof bis-(η^3-alliel)-di-μ-iodo-dipalladium(II), [η^3-(CH$_2$CHCH$_2$)$_2$Pd$_2$I$_2$], wat volledig gekarakteriseer was. Chelaat-vorming deur Te^O-koordinasie het moonlik blyk te wees deur halied presipitasie met behulp van AgBF$_4$. Die komplekse is baie onstabiel en is dit gevolglik nie moontlik om die komplekse suiwer te isoleer en te karakteriseer nie.

ACKNOWLEDGEMENTS

I would like to express my sincere thanks to all those who supported me during my research presented here in this thesis. In particular I would like to thank the following people and institutions: -

- The Lord my God to Whom I owe everything.
- Both my parents who unconditionally supported me through some difficult time during this work.
- Prof. H.G. Raubenheimer for giving me the opportunity to work under him.
- Dr R. Brüll for his advice and many adventurous ideas along the way.
- The NRF, Rand Afrikaans University and the University of Stellenbosch for financial support.
- All the staff at the University of Stellenbosch that gave all the much appreciated support and advice. In particular many thanks to the late Mr. H. Spies for his hours of patience in front of the NMR Spectrometer.
- Special mention must be made of Dr. Bredenkamp for the many thought provoking and inspirational discussions that provided me with the motivation that kept me going when times were really tough.
- Catharine, for all her help in the crystal structure determinations and interpretations.

Different aspects of this study have been presented in the form of: -

- A talk presented by Dr. R Brüll at the 1st Indo Pacific Catalysis Association (IPCAT 1) conference, 26-28 January 1998, Cape Town, South Africa.

- A talk presented by the author at the SACI young chemists meeting at JC Le Roux Wine Estate, Stellenbosch, South Africa.

Contents

Contents

Chapter 3

Chapter 4

Abbreviations

Å	Angstrom (10^{-10}m)
COD	1,5-Cyclooctadiene
Et	Ethyl
FAB-MS	Fast Atom Bombardment Mass Spectrometry
FT	Fourier Transform
^{i}Pr	Isopropyl
IR	Infrared
K	Equilibrium constant
K	Rate constant (Hz)
M.p.	Melting point
M.W.	Molecular weight
Me	Methyl
MS	Mass spectrometry
η	Eta (polydispersity: M_w/M_n)
NMR	Nuclear Magnetic Resonance
Ph	Phenyl
ppm	Parts per million
R	Alkyl, aryl, or hydrogen group
^{t}Bu	Tertiary butyl
THF	Tetrahydrofuran

NMR

b	Broad
bd	Broad doublet
bm	Broad multiplet
bq	Broad quartet
bs	Broad singlet
bt	Broad triplet
btt	Broad triplet of triplets
Δ	Difference between two values
δ	Chemical shift (ppm)
d	Doublet
dd	Doublet of doublets
dt	Doublet of triplets
J	Coupling constant (Hz)
m	Multiplet
q	Quartet
s	Singlet
t	Triplet
tt	Triplet of triplets

Infrared

s	Strong
w	Weak
vs	Very strong
vw	Very weak

Catalysis – A General Introduction and Research Aims.

1.1 General Background.

In the preparation of approximately 60-70% of all industrial chemicals, a catalytic process forms part of the procedure.[1] The catalysts used in these processes can be divided broadly into three classes, namely homogeneous catalysts, supported catalysts and heterogeneous catalysts. The role of homogeneous catalytic processes has become increasingly important in recent years with 10–15% of all industrial catalytic reactions currently applying homogeneous catalytic processes.

One of the greatest advantages of homogeneous catalytic processes over heterogeneous processes is that the reaction conditions are generally much milder. A second advantage is that the homogeneous processes generally offer a greater degree of selectivity with respect to catalytic products.[2, 3]

Transition metal organometallic complexes in particular have been proven to be very useful as homogeneous catalysts. The catalysts sought from the transition metals must have a high degree of selectivity, high activity and high durability.

A great variety of chemical reactions are currently catalysed by nickel compounds. A few of these reactions include hydrogenation, hydrocyanation and carbonylation. The most prominent application of homogeneous nickel catalysis is found in the oligomerisation of olefins. This application is used in the Shell Higher Olefin Process (SHOP) and the Dimersol® process of the Institut Francais du Pétrole. The products of oligomerisation and dimerisation are of great commercial importance e.g. co-monomers in polymerisation, starting materials for plasticisers, detergents and enhancers of the octane number.

The name Wilhelm Keim is always connected with much of the ground-breaking work that has been done in the field of homogeneous catalysis with particular reference to nickel and palladium catalysts. His work in the development of the Shell Higher Olefin Process has set milestones in the understanding of the role of ligands within catalyst precursors.[4]

Homogeneous catalysis in organometallic processes is thought to involve several reaction steps, for example:

- Coordination of the substrate molecules to the catalyst metal;
- Insertion of olefin/etc. into a metal-carbon or metal hydride bond;
- Insertion of carbon monoxide in metal-carbon bonds (where applicable);
- Attacks on coordinated ligands;
- Oxidative addition or reductive elimination.

In an attempt to understand the above processes, the design and development of better catalysts has been done through 'ligand tailoring'.

The development of the concept of hemilability in homogeneous catalysis in the 1970's created the possibility of achieving higher catalytic activity and stability than previously thought possible. The role of hemilability of the ligands chelated to metals has to a large degree become a prime focus within Keim's research group in the investigation of catalyst customization, catalytic activity, efficiency and steroselectivity. An example of a complex with this kind of characteristic is illustrated in Figure 1.1 below.

$$(CH_2)_n \quad P_1 \quad O$$

n = 1 - 6
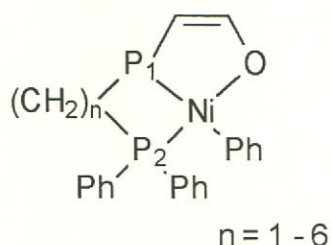
Figure 1.1 : An example of a nickel catalyst complex with a hemilabile P^P^O ligand system.

The terminal P_2-donor atom takes over a hemilabile function similar to that of a windscreen wiper by alternately blocking or vacating a coordination site on the nickel metal allowing a solvent or reactant molecule to coordinate.

The successful application of hemilability within catalysis has sparked much research in this field. Many novel homogeneous catalysts with hemilabile P^O chelating ligands exhibiting a high degree of selectivity and activity have been prepared from various transition metals. Most of this research focused on complexes with well known hemilabile P^O ligands while other possible hemilabile ligands were largely neglected.[5]

First mentioned by Ewers[6] and Jones[7] in the 1960's, chelating β-diketonates were later systematically investigated by Keim and co-workers.[8] They have established an almost linear relationship between the pK_a–value of the β-diketone and the catalyst activity. The hydride (Figure 1.2 below) was accepted as being the active species within the oligomerisation processes in which these catalysts were applied. Wilke et al.[9] did much of the pioneering work in the field of characterization of homogeneous catalyst precursors and active catalyst species. Sulphur- and hemisulphur analogue catalysts of β-diketonates were published by Cavell et al. in 1994.[10]

PCy$_3$
|
O$\cdots$Ni—H
|
O—|
PCy$_3$

O^O = hFacac
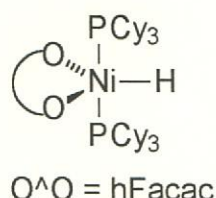
Figure 1.2 : An example of a nickel hydride species postulated as being the active species within the catalytic cycle.

The investigation into the preparation of 'tailored' complexes that contain ligands with potential hemilabile activity could be of vital importance in the further development of catalysis and its application in industry.[11] The present study involved the preparation and characterization of novel palladium and tellurium complexes containing potential catalytic activity in view of them being coordinated by hemilabile ligand systems.

1.2 Current Study – outline and objectives.

In 1998, work conducted in our laboratory showed that the thallium salts of alkylthioethercarboxylic acids react with *trans*-[PdCl(Ph)(PPh$_3$)$_2$] to form palladium(II) complexes with S^O ligands that exhibit hemilabile properties.[12] This hemilability of the S^O ligand was directly observed by NMR spectroscopy. The equilibrium that occurs within this group of complexes investigated is illustrated in figure 4.3 below.

Ph
|
Ph$_3$P—Pd—PPh$_3$
|
O
S—R

⇌

Ph   R
|
Ph$_3$P—Pd—S
O
C
O

+   PPh$_3$

R = ^{i}Pr (*d$_1$*-chloroform),
^{t}Bu (*d$_1$*-chloroform, *d$_6$*-benzene)
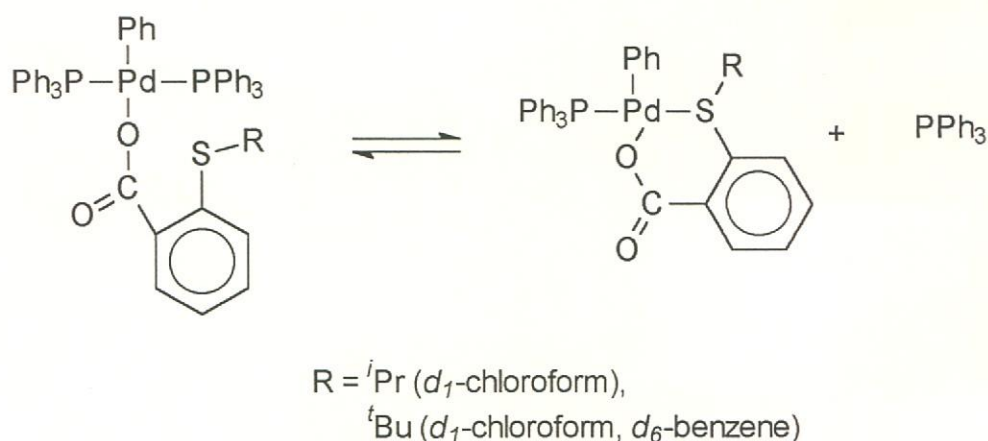
Figure 4.3 : Observed equilibrium of palladium(II) complexes containing hemilabile S^O ligands.

In the light of the complexes previously prepared and characterised within our group, it was decided to prepare and characterise the palladium and palladium/tellurium bimetallic complexes described in this study. The complexes have been divided into three groups namely: -

> Neutral palladium complexes with ß-diketonate type ligands – Chapter 2.

> Neutral η^3-hetero allyl palladium(II) complexes – Chapter 3.

> η^3-Allyl palladium(II)-tellurium(II) bimetallic complexes – Chapter 4. Unfortunately due to their instability, the products could not be isolated in pure form. The preparation attempts of these products are not described in this thesis.

Each chapter begins with an overview of previously reported work and trends with respect to complexes of a similar nature. This is followed by a brief description of the general synthetic methodology used for the preparation of complexes within that chapter. The NMR, infrared and MS (where available) spectroscopic data as well as crystallographic data (where available) are then tabulated and discussed for each complex prepared. The chapter closes with a detailed experimental section that describes in detail the synthesis of each ligand and complex prepared. A summary and conclusion section describes trends and characteristics observed within the spectroscopic data of the complexes prepared in the chapter.

Chapter 2.

The work described in this chapter was embarked upon to answer the question whether a negative charge could be accommodated in a delocalised fashion by an –S=O or–P=O end-group in the same manner in which it is accommodated by the carbonyl groups in acetylacetonate when it is bidentately coordinated to a transition metal through the oxygens of both carbonyl groups. For comparative purposes, acetylacetonate was reacted with *trans*-[PdCl(Ph)(PPh$_3$)$_2$] to yield a bidentate complex by phosphine and halide substitution. This complex was fully characterised (including a crystal structure

analysis) and used as a model for new complexes which contained the –S=O group and the –P=O groups respectively.

Chapter 3.

The work described in this chapter was undertaken to prepare and fully characterise neutral η^3-hetero allyl palladium(II) complexes. Such complexes have not yet been successfully utilized in catalytic reactions involving olefins. Of prime interest, apart from the synthetic methodology development, was to investigate the influence of the different atom types within the η^3-coordination sphere on the stability of the complex. The possible steric effect of trimethylsilyl groups bonded to nitrogen donor atoms upon the stability of the resulting η^3-complexes, was also investigated. An impoertant goal of the study was to characterize one or more of the products by single crystal structure determination.

Chapter 4.

Although sulphur and selenium donor ligand systems are well established in coordination chemistry, this is not true for the more metallic tellurium-based ligands.[12] Unfortunately the goal of preparing such complexes that are potentially hemilabile could not be achieved due to the instability of the products obtained. Nevertheless, an excellent crystal structure determination of prepared starting material, bis-(η^3-allyl)-di-μ-iodo-dipalladium(II), could be carried out.

Cited References.

[1] W. Keim, *Angew. Chem. Int. Ed. Engl.*, 29, **1990**, 235.

[2] B.M. Torst, P.E. Strege, I. Weber, T.J. Dietsche, *J. Am. Chem. Soc.*, 100, **1978**, 3407.

[3] G.J.P. Britovsek, V.C. Gibson, B.S. Kimberley, P.J. Maddox, S.J. McTavish, G.A. Solan, A.J.P. White, D.J. Williams, *Chem. Comm.*, **1998**, 849.

[4] D. Vogt, Applied Homogeneous Catalysis with Organometallic Compounds, eds. B. Cornils and W.A.Herrmann, V.C.H. Weinheim, **1998**, 251.

[5] A. Bader, E. Linder, *Coord. Chem. Rev.*, 108, **1991**, 27.

[6] J. Ewers, *Angew. Chem. Int. Ed. Engl.,* 5, **1966**, 584.

[7] J. R. Jones, *J. Chem. Soc. C*, **1971**, 1117.

[8] W. Keim, A. Behr, G. Kraus, *J. Organomet. Chem.* 251, **1983**, 377.

[9] B. Bogdanovic, B. Henc, B. Meister, H. Pauling, G Wilke, *Angew. Chem. Int. Ed. Engl.*, 11, **1972**, 1023.

[10] K.J. Cavell, *Aust. J. Chem.*, 47, **1994**, 769.

[11] W. Keim, *Angew. Chem. Int. Ed. Engl.*, 29, **1990**, 235.

[12] W. H. Meyer, R. Brüll, H.G. Raubenheimer, C. Thompson, G.J Kruger, *J. Organomet. Chem.*, 553, **1998**, 83.

2

Neutral Palladium Complexes with β-diketo type ligands

This chapter is concerned with the preparation and spectroscopic studies of several palladium(II) complexes of symmetric and unsymmetric ß-dicarbonyl-type compounds. The goal of this study was to synthesize and characterize these complexes by means of melting point, IR, MS (where possible), NMR spectroscopy and X-ray crystal structure determination.

2.1.1 Introduction.

General Background.

The presence of β-dicarbonyl groups with at least one proton on the carbon between the carbonyl groups allows keto-enol tautomerism. Under appropriate conditions, the enolic proton can be removed. Complexes, which form when the proton is replaced by a metal, are the subject of this investigation.

The ligands that give "wings to metals" have now been studied for almost a hundred years,[1] yet very much still remains to be understood.[2]

New complexes with β-dicarbonyl-type ligands are useful not only for comparative studies with various other metal ions, but also as starting materials for the preparation of other organometallic compounds and as catalysts for organic synthesis. As a result, numerous papers have been published which discuss behavioral characteristics of complexes containing ß-dicarbonyl compounds as ligands.[3]

Recent structural studies of inorganic derivatives of acetylacetone render these compounds cogent and fascinating examples of linkage isomerism and related structural phenomena arising from variable metal-ligand interactions.[4] Several distinct bonding and structural types involving acetylacetone and its enolate anion are known. The two resonance forms of the enolate anion of acetylacetone are shown in Figure 2.1 below.
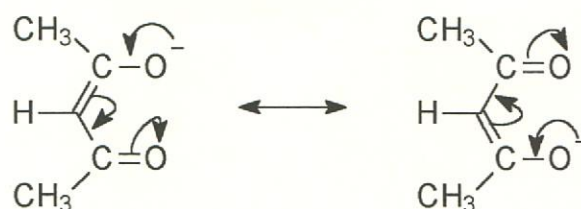
Figure 2.1 : Enolate anion equilibrium of acetylacetone.

By far the most frequently occurring acetylacetonate derivatives are those in which the enolate anion is coordinated to a central metal atom through both oxygen atoms. The ubiquity of oxygen-chelated acetylacetonate complexes can be appreciated from the fact that such complexes have been reported for all the main group transition elements (except technetium), and lanthanide elements (except promethium) as well as numerous main group and acitinide elements.

A second type of oxygen-chelated complex is formed when the acetylacetone does not lose its acidic proton to form an enolate ion. Rather the neutral keto tautomer donates electrons from the oxygens of each carbonyl to an acceptor or acidic species. An example of this type of coordination is illustrated in Figure 2.2 below.
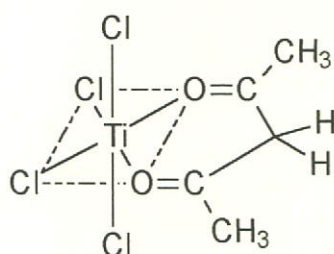
Figure 2.2 : Neutral keto tautomer coordination mode of acetylacetone to a metal.

Far less numerous than oxygen-chelated acetylacetonate derivatives are those in which the metal atom is bonded directly to the central carbon of the enolate anionic ligand rather than through the two oxygen atoms. Metal complexes of this type were first characterized in 1962.[5]

In another boding mode that has been characterized for the acetylacetonate complexes, the anionic ligand bonds through one of the two terminal carbons and not simultaneously through both of the two terminal oxygens or the central carbon. However, this bonding mode of the ligand is rare[6]. A tellurium compound illustrating such bonding mode is shown in Figure 2.3 below.
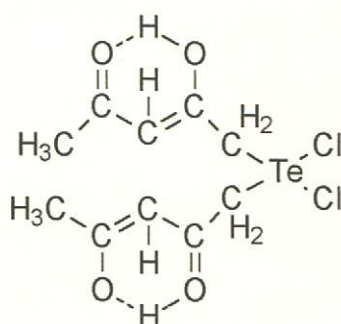
Figure 2.3 : Mono-carbon bonding mode of acacH to a metal ion

A final class of acetylacetonate derivatives contains bridging enolate ligands giving rise to oligomeric or polymeric complexes. Within this class, three types of complexes may be distinguished: -[7]

a) oxygen-chelated oxygen bridged complexes

b) oxygen-bonded two center β-diketonato complexes

c) bridge-bonded complexes

2,4-Pentanedione (acacH) and other ß-dicarbonyl compounds (ß-dikH) mostly react with a wide variety of metal ions to form the (O,O') chelates of the [M(ß-dik)$_n$] type which are usually soluble in organic solvents.[8] Apart from the basic bonding modes described above, these types of ligands are also capable of various reversible inter-conversions that will be briefly described here.

Due to the various bonding modes of ß-diketone ligands such as acetylacetone to metals, various linkage isomerisms result.[9, 10] For example, the reversible rearrangement of an acetylacetonate (acac) ligand from a bidentate O-bonded structure in dimethyl(acetylacetonato)gold(III) to a unidentate C-bonded adduct, dimethyl(acetylacetonato)phosphinegold(III).[11] It would appear as if steric factors play a role in the rearrangement from O-bonded acetylacetonate to C-bonded acetylacetonate.

There are however, only a few examples of the interconversion of O-bonded and C-bonded acac complexes. Rearrangement of one of the O-bonded acac ligands in Pd(acac)$_2$ to the C-bonded ligand is induced by phosphines and nitrogen bases, L, during the formation of the adduct, Pd(acac)$_2$L.[12]

The formation of the C-bonded acac-complexes can be likened to the formation of alkylmetals, in which the most stable transition metal complexes are generally found among the heavier elements with the highest electronegativities e.g. platinum-, palladium-, Rh- and Ir ß-diketonate complexes.[13]

Since interest in the inorganic and organometallic derivative chemistry of β-diketones shows no sign of diminishing, it is likely that additional unusual bonding and structural phenomena will be uncovered.

Work stems from the question, *"How will heteroatom-containing acac-analogue complexes* (3 and 4 in Figure 2.4 below), *behave in comparison with acac⁻,"* (as described in the discussion above). It was not known whether the potentially delocalized negative charge will be accommodated by the sulphur or phosphorous atom in the same manner as it is by the carbon atoms in deprotonated acacH.

2   **3**   **4**
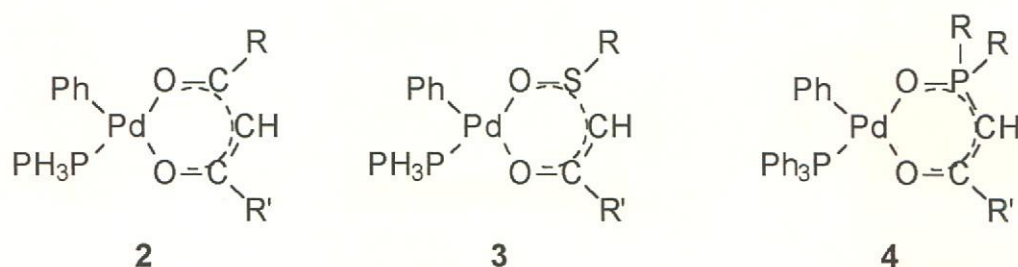
Figure 2.4

Target complexes to be prepared.

General background for the use of deprotonated acacH as an anionic ligand
for complexation with starting complex 1, trans-[(Ph₃P)₂(Ph)PdCl].

For the undeprotonated free ligand, acacH, used to prepare complex **2**, [(Ph₃P)(Ph)Pd(acac)], the following equilibrium and resonance forms must be considered prior to deprotonation of the central –CH₂ group: -[14]
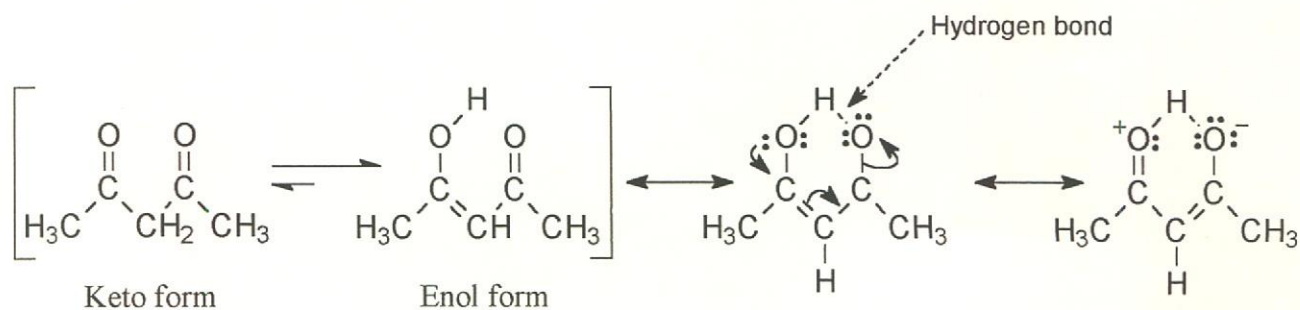
Figure 2.5 : Keto-enol tautomerization equilibrium of the free ligand precursor, acacH, with the resulting hydrogen bonding resonance.

The surface of ordinary laboratory glassware is able to catalyze and establish the equilibrium between the two constitutional isomers illustrated in Figure 2.5 above. As illustrated in Figure 2.5 above, in compounds with two carbonyl groups separated by one $-CH_2-$ group, the amount of enol present at equilibrium is higher. The greater stability of the enol form of ß-dicarbonyl compounds can be attributed to stability gained through resonance stabilization of the conjugated double bonds and through the hydrogen bonding.

The sulphur-containing acac⁻- analogue.

There are many reported cases in the literature where a sulphur atom has been used to replace one of the oxygens in the acac⁻-type ligand and has been coordinated or bonded directly to a transition metal. There are however, no reported examples where it has been used to coordinate to a transition metal through a delocalized [acac]⁻-type bond as indicated in Figure 2.4.[15] Reference is made in the literature to an -S=O group within a ligand which is coordinated to a metal through the oxygen (see Figure 2.6 below).[16]
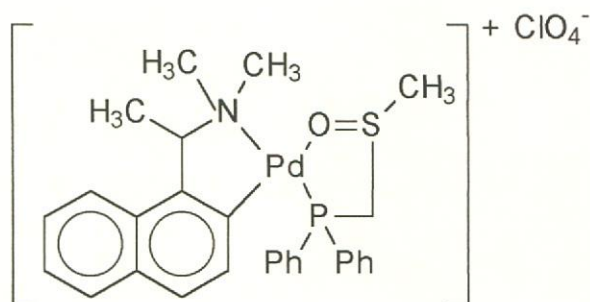
Figure 2.6 : Dative covalent bonding of an -S=O group to palladium.

In this study, ligands of the type $[RS(O)CH_2C(O)R']$ were prepared, deprotonated on the central $-CH_2$ group with NaH and bidentately coordinated to palladium(II) to form six-membered chelate rings. The resulting experimental data were compared to that of complex **2** and to that of related complexes reported in the literature.

The phosphorus-containing acac⁻-analogue.

Examples exist wherein there has been a direct coordination of the neutral $[R_2P(O)]CH_{2n}[R_2P(O)]$, or analogous ligand types, to a metal see Figure 2.7.[17]

Interest in complexes such as those illustrated in Figure 2.7 was generated as a result of its potential catalytic activity and biological activity. Biological activity arises from the O-Sn coordination bonds within such molecule.
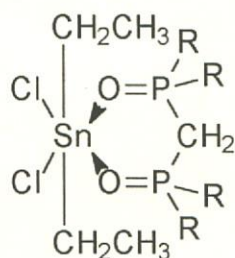
Figure 2.7 : Neutral phosphorus-containing acacH-type ligand coordination to a metal.

As far as can be ascertained, phosphorus has never been used in hetero-acac⁻-type ligands in the same manner as carbon.[18]

The reported complexes produced using the $[R_2P(O)CH_2]_2$-type ligands are monomers as well as complexes wherein the bidentate ligand behaves as a bridge in producing polymeric or binuclear complexes.[19] Many complexes have been produced using these types of ligands with iron(II) or iron(III) as the central metal ion.[20]

For the present investigation, ligands of the type $R_2P(O)CH_2C(O)R'$ were prepared, de-protonated on the central CH_2-group and coordinated to palladium to form 6-membered chelates. The resulting experimental data was compared to that of complex **2** and to that of similar complexes reported in the literature. The probable structures of the complexes produced in this manner are illustrated in Figure 2.8 below.
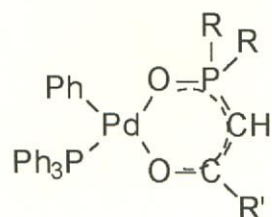
Figure 2.8 : Phosphorus-containing acac⁻-analogue complexes.

Application of acac⁻-type complexes in catalysis.

Transition-metal alkyl complexes are believed to be intermediates in a variety of catalytic processes such as carbonylation and oligomerisation.[21] Palladium(II) forms a variety of alkyl complexes of varying stability and hence is often employed in model systems for studying important steps in these catalytic reactions. In most cases it is believed that a metal hydride species is formed as an active intermediate in the catalytic pathway. Little is known about how the chelating ligand directs individual steps during the catalytic process.

The insertion of small molecules such as carbon monoxide into four coordinate d^8 metal-carbon bonds is an important step in homogenous catalysis. The influence of ligands on this process is a major consideration in catalyst design. Few studies on the mechanism of carbon monoxide insertion in complexes have been done using chelating ligands,[22, 23, 24] and even fewer on complexes of the ß-diketone (ß-dik) type ligands,[25] which is surprising considering the significance of the ligands in the various catalytic processes. These carbonylation studies also represent an important addition to the limited studies carried out on complexes containing dissimilar coordinating atoms.[26]

For future study, it would be interesting to attempt to correlate the nature of the chelate ligand with the activity of carbonylation process as well as other catalytic processes. An investigation into the influence of the coordinating atoms of these ligands, as well as that of the other alkyl groups on the chelate ring, on these catalytic processes would also be of interest.

Palladium and platinum acac⁻-type complexes, related to complex **2,** have been extensively reported. However, complex **2** was primarily synthesised in order to help monitor, predict and characterize the other complexes synthesised in the series of this chapter as it proved problematic to obtain crystals suitable for single crystal structure determination.

2.1.2 *Goals and scope of this section of the project.*

There has been some interest in the role of the chelating phosphine ligands in directing the mechanism for carbon monoxide insertion during the carbonylation of palladium- and platinum-heterocarbonyl complexes.[27, 28, 29] No references describing complexes as illustrated in Figure 2.9 below have been found.[30]
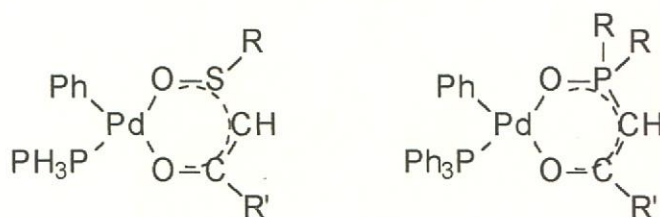
Figure 2.9 : Sulphur- and phosphorus-containing acac⁻-analogue complexes prepared.

The main goal of this study was to prepare and characterize complexes of the type illustrated in Figure 2.9 and to obtain suitable crystals for structure characterization. Structure characterization enables the investigation of the metal ligand bonding in these types of complexes in an attempt to correlate structural parameters with ligand influences. Future studies should include the correlation of these structural parameters with complex reactivity in catalytic reactions e.g. carbon monoxide insertion. The investigation of the catalytic activity of these types of complexes however falls outside the scope of this investigation.

The synthetic route used to prepare complex **2** is illustrated in Scheme 2.1 below and is applicable to all the complexes prepared in this chapter. It finally involves the reaction of the deprotonated ligand with starting complex **1** by

displacement of a triphenylphosphine group. Readily removable sodium chloride forms as a byproduct.

$$CH_3-\underset{\underset{O}{\|}}{C}-CH_2-\underset{\underset{O}{\|}}{C}-CH_3 \quad + \quad NaH \quad \longrightarrow \quad CH_3-\underset{\underset{O}{\|}}{C}-\underset{\underset{Na}{|}}{CH}-\underset{\underset{O}{\|}}{C}-CH_3 \quad + \quad H_2(g)$$

$$CH_3-\underset{\underset{O}{\|}}{C}-\underset{\underset{Na}{|}}{CH}-\underset{\underset{O}{\|}}{C}-CH_3 \quad + \quad \underset{\underset{Cl}{|}}{\overset{Ph}{Ph_3P-Pd-PPh_3}} \quad \xrightarrow[-NaCl]{-PPh_3}$$

2
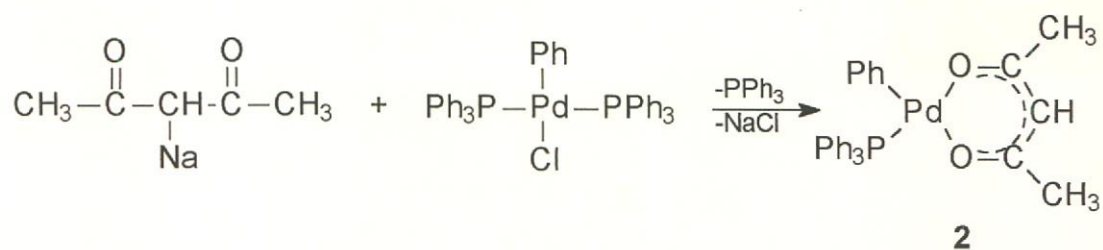
Scheme 2.1 : General synthetic route used to prepare complexes described in chapter 2.

2.2 *Results and Discussion*

2.2.1 Complex 1, *trans*-[(Ph₃P)₂(Ph)PdCl].

I) Preparation of complex 1, trans-[(Ph₃P)₂(Ph)PdCl].

Trans-[(Ph₃P)₂(Ph)PdCl] was synthesised according to the method described by Herrmann and his co-workers and is illustrated in Scheme 2.2 below.[31] It involved the reaction of palladium chloride with triphenylphosphine to deliver palladium tetrakis triphenylphosphine. The final step of preparation involved an oxidative addition of phenyl chloride to produce complex **1**. The clean product was obtained by crystallization from a 1:1 mixture of anhydrous dichloromethane and pentane.

$$PdCl_2 \xrightarrow{4PPh_3} Pd(PPh_3)_4 \xrightarrow{C_6H_5-Cl}$$

$$Ph_3P-Pd-PPh_3$$

1
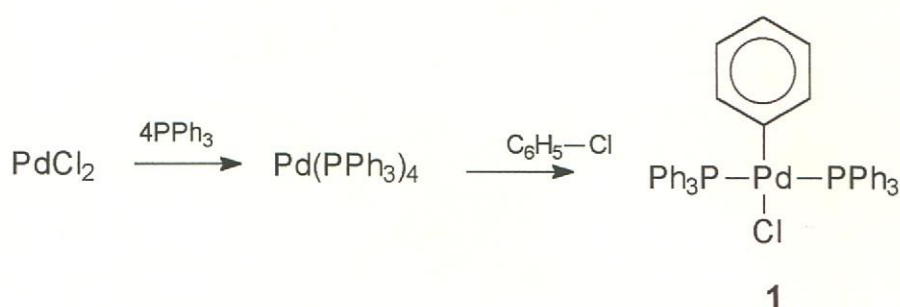
Scheme 2.2 : Preparation of complex **1**.

Trans-[(Ph₃P)₂(Ph)PdCl] as synthesised according to Scheme 2.2, was used as the starting complex for all the neutral palladium complexes prepared.

II) NMR Spectroscopic analysis of complex 1, trans-[(Ph₃P)₂(Ph)PdCl].

The ^{1}H and ^{13}C NMR data for complex **1** are summarised in Table 2.1 below. The ^{1}H and ^{13}C spectra for complex **1**, are reported in both d^2-dichloromethane and d^6-benzene. The complexes that were synthesised from complex **1** were recorded in both of the above solvents in order to enable all proton and carbon groups present to be individually assignable.

Starting Complex **1**.

Ph$_3$P—Pd—PPh$_3$
d c   a b
       |
       Cl

Solvent : CD$_2$Cl$_2$ (TMS used as internal standard)	Solvent : C$_6$D$_6$ (TMS used as internal standard)

Proton (δ-values)

a:	---	---
b:	7.19 – 7.88 (m, 30H)	6.99 – 7.82 (m, 30H)
c:	---	---
d:	7.19 – 7.88 (m, 30H)	6.99 – 7.82 (m, 30H)
e:	---	---
f:	6.59 (d, 2H, J_{H-H} = 6.6Hz)[i]	6.91 (d, 2H)
g:	6.19 (t, 2H)[i]	6.34 (t, 2H)
h:	6.34 (t, 1H)[i]	6.31 (t, 2H)

Carbon 13 {^{1}H} (δ-values)

b:	122.5 – 155.5 (m)	122.3 – 137.8
d:	122.5 – 155.5 (m)	122.3 – 137.8
e:	155.5	156.7
f, g, h:	122.5 – 155.5 (m)	122.3 – 137.8

Phosphorus 31 {^{1}H} (δ-values[ii])

a:	24.41	24.62
c:	24.41	24.62

Table 2.1

^{1}H and ^{13}C data for complex **1**.

---

[i] Peak assignments done largely on the grounds of signal multiplicity and integration values for the Pd-Ph group. It is virtually impossible to assign specific peaks for the triphenylphosphine groups due to the complex multiplet that these triphenylphosphine groups deliver.

[ii] δ-values are relative to H_3PO_4 used as an external standard.

III) Single crystal structure determination of complex 1.

Although the synthesis of complex **1** has been known for some time, the crystal structure has now been solved.[32]

Suitable crystals for crystal structure determination were obtained by crystallization of complex **1** from a solution of dichloromethane layered in a 1:1 ratio with pentane.

A colourless crystal of *trans*-[$(Ph_3P)_2(Ph)PdCl$] was mounted on a glass fiber and transferred to a Phillips PW1100 diffractometer. All data were collected at room temperature with graphite monochromated Mo-K$_\alpha$ radiation with $2\theta = 23°$ and corrected for Lorentz and polarization effects. Absorption corrections were applied by the empirical method. Unique sets of data with intensities greater than two times the standard deviation were used to solve the structure by the heavy atom (Patterson) method. Refinements were done using least squares refinement. All non-hydrogen atoms were refined anisotropically. For structure solution and refinement the ShelX-97 software package was used[33]. Structure figures were generated using Ortep-3[34].

Selected crystallographic bond lengths and angles are listed in Tables 2.2 and 2.3 respectively. The crystal structure is illustrated in Figure 2.12 below and the unit cell is illustrated in Figure 2.13. All other crystallographic information is available Dr. C. Esterhuysen Department of Chemistry, Stellenbosch University, Private Bag X1, 7602 Matieland, South Africa.

Selected bond lengths(Å).			
Pd-C31	2.005 (5)	C134-C135	1.375 (9)
P1-P2	2.3177 (13)	C135-C136	1.376 (8)
P1-P1	2.3233 (13)	C211- C212	1.367 (8)
Pd-Cl	2.4064 (13)	C211-C216	1.389 (8)
P1-C111	1.818 (5)	C212-C213	1.399 (10)
P1-C131	1.825 (5)	C213-C214	1.350 (12)
P1-C121	1.827 (5)	C214-C215	1.349 (12)
P2-C221	1.821 (5)	C215-C216	1.384 (9)
P2-C231	1.822 (6)	C221-C222	1.398 (7)
P2-C211	1.827 (5)	C22-C223	1.372 (8)
C111-C112	1.376 (8)	C223-C224	1.362 (10)
C111-C116	1.389 (7)	C224-C226	1.375 (10)
C112-C113	1.388 (9)	C225-C226	1.367 (9)
C113-C114	1.352 (10)	C231-C236	1.354 (9)
C114-C115	1.366 (10)	C231-C232	1.375 (9)
C115-C116	1.379 (8)	C232-C233	1.384 (11)
C121-C122	1.382 (8)	C233-C234	1.323 (16)
C121-C126	1.384 (8)	C234-C235	1.367 (16)
C122-C123	1.387 (10)	C235-C236	1.413 (11)
C123-C124	1.357 (13)	C31-C32	1.388 (8)
C124-C125	1.353 (12)	C32-C36	1.393 (8)
C125-C126	1.372 (9)	C32-C33	1.378 (9)
C131-C136	1.375 (8)	C33-C34	1.376 (12)
C131-C132	1.391 (7)	C34-C35	1.359 (12)
C132-C133	1.379 (9)	C35-C36	1.387 (9)
C133-C134	1.342 (10)		

Table 2.2

Selected bond lengths (Å) with e.s.d's. in parenthesis for complex **1**.

Selected bond angles(°).			
C31-Pd-P2	90.30 (14)	C221-P2-C211	102.2 (2)
C31-Pd-P1	91.59 (14)	C231-P2-C211	104.2 (2)
P2-Pd-P1	177.20 (5)	C221-P2-Pd	116.51 (17)
C31-Pd-Cl	179.93 (13)	C231-P2-Pd	107.94 (19)
P2-Pd-Cl	89.68 (5)	C211-P2-Pd	119.75 (17)
P1-Pd-Cl	88.43 (5)	C112-C111-C116	118.3 (5)
C111-P1-C131	104.5 (2)	C122-C121-C126	117.0 (6)
C111-P1-C121	102.7 (2)	C136-C131-C132	117.8 (5)
C131-P1-C121	107.6 (2)	C212-C211-C216	118.1 (6)
C111-P1-Pd	117.69 (16)	C225-C221-C222	117.0 (5)
C131-P1-Pd	109.84 (16)	C236-C231-C232	119.1 (7)
C121-P1-Pd	113.72 (18)	C32-C31-C36	117.2 (5)
C221-P2-C231	104.7 (3)	---	---

Table 2.3

Selected bond angles (°) with e.s.d's. in parenthesis for complex **1**.
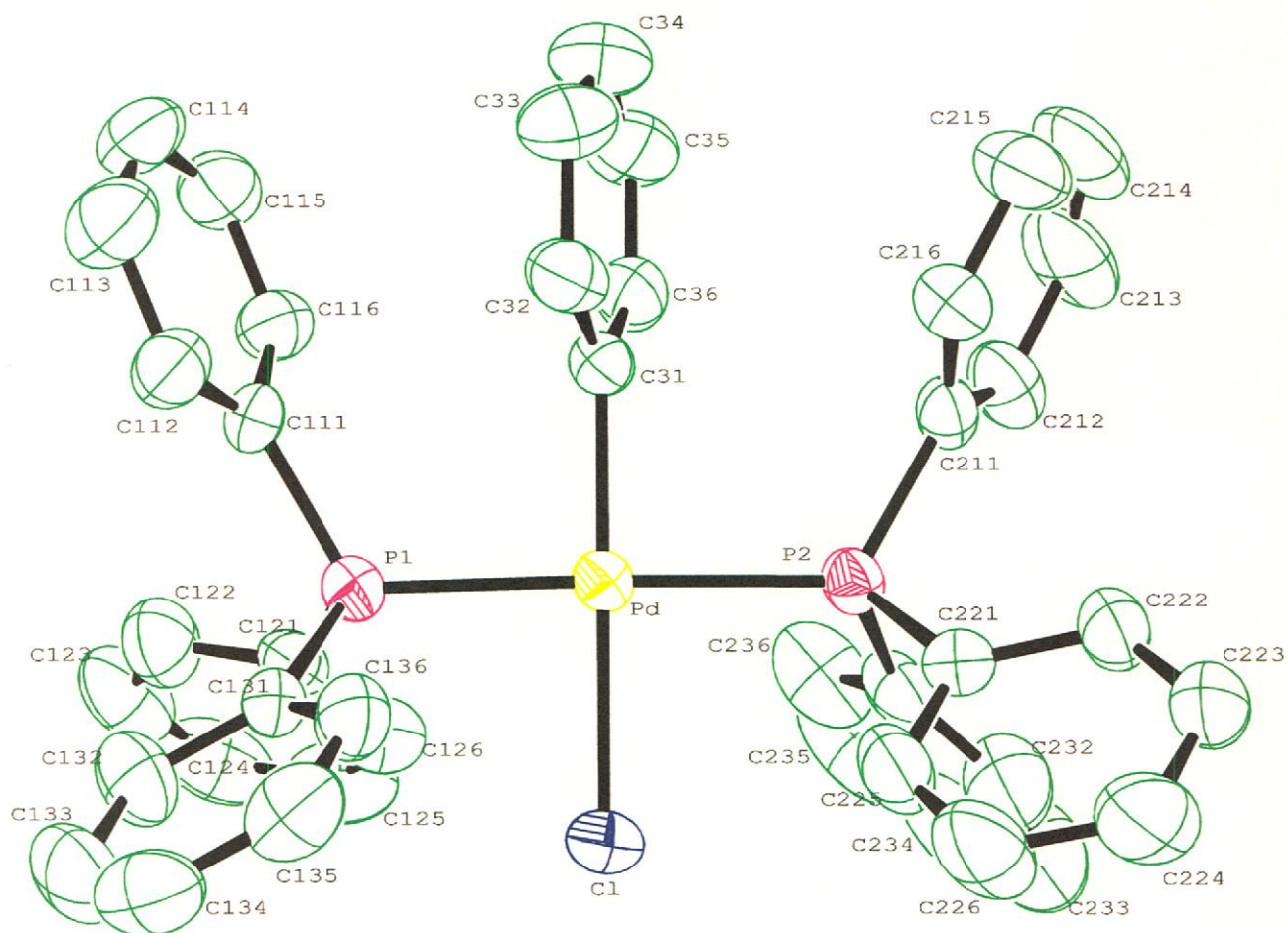
Figure 2.11 : Ortep-3 plot of the molecular structure of complex **1**, *trans*-[(Ph$_3$P)$_2$(Ph)PdCl], at 50% ellipsoid probability showing the numbering scheme used. Hydrogen atoms have been omitted for clarity.
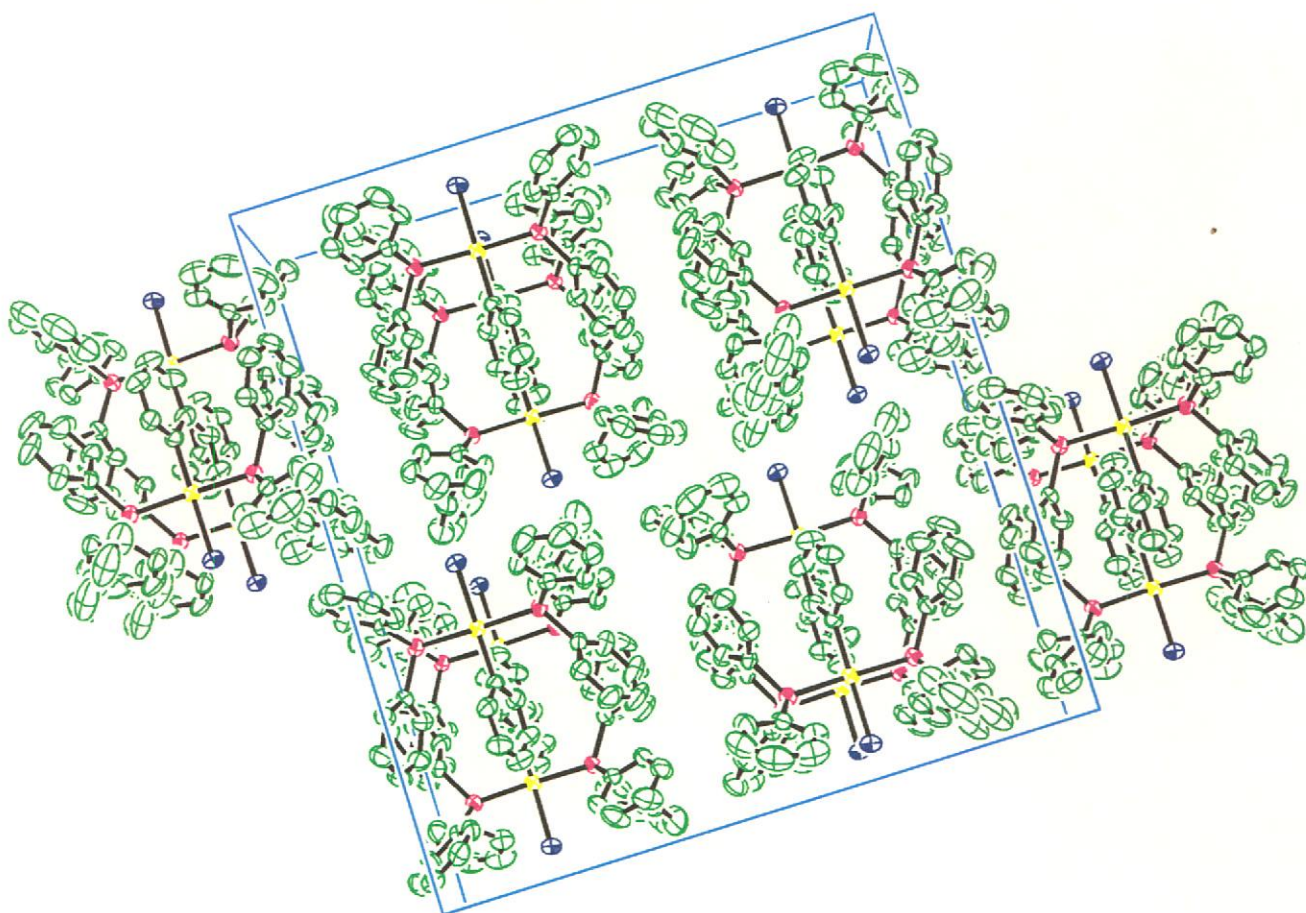
Figure 2.12 : Ortep-3 plot of the unit cell of complex **1**, trans-[(Ph$_3$P)$_2$(Ph)Pd(Cl)], at 50% ellipsoid probability. Hydrogen atoms have been omitted for clarity.

*IV) Discussion of the structure and bonding in complex **1**.*

Most organo-palladium complexes are square-planar[35]. This means that in an ideal molecule, the four atoms surrounding the palladium will lie at right angles to each other in a plane with the palladium. The average deviation in angles around the palladium atom in complex **1** from the ideal square-planar molecule was found to be 1.11° with a maximum deviation value of 2.80°.[36] The average was calculated by taking the absolute value of the differences between the experimental angle and the ideal angle (180° or 90°) and taking the average of the four resulting values, while the maximum was the largest of the six numbers. The root mean square (RMS)[iii] for complex **1** was found to be 0.021 while the maximum deviation from planarity was found to be 0.026Å.

It is clear from the square-planar angle and planar deviation values that complex **1** conforms to the typical square planar geometry of four co-ordinate complexes of palladium(II) with the two triphenylphosphine groups being *trans* to each other. This conformation to square planar configuration is clearly illustrated in Figure 2.12.

Bond Angles: -

The two *trans* triphenylphosphine ligands can take on one of three possible configurations relative to one another. These are eclipsed, staggered and skew. These possible conformations can be identified by inspection of the torsion angle as defined in Figure 2.14 below.

[iii] RMS deviation = $\left[\dfrac{1}{N} \sum \left(x_i - \overline{x} \right)^2 \right]^{1/2}$, N = number of observations, x_i = value of observation i and $\overline{x}$ = mean.
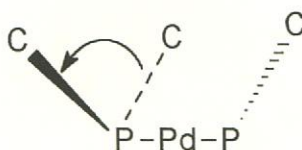
Figure 2.14 : Definition of the torsion angle describing possible conformations of triphenylphosphine groups in complex **1**.

The torsion angles for the eclipsed conformation would thus be ($0°$, $120°$, -$120°$), ($60°$, $180°$, -$60°$) for the staggered conformation and ($90°$, -$30°$, -$150°$) for the skew conformation. The torsion angles for complex **1** were found to be [$131.9(3)°$, $13.7(3)°$, -$111.5(3)°$]. Thus with a distortion of $10°$, the triphenylphosphine groups of complex **1** can be classified as being eclipsed.

As the overall structure is close to square planar, the C31-Pd-P2 angle is close to $90°$ ($90.30°$), but C31-Pd-P1 is greater than $90°$ and is at $91.59°$. These small differences in angle are most likely due to the slightly different spatial arrangement of the bulky phenyl rings in each of the two triphenyl phosphine groups. As this difference in spatial arrangement is small, the two triphenylphosphine groups are sitting close to $180°$ from each other. The P2-Pd-P1 angle being $177.2°$.

In spite of the small differences in the individual spatial arrangement of each phenyl ring in the two triphenylphosphine groups, the opening angles of each phenyl ring within each triphenylphosphine group are equivalent to each other and to those of the opposing triphenylphosphine group.

As illustrated in Figure 2.12, the phenyl group lies at $75.42(16)°$ to the plane containing Pd, P1, P2, C31. The chlorine atom is a fairly bulky ligand and lies trans to the phenyl ligand. It lies in the molecular plane interacting equally with the two triphenylphosphine groups. Since the triphenylphosphine ligands are similarly arranged, these groups do not allow any bending of the phenyl group only twisting. The C34-C31-Pd angle measured in complex **1** is $179.8°$

Bond lengths: -

If the bonds from the central palladium atom to the two phosphorus atoms are compared, it can be seen that the bond lengths are almost equivalent. The Pd-P1 bond length being 2.3233 (13) Å while the Pd-P2 bond length is 2.3177 (13) Å.

The bond lengths from the phosphorus atoms to the ipso-carbon atoms of the respective phenyl rings within each triphenylphosphine group are, as expected, equivalent to each other and equivalent to the P-C_{ipso} bonds in the opposing triphenylphosphine group. The mean carbon-carbon bond lengths within each of the triphenylphosphine rings of each triphenylphosphine group are similar in length.

As can be seen from both Figure 2.12 and the e.s.d's values in Table 2.2, the phenyl rings of P2 have a slightly higher degree of thermal disorder than those of P1.

V) Thermogravimetric analysis of complex 1.

The thermal decomposition of complex **1** was studied to investigate the possible existence of stable intermediate species. No thermogravimetric analysis reference could be found in the literature for similar palladium(II) complexes.

Figure 2.15 is a graphic representation of the thermogravimetric temperature program which involved a $0 - 500^{\circ}C$ temperature range at $5^{\circ}C$ min^{-1}.
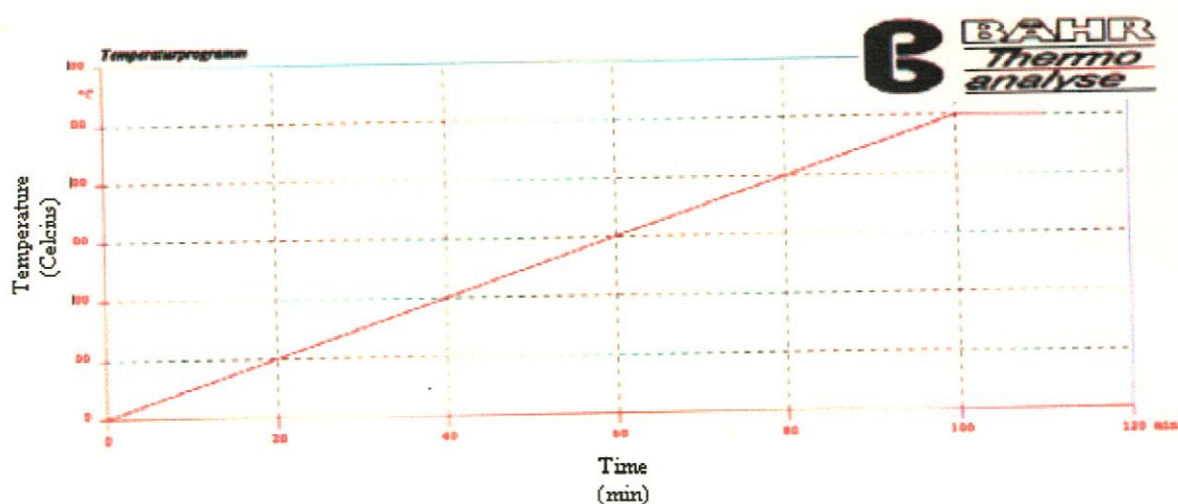
Figure 2.15 : Thermogravimetric analysis temperature program.

Figure 2.16 below is a plot of TG and DTG versus temperature for the thermogravimetric decomposition of complex **1**, while Figure 2.17 is a plot of TG and DTA versus time for the same thermogravimetric decomposition.
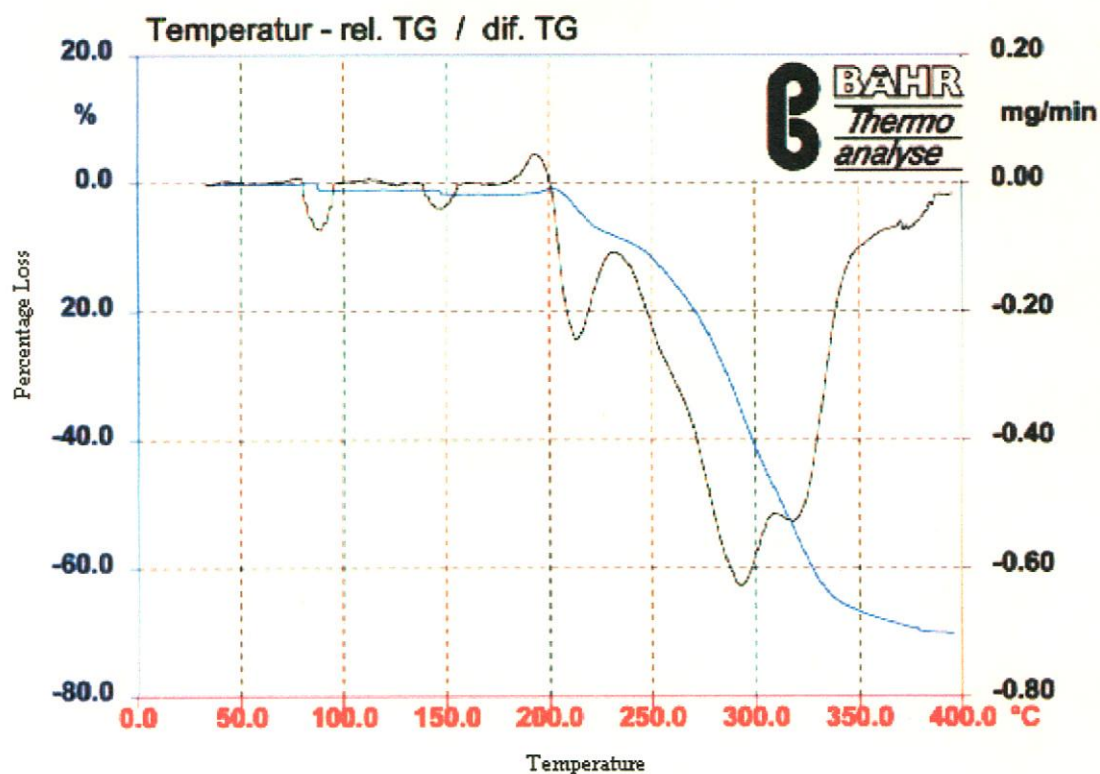
Figure 2.16 : TG and DTG versus temperature plot of the thermogravimetric analysis for complex **1**.
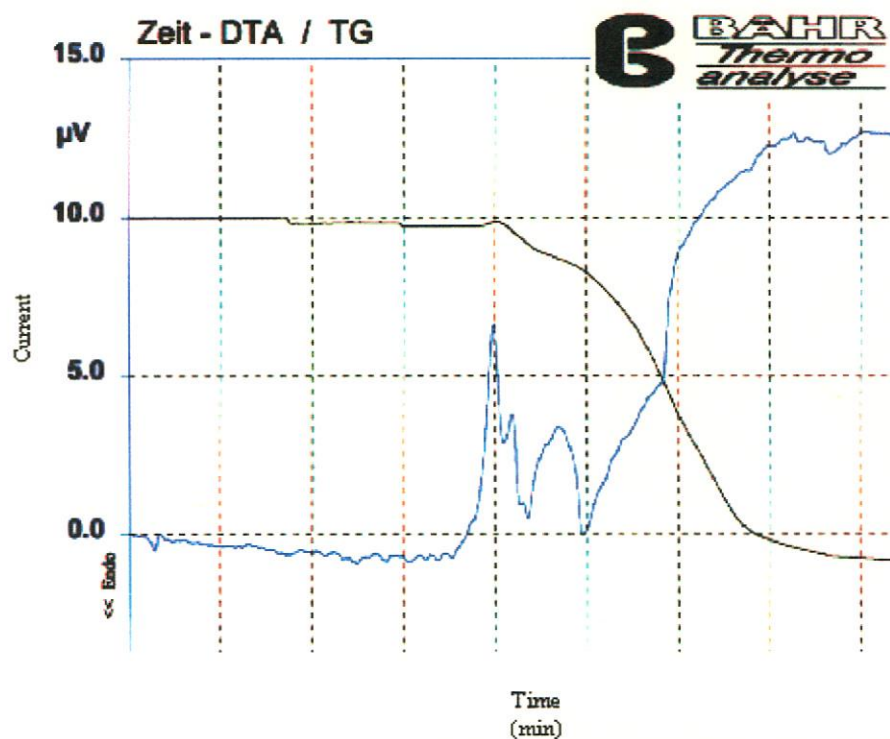
Figure 2.17 : DTA and TG versus time plot of the thermogravimetric analysis for complex **1**.

Based on Figures 2.16 and 2.17 above, Scheme 2.3 below illustrates the suggested decomposition of complex **1**. It is evident from Figures 2.16 and 2.17 that the decomposition occurs in three distinct stages.

$$
\underset{\text{1}}{\underset{\underset{\displaystyle Cl}{|}}{\overset{\overset{\displaystyle Ph}{|}}{Ph_3P-Pd-PPh_3}}} \xrightarrow{\;-\;Cl\;} \underset{\text{2}}{\overset{\overset{\displaystyle Ph}{|}}{Ph_3P-Pd-PPh_3}} \xrightarrow{\;-PPh_3\;} \underset{\text{3}}{\overset{\overset{\displaystyle Ph}{|}}{Ph_3P-Pd}} \xrightarrow{\;-PPh_3\;} \overset{\overset{\displaystyle Ph}{|}}{Pd}
$$
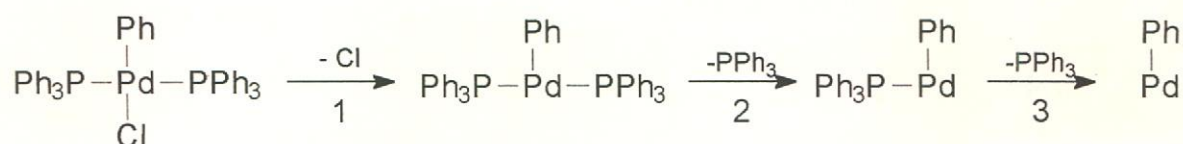
Scheme 2.3 : Suggested thermogravimetric decomposition route of complex **1**.

The decomposition process starts at about 200°C and ends at 350°C. Step one occurs at ca. 200°C, step two at ca.250°C and step three at ca. 300°C. The three steps occur in relatively quick succession and the ideal decomposition curve with distinct individual plateaus is not obtained.

From the above graphs it can be seen that with initial decomposition the chloride is lost followed by the subsequent loss of the two triphenylphosphine groups. The intermediates formed during this decomposition do not appear to be very stable. This lack of stability of the intermediates is evident in Figure 2.16 by the relative rapid sequence of decomposition and lack of plateau definition with particular reference to the third stage. The final fragment obtained is Pd-Ph, which is stable over the following ca. 20° up to 500°C.

2.2.2 Complex 2, [(Ph₃P)(Ph)Pd(acac)].

I) Preparation of complex 2, [(Ph₃P)(Ph)Pd(acac)].

Complex **2** was synthesised according to Scheme 2.4 below. 2,4-Pentanedione was deprotonated under anhydrous, inert conditions with sodium hydride. The sodium acetylacetonate was reacted with complex **1** to substitute a triphenylphosphine group and produce complex **2** with sodium chloride and triphenylphosphine as a by-products.

Scheme 2.4 : Synthesis of complex **2**.

II) NMR Spectroscopic analysis of acetylacetone and complex 2.

The ^{1}H and ^{13}C NMR data for acetylacetone is summarised in Table 2.4 below. The ^{1}H and ^{13}C data for the free ligand is reported for d^2-dichloromethane. The NMR data in Table 2.4 lists the shifts in ppm for both the keto- and enol-form of the free ligand. The keto-enol equilibrium of acetylacetone is described in detail in the introduction to this chapter.

Free Ligand Precursor

| | Keto form | Eno form |

Solvent : CD_2Cl_2 (TMS as internal standard).

Proton (δ-values)

a:	2.02 (s, 9H) (two CH_3 groups from ketone & one CH_3 group from enol form)
b:	2.19 (s, 3H) (One CH_3 group of enol) form
c:	---
	5.52 (s, 2H) (ketone form)
	3.57 (s, 1H) (enol form)

Carbon 13 {¹H} (δ-values)

a:	32.5 (ketone form)
	26.5 (enol form)
b:	204.0 (ketone form)
	193.2 (enol form)
c:	60.3 (ketone form)
	102.1 (enol form)

Table 2.4 : ^1H and ^{13}C NMR data for acetylacetonate.

The ^1H and ^{13}C NMR data for complex **2** are summarised in Table 2.5 below. The ^1H and ^{13}C data are reported for both d^2-dichloromethane and d^6-benzene.

Complex

Solvent : CD_2Cl_2 (TMS used as internal standard).	Solvent : C_6D_6 (TMS as internal standard

Proton (δ-values)

a:	1.91 (s) or 1.67 (s) (3H)	1.75 (br s) (6H)
b:	5.36ppm (s, 1H)	5.34 (s) (1H)
c:	1.91 (s) or 1.67 (s) (3H)	1.75(br s) (6H)
d:	---	---
e:	6.67 – 7.03 (m) (5H)	6.85 – 7.84ppm (m) (20H)
f:	7.51 – 7.30 (m) (15H)	6.85 – 7.84ppm (m) (20H)

Carbon 13 $\{^1H\}$ (δ-values)

a:	27.9	27.9
b:	99.9	100.0
c:	27.9	27.9
d:	188.2 and 187.5	187.7
e:	123.7 – 136.7[iv] (m)	123.7 – 136.9[iv] (m)
e_{ipso}:	149.8	---[v]
f:	123.7 – 136.7[vi] (m)	123.7 – 136.9[vi] (m)
f_{ipso}	150.0	---

Phosphorus 31 $\{^1H\}$ (δ-values)

f:	33.13ppm	Not measured

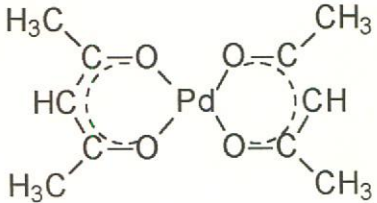**Table 2.5 :** ^1H and ^{13}C data for complex **2**.

[iv] Signal obscured by the signal of protons f.
[v] Impossible to unambiguously assign ipso signal due to overly of phenyl triphenylphosphine signals.
[vi] Signal obscured by the signal of protons e.

The proton and carbon-13 shifts of the ß-dicarbonyl compounds complexed to metals are known to show a variety of different shifts in different NMR solvents due to solvent interaction with the complex. It is known that d^6-benzene has a remarkable effect on the ^{1}H NMR spectra of most measured palladium ß-dicarbonyl complexes[37]. Most signals show a substantial upfield shift in d^6-benzene as compared to those in other solvents. When the NMR of complex **2** is measured in d^2-benzene, a single broader signal for the two terminal –CH$_3$ groups was found in the middle of the ppm shift of the signals produced by the –CH$_3$ groups when analysed in d^2-dichloromethane. The upfield shift in benzene may be attributed to the diamagnetic anisotropy of the solvent molecule interacting with the complex.

Table 2.6 below lists the NMR data of Pd(acac)$_2$ as reported in the literature for various solvents.[38] It illustrates the solvent effect that is reported for these types of complexes in different NMR solvents.

	Proton NMR Data		
	Solvent	*-CH₃*	*-CH-*
	in CDCl$_2$	2.07	5.43
	in C$_6$D$_6$	1.65	4.94
	in (CD$_3$)$_2$CO	1.97	5.49
	in (CD$_3$)$_2$SO	1.97	5.53
	Carbon 13 {^{1}H} NMR Data		
	Solvent	*-CH₃*	*-CH-*	CH$_3$CO
	in CDCl$_3$	25.4	101.6	187.2
	in C$_6$D$_6$	24.9	101.1	186.8
	in (CD$_3$)$_2$CO	25.0	101.4	*vii*

Table 2.6 : Reported NMR spectral data of Pd(acac)$_2$ as collected in various solvents.

When the NMR spectral data of acetylacetone and that of complex **2** are compared, it is evident that deprotonation of the free ligand did occur as well as co-ordination of the free ligand to the palladium. The following characteristics of the spectrum are of note: -

➢ It is evident from the NMR data that the coordination of the ligand to the palladium took place through the two oxygen atoms and not through the central carbon atom as was a possibility. This can be seen by the difference in shifts for the carbonyl carbons ($\delta_{complex}$ - $\delta_{free\ ligand}$, 16.5 and 15.8ppm respectively) in the carbon-13 spectrum. The shifts with respect to these groups, as well as to those compared to the –CH group and the two-CH_3 groups, are in line with that for similar complexes found in the literature.[39, 40, 41]

➢ The position of the central –CH- group in both the carbon-13 (100.0ppm) and proton (5.34ppm) data, relative to its position prior to deprotonation is also consistent with bonding through the carbonyl groups.

➢ Since co-ordination with palladium is square planar, and the other two subsituents are triphenylphosphine and a phenyl group, the two carbonyl groups are not chemically equivalent. This is substantiated by the two different signals that are evident in the carbon-13 data for the two carbonyl groups when measured in d^2-dichloromethane namely 191.6ppm and 187.8ppm. This is in line with the same phenomenon reported in the literature[42]. However, only one signal is evident in the carbon-13 spectrum when measured in d^6-benzene namely 187.7ppm

➢ Due to the square planar geometry of the complex and the resulting relatively high symmetry, the two terminal –CH_3 groups of the acac⁻-ligand are also not equivalent. Two signals are observed for these groups in the proton NMR data, namely δ1.78 (s) and δ1.76 (s).
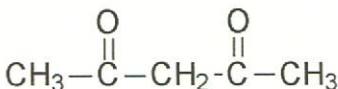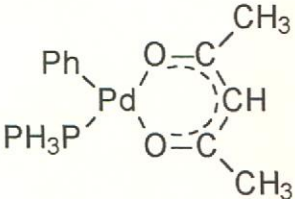

[vii] Signal indiscernible because of poor solubility of the complex.

> An overall downfield shift in the phosphorus-31 spectrum of complex **1**, compared to that of complex **2** is further evidence in support of the suggested co-ordination of the deprotonated acac⁻-ligand.

> When analysed in d^2-dichloromethane, the proton NMR signals of the phenyl rings of the two triphenylphosphine groups appear in the region 7.30-7.51ppm as a complex multiplet. The Pd-Ph proton NMR signals are well separated from the -PPh₃ signals and can easily be distinguished in the region 6.67 - 7.03ppm. However, when analysed in d^6-benzene, the signals of the Pd-Ph group are obscured by the signals of the -PPh₃ group and visa versa thus only enabling the overall δ-assignment for both groups as a whole (6.85 – 7.84ppm).

> It is important to note that two separate, well-defined proton signals are evident for the two –CH₃ groups when the sample is analysed in d^2-dichloromethane, but only one broad singlet is apparent for both groups when analysed in d^6- benzene.

> Due to the non-separation of the signal of the phenyl group from those of the triphenyl phosphine group, when analysed in d^6-benzene, it proved impossible to unambiguously assign the carbon-13 signals for these groups.

> When the NMR proton spectrum of complex **2** measured in d^6-benzene is compared with the proton spectral data as collected in d^2-dichloromethane, an overall upfield shift is apparent in d^6-benzene. This is in line with the literature-reported phenomenon for these types of complexes and is probably due to the diamagnetic anisotropy interaction of d^6-benzene.[43]

III) Infrared spectral data for complex 2, [(Ph₃P)(Ph)Pd(acac)].

Infrared spectroscopy proves invaluable in the characterization of acetylacetonate-type complexes. Extensive infrared studies have been carried out in the characterization of acetylacetonate complexes.[44] It was reported by Collman *et al.* that the central hydrogen atom of these complexes can be replaced under electrophilic conditions. He reported that the unsubstituted acetylacetonate complexes exhibit strong bands at $\sim 1570 cm^{-1}$ and $\sim 1520 cm^{-1}$. Substituted acetylacetonate complexes show only weak absorbtion at $\sim 1520 cm^{-1}$ and the band at $\sim 1570 cm^{-1}$ is shifted to $\sim 1550 cm^{-1}$. It was also reported by Collman that infrared vibrations of different chelate rings in unsymmetrical substituted acetylacetonates in the same complex are nearly independent of each another. It has also been reported that the infrared data for analogous complexes with different metal centers e. g. Rh, Cr, Co are nearly identical.[45]

The infrared data for the free ligand acacH and complex **2** are reported in Table 2.7 below. The infrared data obtained for the free ligand acacH is in agreement with the data reported by Pretch *et al.*[46]

Acetylacetone	Complex 2.
1724 cm-1 (keto form)	1539.8 cm^{-1} (s)
1608 cm-1 (enol form)	1558.7 cm^{-1} (vs)
CO bond order = 2	CO bond order = 1½

Table 2.7 : Infrared spectral data for acacH and complex **2**.

If the carbonyl groups of the deprotonated acetylacetone were to coordinate to the palladium atom through a delocalized negative charge as proposed, the double bond character of these carbonyl group groups would be decreased.

This would cause the stretching frequency of the carbonyl groups to be reduced.[47]

As is evident in Table 2.7 above, there has been a decrease of ~200cm^{-1} in the ν(C=O) stretching vibration. The reduction in the stretching vibration of these carbonyl groups is further support of the NMR data that the coordination of the acetylacetonate to the palladium has occurred through the carbonyl groups and not though the central carbon atom.

*IV. Mass Spectrum for complex **2**.*

The mass spectrum fragmentation pattern for complex **2** is illustrated in Scheme 2.5 below. Relative intensities are given in parenthesis. The molecular ion of the target complex was observed at m/z 546. The subsequent fragmentation occurs primarily along two pathways:

- The first involves the initial loss of the acetylacetonate ligand followed by the further fragmentation of the triphenylphosphine and phenyl groups.
- The second route involves the loss of the triphenylphosphine group followed by the phenyl group. The second fragmentation path is characterized by comparatively low intensities relative to the first.
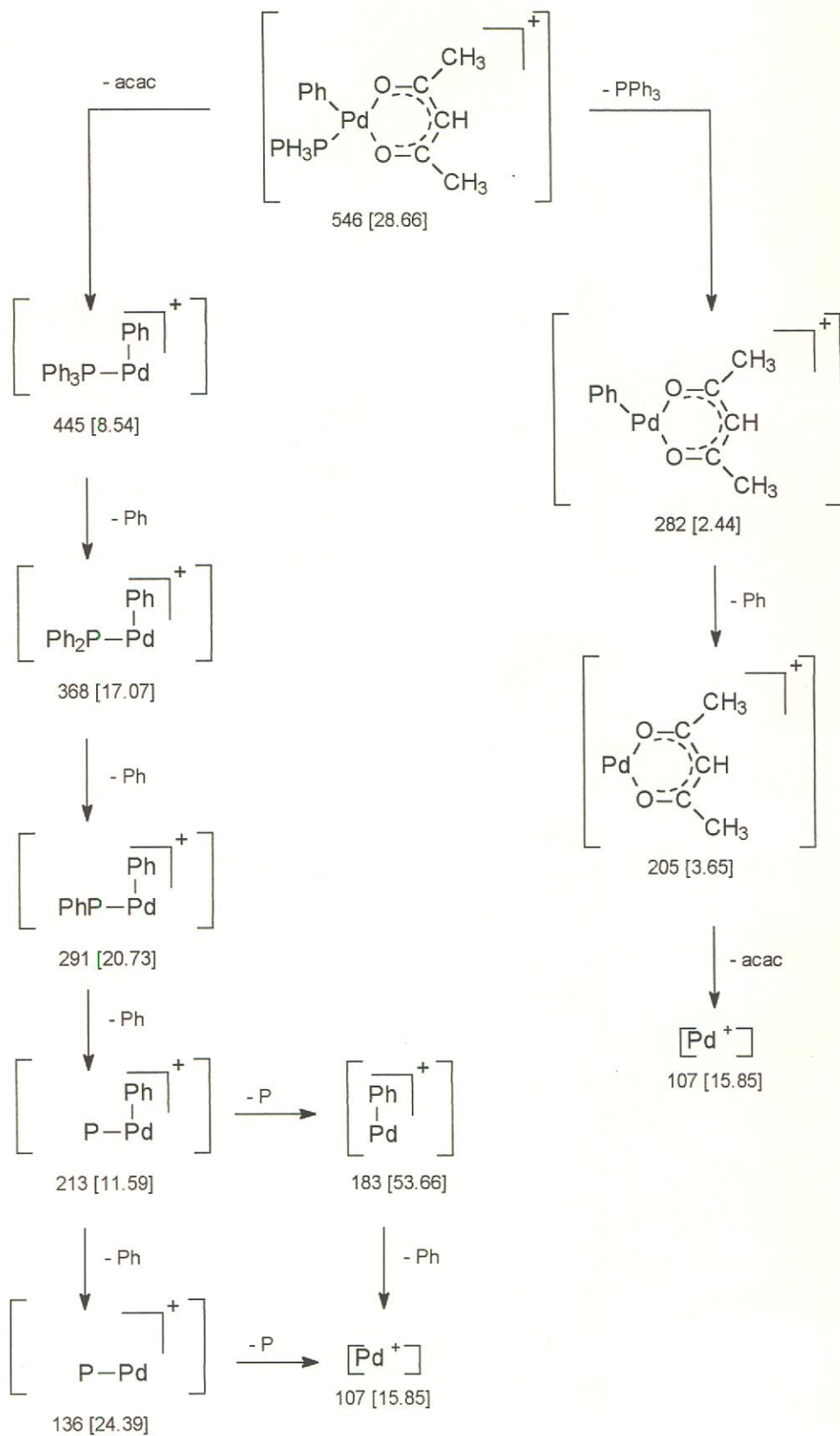
Scheme 2.5 : Mass spectrum for complex 2.

Relative intensities are given in parenthesis.

*V. Single crystal structure determination of complex **2**.*

Suitable crystals for crystal structure determination were obtained by crystallization of complex **2** from a solution of dichloromethane layered in a 1:1 ratio with pentane.

A light yellow crystal of $(Ph_3P)(Ph)Pd(acac)$ was mounted on a glass fiber and transferred to a Phillips PW1100 diffractometer. All data were collected at room temperature with graphite monochromated Mo-K_α radiation with $2\theta = 23°$ and corrected for Lorentz and polarization effects. Absorption corrections were applied by the empirical method. Unique sets of data with intensities greater than two times the standard deviation were used to solve the structure by the heavy atom (Patterson) method. Refinements were done using least squares refinement. All non-hydrogen atoms were refined anisotropically. For structure solution and refinement the ShelX-97 software package was used.[48] Structure Figures were generated using Ortep-3.[49]

Selected crystallographic bond lengths and angles are listed in Tables 2.8 and 2.9 respectively. The crystal structure of complex **2** is illustrated in Figure 2.18 below while the unit cell is illustrated in Figure 2.19. All other crystallographic information is available from Dr. C. Esterhuysen Department of Chemistry, Stellenbosch University, Private Bag X1, 7602 Matieland South Africa.

Atoms bonded	Bond length (Å)	Atoms bonded	Bond length (Å)
Pd1 -C41	1.990 (4)	O1-C1	1.263 (4)
Pd1-O2	2.086 (2)	O2-C4	1.272 (4)
Pd1-O1	2.095 (3)	C1-C3	1.392 (6)
Pd1-P1	2.2325 (10)	C1-C2	1.511 (6)
P1-C11	1.816 (4)	C3-C4	1.381 (6)
P1-C31	1.828 (4)	C4-C5	1.515 (6)
P1-C21	1.843 (4)	---	---

Table 2.8 : Selected bond lengths (Å) with e.s.d's. in parenthesis for complex **2**, [(PPh$_3$)(Ph)Pd(acac)]

Atoms bonded	Bond angle (°)	Atoms bonded	Bond angle (°)
C41-Pd1-O2	87.42 (12)	C11-P1 C31	104.70 (19)
C41-Pd1-O1	176.00 (12)	C11-P1 C21	103.90 (17)
O2-Pd1-O1	89.43 (10)	C31-P1 C21	104.16 (17)
C41-Pd-P1	88.45 (10)	C11-P1 Pd1	111.08 (12)
O2-Pd1-P1	175.55 (8)	C31-P1 Pd1	110.25 (12)
O1-Pd1-P1	94.62 (7)	C21-P1 Pd1	121.32 (13)

Table 2.9 : Selected bond angles (°) with e.s.d's. in parenthesis for complex **2**, (PPh$_3$)(Ph)Pd(acac)]
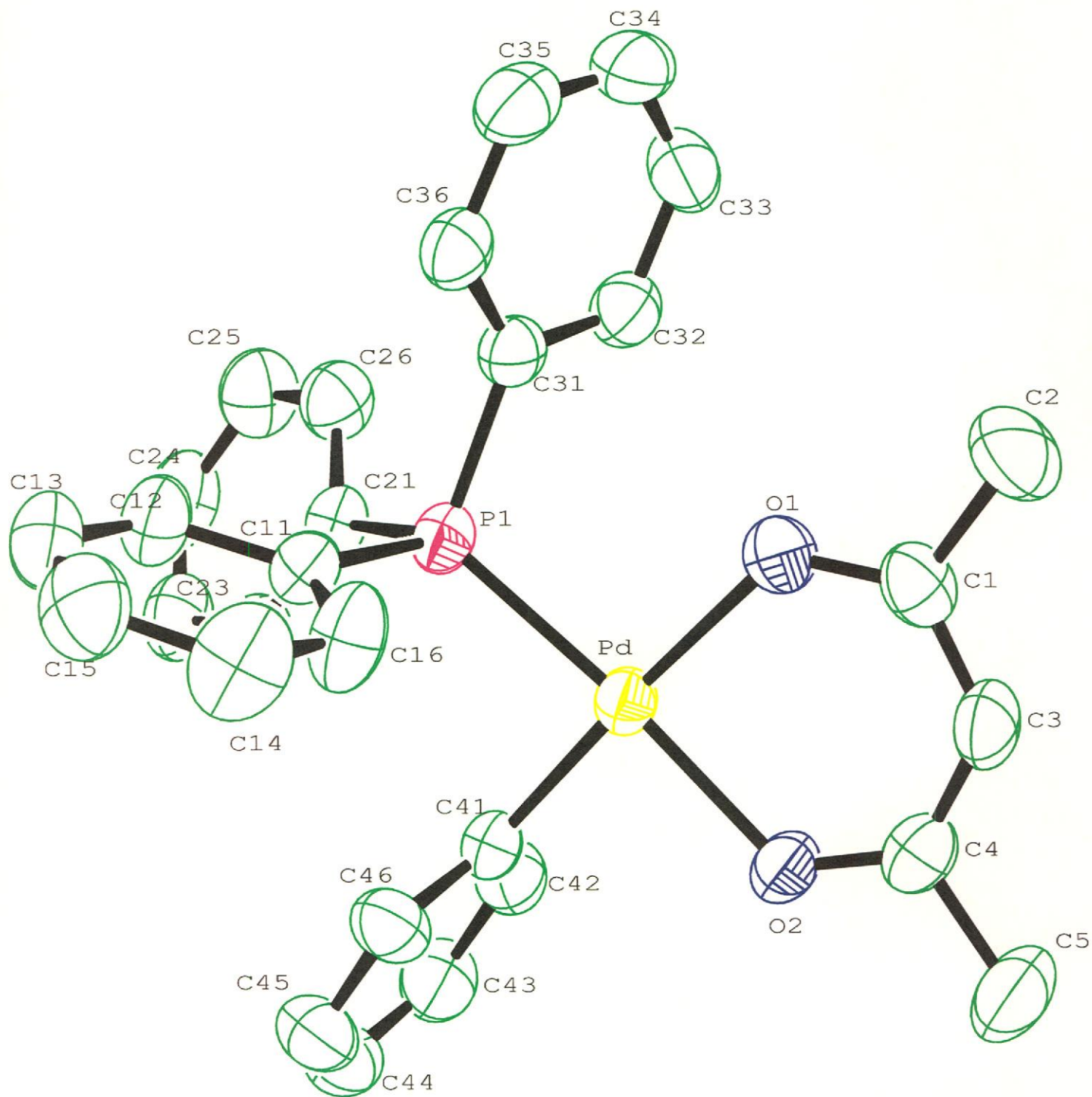
Figure 2.17 : Ortep-3 plot of the molecular structure of [(Ph$_3$P)(Ph)Pd(acac)] at 50% ellipsoid probability showing the numbering scheme used. Hydrogen atoms have been omitted to make viewing easier.
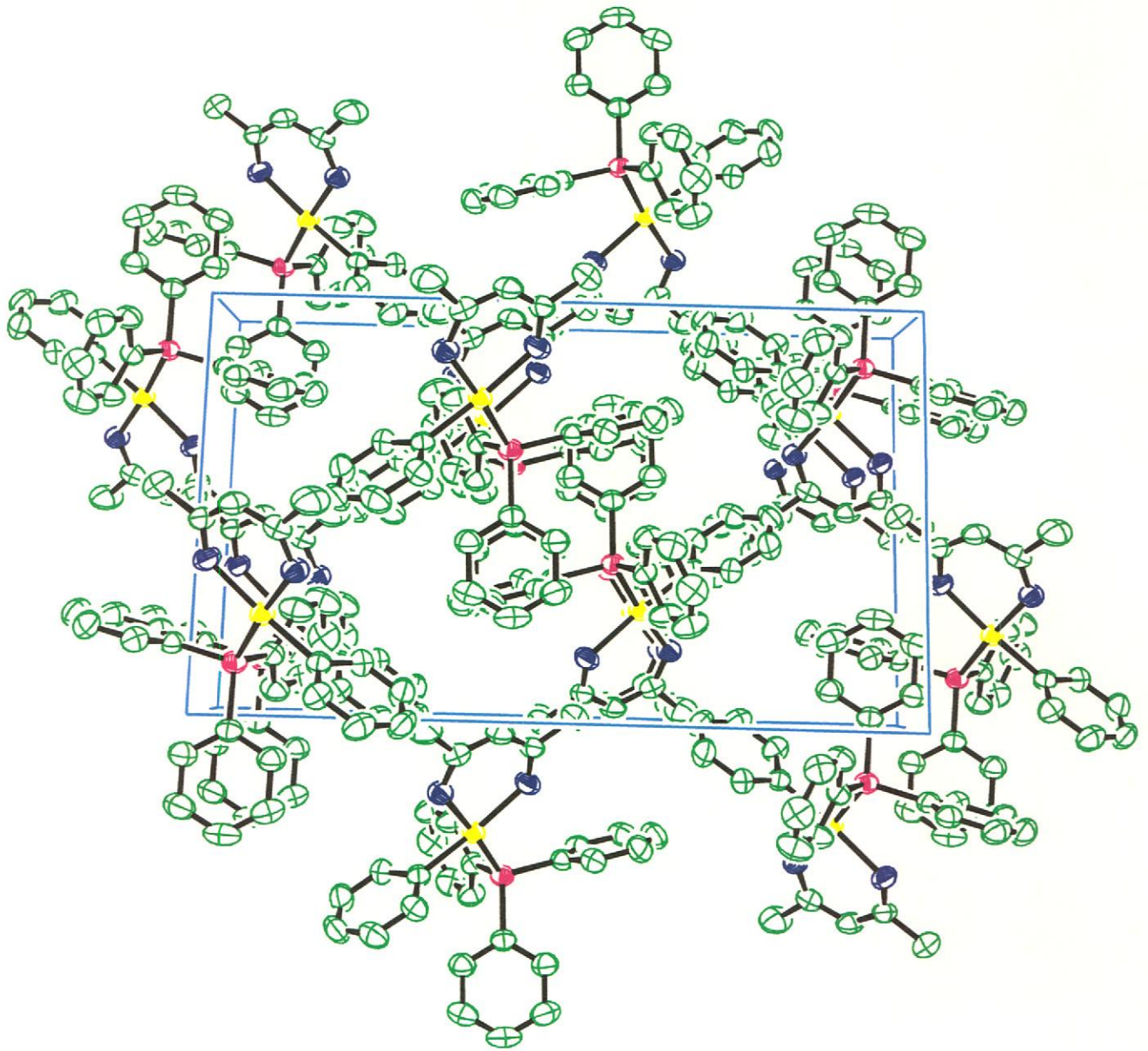
Figure 2.19 : Ortep32 plot of the unit cell of [(Ph$_3$P)(Ph)Pd(acac)] at 50% ellipsoid probability showing the molecular packing. Hydrogen atoms have been excluded to make viewing easier.

VI. _Discussion of the structure and bonding in complex **2**,_
[(PPh₃)(Ph)Pd(acac)].

Bond angles and bond lengths for complex **2** are reported in the tables 2.8 and 2.9 above. The corresponding structure with respect to this data will be discussed here.

Based on an analysis of the Cambridge Crystallographic Structural Database (CCSD), most organo-palladium complexes are square planar. In the ideal molecule the four atoms surrounding the palladium will lie at right angles to each other in the plane with the palladium. The average angle of deviation within complex **2** from the square-planar conformation is 2.96° with the maximum being 4.62°. The average was calculated by taking the absolute value of the difference between the experimental angle and the ideal angle (180 ° or 90°) and taking the average of the four resulting values while the maximum was the largest of the six numbers. The root mean square (RMS)[viii] for complex **2** was found to be 0.017 while the maximum deviation from planarity was found to be 0.027Å. This maximum deviation from planarity is very close to that which was found for complex **1** (0.026Å).

The above values indicate that complex **2** exhibits a typical square-planar coordination with very slight deviation from the plane. In general the trends described below for complex **2** are similar to and in line with similar Pd(II) and Pt(II) complexes reported by Cavell et al.[50]

The C41-Pd-P1-C11 torsion angle for complex **2** is −168.2°. This torsion angle is in sharp contrast to the comparative torsion angle of 131.9° in complex **1**.

The phenyl group, directly bonded to the palladium atom, lies almost perpendicular to the plane containing the Pd, P1, O1 and O2. The phenyl is rotated about the palladium-carbon bond and is being slanted against the

---

[viii] RMS deviation = $\left[\dfrac{1}{N}\sum\left(x_i-\overline{x}\right)^2\right]^{\frac{1}{2}}$, N = number of observations, x_i = value of observation i and $\overline{x}$ = mean.

square-planar plane with a torsion angle of 78.47(9)°. The C41-Pd-P1-C11/C12/C13 torsion angles are 76.2(2)°, -46.2(2) ° and −168.2(2)° respectively.

Since the phenyl group is aromatic, the Pd atom would thus be expected to lie in the same plane as the phenyl ring. However, the phenyl ring has a distinctly bent conformation with the C44-C41-Pd angle being 172.0°. A perfectly straight phenyl ligand would have an angle of 180°. The phenyl ligand takes up this bent conformation to minimize its interaction with the triphenylphosphine group.

Where acetylacetonate bonds to a metal ion in the classical form though the two oxygen atoms, the two chelate ring C-C bond distances and the two C-O bond distances are reported as being equal.[51] This characteristic is present in complex **2** with C1-O1 = 1.263(4) Å, C4-O2 = 1.272(4) Å and C1-C3 = 1.392(6) Å, C3-C4 = 1.381(6) Å. The bond lengths between the palladium and the two oxygen atoms are close enough in length [Pd-O(1) 2.095(3)Å and Pd-O(2) 2.086(2)Å] to be considered equal.

The methyl groups of the ligand are equivalently bonded to their respective carbons within the ligand ring with a bond length of 1.515(6)Å and 1.511(6) Å respectively.

This general equivalency in bond lengths is characteristic of a coordination of the anion of 2,4-pentanedione through the two oxygen atoms to a metal with a delocalization of charge through the resulting chelate ring.

Due to the bulky nature of the phenyl rings within the PPh$_3$ group, the three phenyl rings become constrained causing the P-C(phenyl) bond lengths within the rings not to be equivalent. The P-C21 bond (1.843 (4)Å) is longer in length than the other P-C bonds.

2.2.3 Complex 3, [(Ph₃P)(Ph)Pd(CH₃SCHC(O)Ph)].

*I) Preparation of complex **3**.*

Complex **3** was prepared according to Scheme 2.6 below. The precursor for the ligand, ω-(methylsufinyl)acetophone [CH₃S(O)CH₂C(O)Ph], was prepared, de-protonated on the central -CH₂ group with NaH and bidentately coordinated in complex **1** through the two forming a six-membered chelate. During the reaction one triphenylphosphine group of complex **1** was displaced to furnish complex **3**. Readily removable sodium chloride forms as a byproduct.
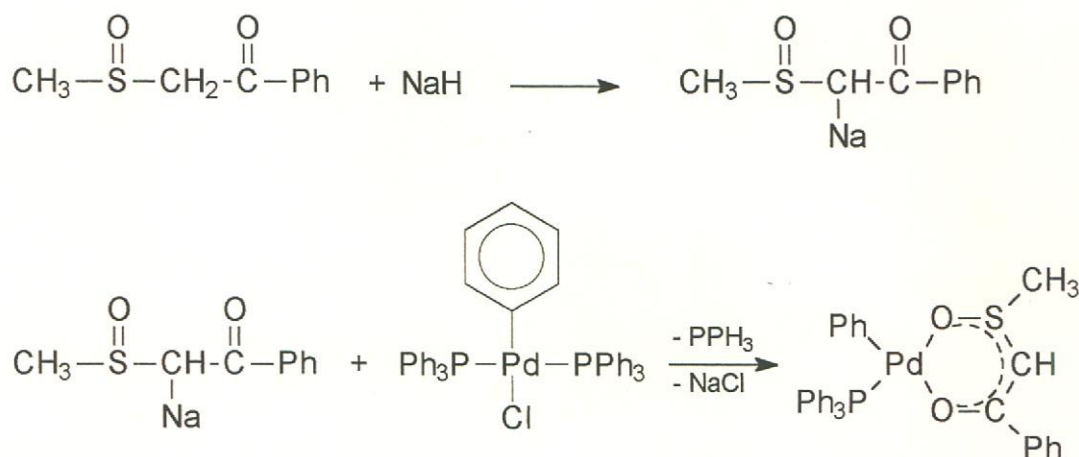
Scheme 2.6 : Preparation of complex 3, [(Ph₃P)(Ph)Pd(CH₃SCHC(O)Ph)].

*II) Spectroscopic analysis of the precursor of the free ligand, ω-(methylsufinyl)acetophone, and complex **3**.*

The ^{1}H and ^{13}C NMR data for the precursor of the free ligand ω-(methylsufinyl)acetophone, are summarised in Table 2.10 below. The ^{1}H and ^{13}C spectra for ω-(methylsufinyl)acetophone, are reported for both d^2-dichloromethane and d^6-benzene since the NMR data of complex **3**, synthesised from deprotonated ω-(methylsufinyl)acetophone, were recorded in both solvents to enable all protons and carbons present in the synthesised complex to be individually visible.

Free Ligand Precursor

$$CH_3-\overset{\overset{\displaystyle O}{\|}}{S}-CH_2-\overset{\overset{\displaystyle O}{\|}}{C}-Ph$$
$$abcd$$

Solvent : CD_2Cl_2 (TMS as internal standard).	Solvent : CD_2Cl_2 (TMS as internal standard).

Proton (δ-values)

a:	2.73 (s, 3H)	2.11 (s, 3H)
b:	4.38 (dd, 2H)	3.74 (dd, 2H)
c:	---	---
d:	7.54 - 8.05 (m, 5H)	7.02 – 7.84 (m, 5H)

Carbon 13 {^{1}H} (δ-values)

a:	40.0	39.3
b:	62.8	62.2
c	193.2	192.8
d_{ortho}	129.2 - 129.6 (m)	27.8 – 129.7 (m)
d_{meta}	129.2 – 129.6 (m)	127.8 – 129.7 (m)
d_{para}	134.9	134.3
d_{ipso}	136.9	137.3

Table 2.10 : NMR spectral data for the precursor of the free ligand, ω-(methylsufinyl)acetophone.

The hydrogen atoms of the central -CH_2 group are diastereotopic and thus are visible in the proton NMR spectrum as a doublet of doublets.

The ^{1}H and ^{13}C NMR data for complex **3** are summarised in Table 2.11 below. The ^{1}H and ^{13}C data are reported for both d^2-dichloromethane and d^6-benzene.

Complex

Solvent : CD_2Cl_2 (TMS as internal standard).	Solvent : C_6D_6 (TMS as internal standard).
Proton (δ-values)	
a: 2.67 (s, 3H)	2.46 (s, 3H)
b: 5.72 (s, 1H)	5.90 (s, 1H)
c: ---	---
d: 6.70 – 7.63 (m)	6.89 – 7.52 (m)[ix]
e: 6.70 – 7.63 (m)	6.89 – 7.52 (m)[ix]
f: 6.70 – 7.63 (m)	6.89 – 7.52 (m)[ix]
Carbon 13 {¹H} (δ-values)	
a: 43.3	44.3
b: 94.3	96.8
c: 178.4	179.78
d: 123.1 – 134.8 (m)	124.2 – 138.8 (m)[ix]
e: 123.1 – 134.8 (m)	124.2 – 138.8 (m)[ix]
f: 123.1 – 134.8 (m)	124.2 – 138.8 (m)[ix]
Phosphorus 31 {¹H} (δ-values)	
f: 27.85	24.58

Table 2.11 : NMR spectral data for complex **3**.

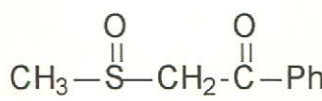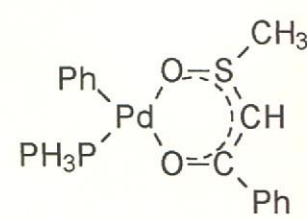[ix] Signals are obscured by the C_6D_6 signal and it is impossible to unambiguously assign individual phenyl group signals

The characteristics of the NMR spectral data of complex **3** relative to that of the free ligand precursor, ω-(methylsufinyl)acetophone, can be summarized as follows: -

➤ A slight downfield shift occurs in the proton spectrum of the –CH_3 group. This shift is more evident in the carbon-13 spectrum where a downfield shift of 3.5ppm has occurred.

➤ The position of the –CH- group in both the carbon-13 and proton data, relative to it's position prior to de-protonation, suggests that significant de-shielding (±34ppm) has occurred. This is consistent with de-localized bonding through the carbonyl- and sulphoxide group. This deshielding is consistent with the deshielding of the central –CH group of acac⁻ that occurred upon its chelation with palladium in complex **1** which is in opposition to the shielding that occurs due to the negative charge formed as a result of the deprotonation of the neutral ligand. This downfield shift in complex **3** is more dramatic in the carbon-13 spectrum where a shift of 31.5ppm in CD_2Cl_2 has occurred.

➤ An overall upfield shift from free ligand to complex has occurred for the phenyl group of the ligand in both the carbon –13 (6.1ppm) and proton (0.84ppm) spectra.

➤ A sharp upfield shift of 14.8pmm has occurred for the carbonyl signal. This upfield shift is further support for coordination of the ligand to the palladium. This marked upfield shift indicates that the carbonyl groups have experienced a greater degree of shielding due to the anionic ligand used in contrast to the neutral compound used as reference. This marked upfield shift was also observed in the carbon-13 spectra of complex **2**.

➤ Overall the trends exhibited here are similar to those observed for complex **2** whose molecular structure is confirmed by MS-, IR-, NMR spectroscopy and X-ray crystal structure determination.

III) Infra-red spectral data for the free ligand, ω-(methylsufinyl)acetophone, and complex 3.

The infrared data for ω-(methylsufinyl)acetophone and complex **3** is listed in Table 2.12 below.

Free ligand Precursor	Complex
$CH_3-\overset{\overset{O}{\|\|}}{S}-CH_2-\overset{\overset{O}{\|\|}}{C}-Ph$	
ν(C=O) : 1710.6 cm^{-1}	ν(C=O) : 1564.2 cm^{-1}
CO bond order = 2	CO bond order = 1½.

Table 2.12 : Infrared spectral data for ω-(methylsufinyl)acetophone and complex **3**.

There has been a decrease of 146.4 cm^{-1} in the ν(C=O) stretching vibration. This reduction is in-line with the reduction of double bond character that would occur if deprotonated ω-(methylsufinyl)acetophone were to coordinate to the palladium atom through the carbonyl group by means of a delocalized charge. This change is parallel to that in the infrared spectral data that was observed for complex **2** relative to the ligand precursor whose structure was confirmed by a single crystal x-ray structure determination (see Table 2.7).

Despite attempting various methods of crystallization, no crystals suitable for crystal structure determination formed. Complex **3** may occur as two possible isomers. NMR data indicated that only one is present. These isomers are illustrated in Figure 2.19 below.
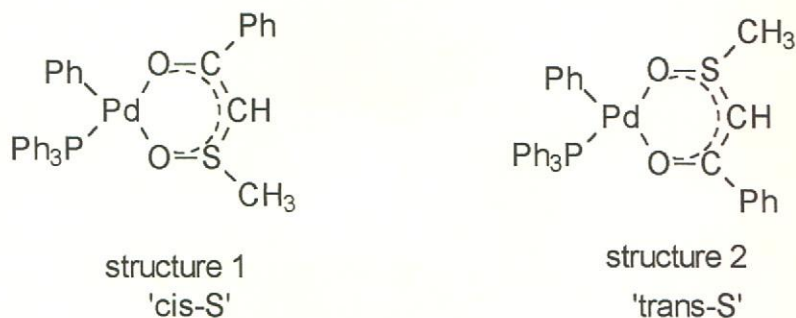
Figure 2.19 : Possible isomeric forms of complex **3**.

In the first isomer, structure 1 above, the OS-CH$_3$ unit is situated cis to the triphenylphosphine group. In the second isomer, structure 2, the OS-CH$_3$ group occurs trans to the triphenylphosphine group. Due to the relatively bulky nature of both the phenyl and triphenylphosphine groups, it is proposed that the cis configuration (structure 1, Figure 2.19 above) is preferred configuration for complex **3**.

*IV) Mass Spectrum of complex **3**, (Ph$_3$P)(Ph)Pd (CH$_3$S(O)CH$_2$C(O)Ph)]*

The mass spectrum for complex **3** is illustrated in Scheme 2.7 below. Relative intensities are given in parenthesis. The molecular ion was observed at m/z 630 with relative high intensity.

The fragmentation pattern illustrated in Scheme 2.7 is similar in many respects to that in Scheme 2.5 for complex **2**. Fragmentation of complex **3** also occurs primarily along two pathways:

- The first fragmentation pathway involves the loss of the triphenylphosphine group followed by the loss of the phenyl group. Further fragmentation involves the loss of the bonded sulphur-containing ligand.
- The second fragmentation pathway involves the initial loss of the sulphur-containing ligand followed by further fragmentation of individual phenyl groups.
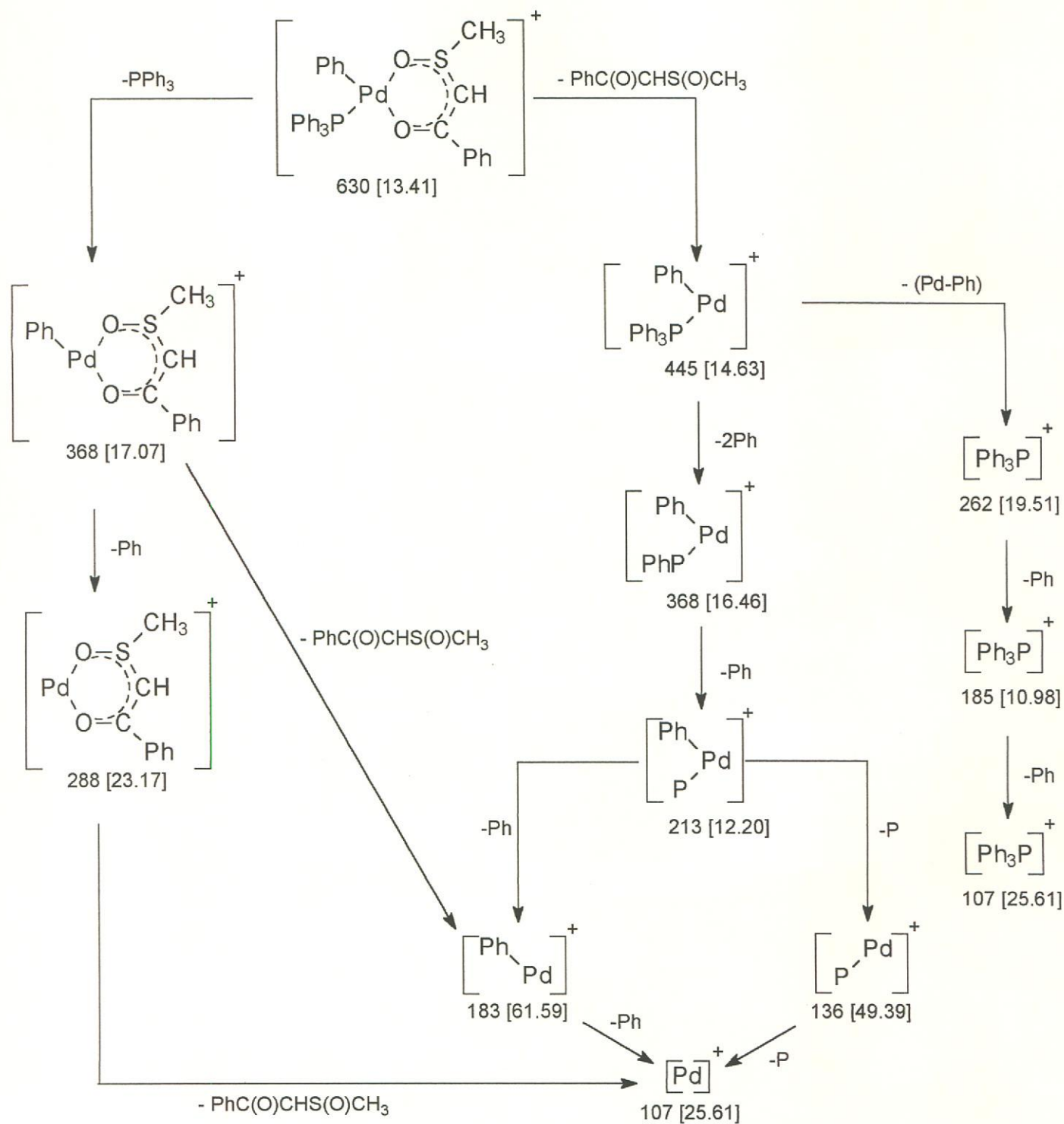
Scheme 2.7 : Mass spectrum for complex **3**.

Relative m/z intensities are in parenthesis.

2.2.4 *Complex 4, [(PPh₃)(Ph)Pd{(CH₃CH₂O)₂P(O)CHC(O)CH(CH₃)₂}].*

I)Preparation of complex 4.

The precursor of the free ligand, 1-diethyl-3-methyl-phosphino-2-butanone, was prepared according to modified literature methods.[52] Complex **4** was prepared according to Scheme 2.8 below. The precursor of the free ligand was deprotonated on the central -CH₂ group with a 1.1 mole equivalent of sodium hydride. The resultant isolated sodium salt was re-dissolved and bidentately coordinated to the palladium in complex **1** by substituting a triphenylphosphine group forming a 6-membered chelate ring. Readily removable sodium chloride is formed as a byproduct.
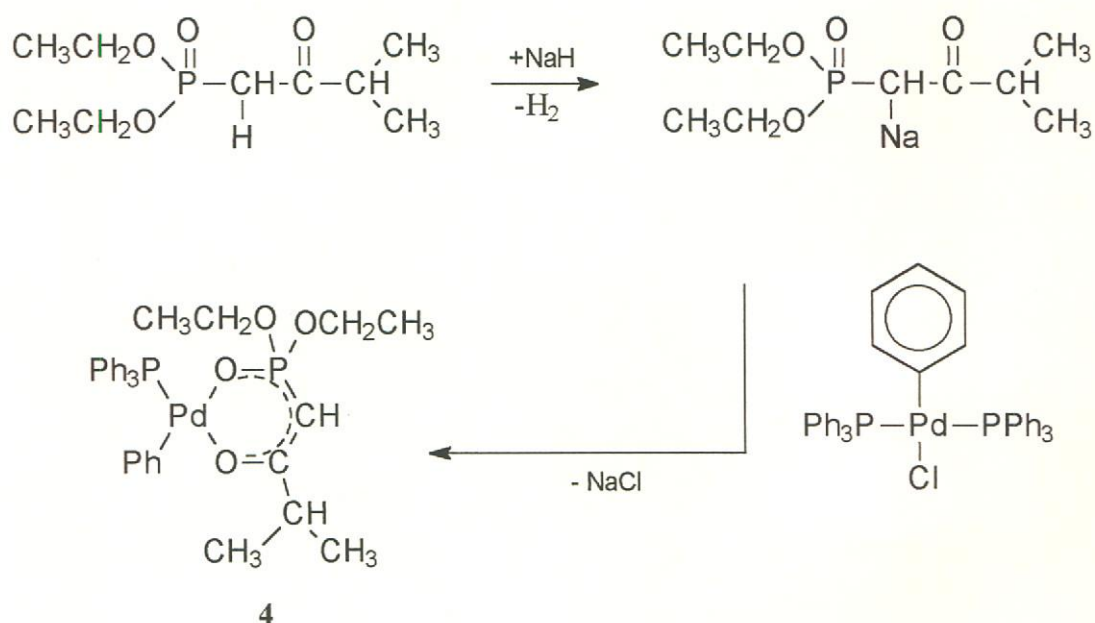
Scheme 2.6 : Formation of complex **4**.

II) Spectroscopic analysis of the free ligand 1-diethyl-3-methyl-phosphino-2-butanone, and complex 4.

The ^1H and ^{13}C NMR data for the free ligand 1-diethyl-3-methyl-phosphino-2-butanone, are summarised in Table 2.13 below, while the ^1H and ^{13}C NMR data for complex **4** are reported in Table 2.14. The NMR data for both the precursor to the free ligand and the prepared complex were measured in d^2-dichloromethane using TMS as an internal standard.

Complex **4** proved to be relatively unstable and decomposed in solution during NMR analysis despite the inert, anhydrous conditions under which the NMR solution was prepared. Due to the complex's unstable character, it proved impossible to obtain perfectly clean NMR spectrums. This instability resulted in the NMR spectra having several decomposition peaks in both the ^1H and ^{13}C spectrums that increased in intensity with time. In spite of this decomposition, it was possible to assign prominent peaks and to identify trends in the spectra that were also present in the NMR spectra for complexes **2** and **3**.

Free Ligand Precursor

$$CH_3CH_2O \underset{a\quad b}{\diagdown} \underset{f}{\overset{O}{\overset{\|}{P}}} - \underset{c}{CH_2} - \underset{g}{\overset{O}{\overset{\|}{C}}} - \underset{d}{\overset{e}{\underset{\underset{e}{CH_3}}{CH}}} \overset{e}{CH_3}$$

CH₃CH₂O ... P—CH₂-C—CH ... CH₃

Solvent : CD_2Cl_2 (TMS as internal standard)

Proton (δ-values)

a:	1.31 (t, 6H)
b:	4.13 (m, 4H)
c_i	3.15 (br s, 1H)
c_{ii}:	3.07 (br s, 1H)
d:	2.85 (m, 1H)
e:	1.03 (d, 6H)

Carbon 13 {¹H} (δ-values).

a:	18.2
b:	63.0
c_i:	39.8
c_{ii}:	41.5
d:	42.2
e:	16.7
f:	---
g;	207.0

Phosphorus 31 {¹H} (δ-values).ˣ

f:	20.71

Table 2.13 : NMR spectral data for the precursor to the free ligand 1-diethyl-3-methyl-phosphino-2-butanone.

The hydrogen atoms of the central $-CH_2$ group are diastereotopic and are thus visible in the proton NMR spectrum as two individual signals.

ˣ (δ-values are relative to H_3PO_4 which was used as an external standard.

Complex **4**.

$$CH_3CH_2O \quad OCH_2CH_3$$

(structure diagram of palladium complex with labels a, b, h, f, c, Pd, i, Ph, g, d, e, CH_3, CH_3, Ph_3P, O=P, O=C)

Solvent : CD_2Cl_2 (TMS as internal standard).

Proton (δ-values).

a:	1.21 (d, 6H)
b:	3.89 (m, 4H)
c:	obscured by peak b
d:	peak not observed
e:	1.02 (d, 6H)
f:	---
g:	---
h, i:	6.64 – 7.71 (m, 20H)

Carbon 13 {^{1}H} (δ-values).

a:	21.6
b:	60.6
c:	62.6
d:	40.6
e:	16.5
f:	---
g:	196.4
h, i:	123.4 – 137.1

Phosphorus 31 {^{1}H} (δ-values).[xi]

f:	27.66
h:	30.37

Table 2.14 : NMR spectral data for complex **4**.

[xi] (δ-values are relative to H_3PO_4 which was used as an external standard.

The spectral shifts, characteristics and trends evident in the NMR spectral data of the neutral precursor of the free ligand, 1-diethyl-3-methyl-phosphino-2-butanone, versus that of complex **4** in the Tables 2.13 and 2.14 above can be summarized as follows: -

➢ A slight upfield shift has occurred in the proton spectra for proton groups a and b. This upfield shift is mirrored in the carbon-13 spectra for carbon group b, but not for carbon group a where a small downfield shift occurred.

➢ Virtually no spectral shift changes were evident for proton or carbon groups e.

➢ A sharp upfield shift of 10.6ppm from the precursor to the free ligand to complex has occurred for the carbonyl group g in the carbon-13 spectrum. This sharp upfield shift of the carbonyl group was observed in the carbon-13 spectra of both complex **2** and **3**.

➢ There has also been a dramatic upfield shift of 18.44ppm from free ligand to complex in the phosphorus group of the original free ligand precursor. This upfield shift takes place parallel to the shift that has occurred for the carbonyl group g in the carbon-13 spectrum. This significant upfield shift in the phosphorus-31 spectrum of the -P=O group suggests that the coordination of this group to the palladium metal is stronger than the coordination of the comparable carbonyl groups to the palladium metal in complex **2**, **3** and **4**.

It is suspected that the steric hindrance imposed by the iso-propyl, phenyl and triphenylphosphine groups along with the thermal lability of the ethoxide groups are responsible for complex **4**'s instability despite the comparative strong bonding of the –P=O group to the palladium. Due to the instability of the complex, it proved impossible to obtain crystals suitable for X-ray crystal structure analysis despite several methods of crystallization that have been repeatedly employed.
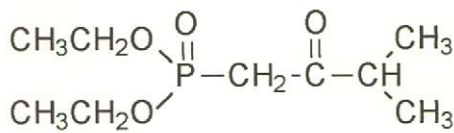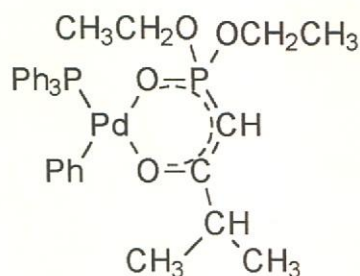
Attempts at purification of complex 4: -

It is not possible to use column chromatography (SiO$_2$) for the separation of our palladium complexes as they streak and decompose on these columns. Extraction attempts with various solvents proved fruitless, as impurities

appeared to be largely soluble in the same solvents as complex **4**. The only other possible purification technique available was crystallization. This technique however, also proved to be fruitless since all the crystallization attempts resulted in total decomposition. The crystallization techniques that were attempted included solvent concentration, cooling, solvent layering and solvent diffusion. The route of decomposition for complex **4** is not known and attempts to assign NMR peaks to possible decomposition products proved ambiguous and inconclusive. This was in-spite of attempts to monitor the decomposition process with proton and carbon-13 NMR spectroscopy over time.

III) *Infrared spectral data for the precursor to the free ligand , 1-diethyl-3-methyl-phosphino-2-butanone, and complex* **4**.

The infrared spectral data for the precursor to the free ligand, 1-diethyl-3-methyl-phosphino-2-butanone and complex **4** is summarized in Table 2.15 below. The infrared samples were measured in liquid cells using anhydrous dichloromethane with 16 scans at 4cm^{-1} resolution.

Free ligand	Complex
ν(C=O) : 1710.6 cm^{-1}	ν(C=O) : 1564.2 cm^{-1}
CO bond order = 2.	CO bond order = 1½.

Table 2.15 : Infrared spectral data for the precursor to the free ligand, 1-diethyl-3-methyl-phosphino-2-butanone and complex **4**.

For the ligand to be coordinated to the palladium metal center through a delocalized bond involving the P=O and –C=O groups, the double bond character of these groups would have to be reduced. This reduction in double bond character of the carbonyl group can easily be monitored by infrared spectroscopy. As can be seen in the infrared data in Table 2.15, there has been a reduction of 146.4cm^{-1} in the ν(C=O) stretching vibration. This supports the suggested bonding mode of the deprotonated ligand to the palladium centre.[53]

IV) *Mass Spectrum of complex 4.*

The mass spectrum for complex **4** is illustrated in Scheme 2.9 below. Relative intensities are given in parenthesis. The molecular ion of the target complex was observed with relatively high intensity at m/z 668.

The fragmentation pattern exhibited for complex **4** is similar to that of complexes **2** and **3** in that the fragmentation, once again, occurs primarily along two main routes.

➢ The first involves the initial loss of the palladium-phenyl-triphenylphosphine section of the complex followed by further fragmentation of the original phosphorus ligand.

➢ The second route of fragmentation involves the fragmentation of complex **4** as a whole with the initial loss of the ethoxy- and phenyl-groups. This second route is characterized by relatively low intensities as compared to the first.

Scheme 2.9 : Mass spectra for complex **4**.

(Relative intensities are given in parenthesis).

2.3 *Conclusion.*

In conclusion, the structure of complex **2** was solved by single crystal X-ray diffraction confirming that the target complex had been synthesised. The acac⁻ -ligand is bidentately coordinated by means of the oxygen atoms carrying a delocalized negative charge resulting from two resonance structures as illustrated in Figure 2.20 below. The NMR, infrared and MS spectroscopic data were analysed, peaks assigned and trends described. Similar data trends were observed in the NMR, infrared and MS spectra of complexes **3** and **4**. Changes that occurred in the NMR spectral data from the precursor of the free ligand to coordinated ligand of complexes **3** and **4** were also compared to those of the model system in complex **2**. Until conclusive crystal structure data become available, it is concluded on the basis of MS, IR- and NMR spectral data, that electron delocalization does take place through the – S=O and –P=O groups of complexes **3** and **4** in a similar fashion to that which occurs through the carbonyl groups of acac⁻ in complex **2**.
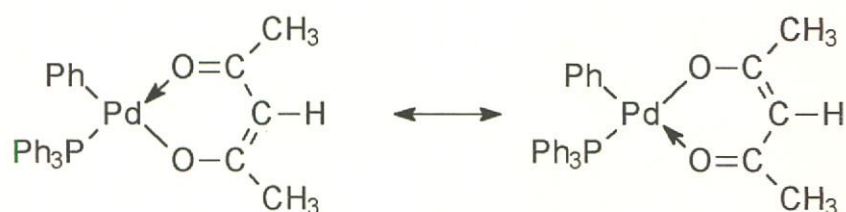
Figure 2.20 : Resonance structures of complex **2**.

2.4 Experimental.

2.4.1 Materials

Solvents:

High spectroscopic grade solvents were used during synthesis and were pre-dried over 4Å molecular sieves for at least 48 hours prior to use.

Diethyl ether, tetrahydrofuran (THF), benzene and hexane were distilled under nitrogen over sodium using benzophenone as indicator. Dichloromethane was distilled under nitrogen over calcium hydride. All alcohols were distilled under nitrogen from magnesium shavings. Alkyl lithium reagents were standardized by literature methods.[54]

All deuterated solvents, dichloromethane (d^2-CD_2Cl_2) and benzene (d^6-C_6D_6), that were used in the spectroscopic investigations for the complexes and ligands in this series were purchased from Aldrich. All deuterated NMR solvents were stored over 4Å molecular sieves under argon in order to keep them free from moisture and oxygen.

2.4.2 Physical Methods.

A. General:

Unless otherwise noted, all reactions and manipulations were carried out under an inert atmosphere with a positive gas flow of argon or nitrogen using standard vacuum line and Schlenk techniques. Solutions were stirred magnetically with Teflon coated stirrer bars. Room temperature refers to about 22-24°C. Clean Glassware was taken from a drying oven at ±120°C, assembled while hot and cooled under vacuum.

B. Instrumentation.

➢ *Melting points.*

Melting points were determined on a standard Büchi 535 apparatus and are uncorrected.

➤ *Mass Spectroscopy.*

MS spectra were obtained by either one of the following techniques and the applicable method is indicated: -

- FAB-MS (Fast Atom Bombardment Mass Spectra) spectra were recorded on a Micromass DG 70/70E double focussing mass spectrometer coupled to an Ion Tech fast atom bombardment unit using Xenon gas as bombardment atoms.

- Standard MS Spectra were obtained by means of the electron impact mass spectrometry technique on an AMD INTECTRA GmbH 604 double focusing mass spectrometer.

➤ *Infrared Spectroscopy.*

Infra red spectral data was obtained using either one of the following two apparatus and the respective apparatus used is indicated in the relevant section: -

- Perkin Elmer FT1600 series (4000 to 600cm^{-1}) with samples prepared as films between NaCl plates using hexachloro-1,3-butadiene or as standard liquid cell solutions in anhydrous dichloromethane with 16 scans at 4cm^{-1} resolution.

- Perkin Elmer 841 IR spectrometer (4000 to 600cm^{-1}) with samples prepared as films between NaCl plates using hexachloro-1,3-butadien.

➤ *Nuclear Magnetic Resonance Spectroscopy*

^{1}H, ^{13}C{^{1}H}, ^{31}P{^{1}H}, ^{125}Te{H} NMR data were recorded on a Varian VXR 300 FT spectrometers. NMR data are expressed as parts per million (ppm) downfield from an internal (TMS) or external standard used. (See Table 2.16 for NMR conditions used for the respective nuclei).

The respective nuclei were recorded under the following parameters: -

Nucleus	Frequency	Standard
^{1}H	300 MHz	$(CH_3)_4Si$ as internal standard
^{13}C $\{^{1}$H$\}$	75 MHz	$(CH_3)_4Si$ as internal standard
APT $\{^{1}$H$\}$	75 MHz	$(CH_3)_4Si$ as internal standard
^{31}P $\{^{1}$H$\}$	121 MHz	85% H_3PO_4 as external standard

Table 2.16 : NMR parameters.

➤ *X-ray crystallography.*

Crystals that were suitable for use in diffraction intensity measurements at room temperature were mounted on a glass fiber using fast adhesive. Crystal structure data collection and correction procedures were carried out on a Phillips PW1100 diffractometer by Dr. C. Esterhuysen Department of Chemistry, Stellenbosch University, Private Bag X1, 7602 Matieland South Africa. All systematic absences were consistent with the space groups assigned in each case. The positions of the hydrogens were calculated by assuming idealized geometries.

C. General preparation of starting materials and ligands:

Several of the starting materials and the ligands were synthesized directly according to literature and have been referenced accordingly. However, almost all of the literature methods used have been modified to varying degrees since they refer to similar, but somewhat different products. For this reason, detailed preparative methods are given for all the ligands and starting materials used in this chapter.

D. General Preparation of Complexes.

For the preparation of the palladium ß-dicarbonyl-type complexes described in this chapter, standard Schlenk techniques were employed throughout and all manipulations were carried out under an inert atmosphere. All general reagents, unless otherwise stated, were used as received.

The complexes described in this series, apart from complex **1**, were prepared according to the general reaction scheme below: -
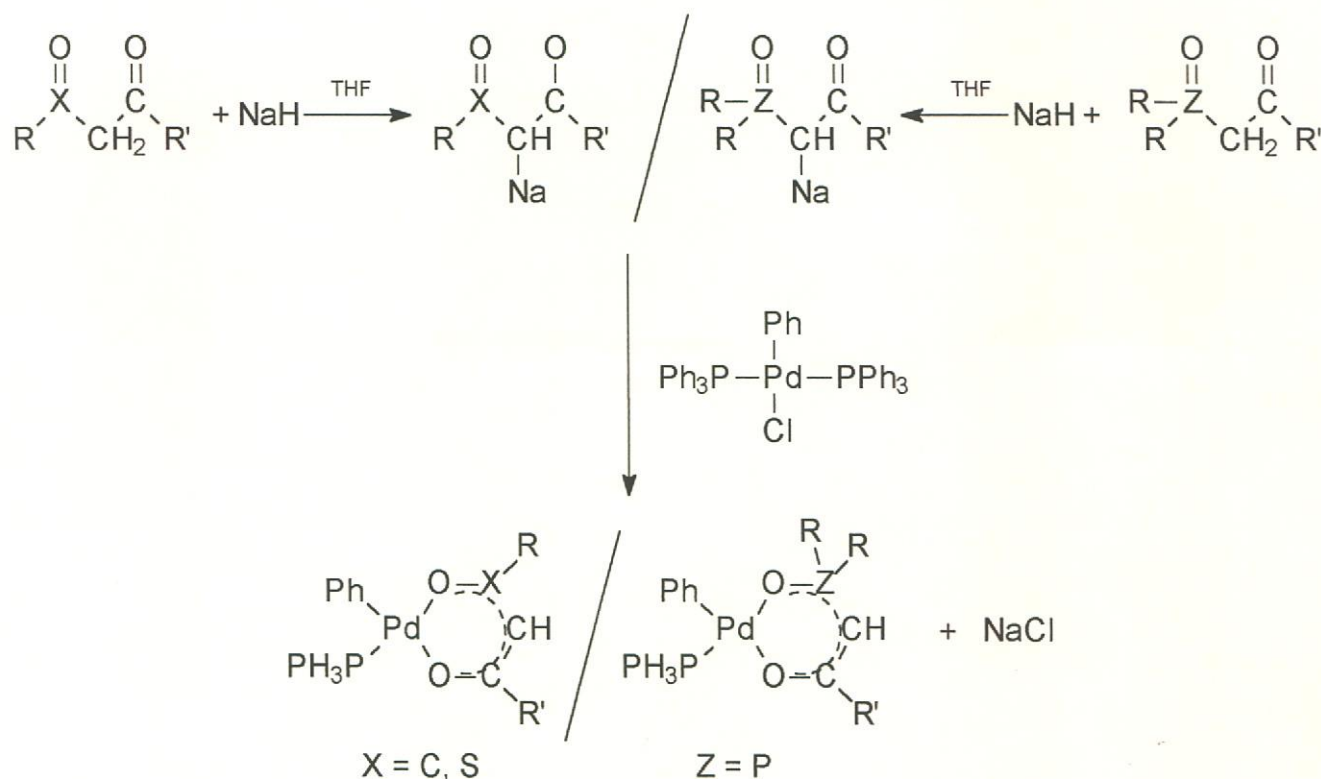
Scheme 2.10 : General preparation of complexes within this series

2.4.2.1 Preparation of complex 1, trans-[(Ph₃P)₂(Ph)PdCl]

Complex **1** was prepared according to Scheme 2.11 below.

Scheme 2.11 : Preparation of complex 1.

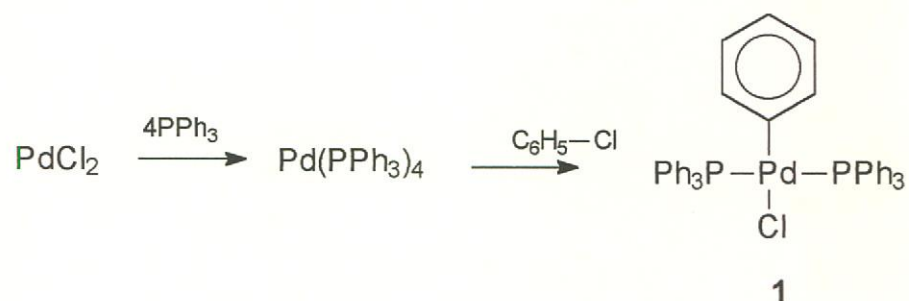3.00g (1.69×10^{-2}mol) of palladium chloride powder and 22.19g (8.46×10^{-2}mol) of triphenylphosphine was added to 180ml of DMSO. The solution was heated to ~150°C while stirring until all the reagents had fully dissolved.

3.30ml (0.11mol) of hydrazin hydrate was added dropwise with vigorous stirring of the solution. $N_{2(g)}$ was produced during the addition. After all the hydrazin hydrate had been added the solution was placed into an ice bath and allowed to cool. The reaction mixture was filtered and washed with ethanol (2 x 40 ml) followed by further washing with ether (2 x 50 ml).

Chlorobenzene (400 ml) was distilled under nitrogen and 20.30g of the $Pd(PPh_3)_4$ synthesised above was added. The solution was refluxed overnight.

Most of the remaining chlorobenzene was removed under reduced pressure leaving enough to aid the transfer of the remaining solid to a sinter glass filter. The product was washed with anhydrous ether until almost white.

The off-white product was re-dissolved in anhydrous dichloromethane and filtered. The solution was concentrated under reduced pressure and layered in a 1:1 ratio with anhydrous ether and left to crystallize at room temperature overnight.

The following day the solvent was removed from the crystals with a syringe and the remaining crystals were washed three trimes with anhydrous ether to remove any remaining impurities leaving a white, crystalline product.

Yield = 92.3% (based on mole palladium chloride used).

Molecular structure determination of complex **1**.

Suitable crystals for crystal structure determination were obtained by crystallization of complex **1** from a solution of dichloromethane layered in a 1:1 ratio with pentane.

A colourless crystal of *trans*-[(Ph$_3$P)$_2$(Ph)PdCl] was mounted on a glass fiber and transferred to a Phillips PW1100 diffractometer. All data were collected at room temperature with graphite monochromated Mo-K$_\alpha$ radiation with $2\theta = 23°$ and corrected for Lorentz and polarization effects. Absorption corrections were applied by the empirical method. Unique sets of data with intensities greater than two times the standard deviation were used to solve the structure by the heavy atom (Patterson) method. Refinements were done using least squares refinement. All non-hydrogen atoms were refined anisotropically. For structure solution and refinement the ShelX-97 software package was used[55]. Structure Figures were generated using Ortep-3.[56] Important crystallographic parameters and refinement details are given in Table 2.17 All other crystallographic information is available from Dr. C. Esterhuysen Department of Chemistry, Stellenbosch University, Private Bag X1, 7602 Matieland South Africa.

Table 2.17 : Crystal data, collection and refinement details for complex **1**.

Structure	
	Ph$_3$P—Pd—PPh$_3$
	Cl
Empirical formula	C$_{42}$H$_{35}$ClP$_2$Pd
Formula weight (g.mol^{-1})	743.49
Temperature	293(2) K
Radiation wavelength	Mo Kα, 0.71073 Å
Crystal system, space group	Orthorhomic, P bca
Unit cell dimensions	a = 11.8828(2) Å α = 90.00°
	b = 23.7783(2) Å β = 90.00°
	c = 25.5420(1) Å γ = 90.00°
Volume	7216.9(11) Å^3
Z, Calculated density	8, 1.369 Mg/m^3
Reflections for cell parameters	42
Absorption coefficient	0.705 mm^{-1}
Absorption correction method	none
F(000)	3040
Crystal size	0.40 x 0.30 x 0.18 mm^3
Crystal colour	Colourless
Diffractometer type	Philips PW1100
Scan type	ω-2θ
Theta range for collection	2.34 to 24.00°
Index ranges	-5 $\leq$ h 13
	-4 $\leq$ k $\leq$ 27
	-1 $\leq$ l $\leq$ 29
Reflections collected / unique	6086 / 5660 [R(int) = 0.0055]
Refinement method	Full-matrix least-squares on F^2
Data / restraints / parameters	5660 / 0 / 537
Reflections observed [I>2σ(I)]	4023
Goodness-of-fit on F^2	1.182
Final R indices [I>2σ(I)]	R1 = 0.043, wR2 = 0.109
R indices (all data)	R1 = 0.081, wR2 = 0.143
Weighting scheme (calculated)	W=1/[σ^2(F$_o$^{2})=(0.0761P)2]
	where P=(F$_o$^{2}+2F$_c$^{2})/3
Maximum shift/esd	0.014
Largest diff. peak and hole	0.981 and −0.547 e.Å^{-3}

2.4.2.2 Preparation of complex 2, [(Ph₃P)(Ph)Pd(acac)].

Complex **2** was prepared according to Scheme 2.12 below.

$$CH_3-\overset{\overset{O}{\|}}{C}-CH_2-\overset{\overset{O}{\|}}{C}-CH_3 \ + \ NaH \ \longrightarrow \ CH_3-\overset{\overset{O}{\|}}{C}-\underset{\underset{Na}{|}}{C}H-\overset{\overset{O}{\|}}{C}-CH_3 \ + \ H_2(g)$$

$$CH_3-\overset{\overset{O}{\|}}{C}-\underset{\underset{Na}{|}}{C}H-\overset{\overset{O}{\|}}{C}-CH_3 \ + \ \underset{\underset{Cl}{|}}{\overset{\overset{Ph}{|}}{Ph_3P-Pd-PPh_3}} \ \xrightarrow[-NaCl]{-PPh_3} \ \text{2}$$

Scheme 2.12 : Preparation of complex **2**.

NaH (1.06×10^{-2} mol) was added to acetylacetone (1.06×10^{-2} mol) dissolved in anhydrous ether (5.00cm^3) and stirred for 5 minutes. Gas evolution was evident. The solvent was removed under reduced pressure.[57] The resulting sodium salt was dissolved in 7ml of anhydrous tetrahydrofuran and 2ml of anhydrous ethanol. Total solution was ensured before proceeding.

The palladium starting complex **1** was dissolved in 7ml of anhydrous tetrahydrofuran and the dissolved Na(acac) ligand was added dropwise over several minutes with vigorous stirring. The resulting mixture was stirred for a further 48 hours at ambient temperature. The solution initially exhibited a milky white colour, that gradually turned milky yellow during the 48 hours stirring period.

An anhydrous magnesium sulphate packed sinter glass filter was prepared by repeatedly washing the magnesium sulphate with anhydrous ether and removing the remaining ether under reduced pressure. The resulting reaction suspension was filtered and evaporated to dryness under reduced pressure.

To obtain crystal suitable for crystal structure determination, the product was then re-dissolved in dichloromethane and layered with anhydrous pentane

(1:1.3) to afford very pale yellow, almost colourless, crystals. An NMR analysis of the crystals was done using both d^2-dichloromethane and d^6-benzene with TMS as an internal reference.

Yield :

Microcrystals obtained = 78% (based on mole complex **1** initially used)

Single crystals = 2% (based on mole complex **1** initially used)

Melting Point of complex **2**, [(Ph$_3$P)(Ph)Pd(acac)].

The melting point of the complex was measured on a standard Büchi 535 melting point apparatus and was uncorrected. The complex melts with total decomposition at 176.9 – 177.4°C.

Molecular structure determination of complex **2**.

Suitable crystals for crystal structure determination were obtained by crystallization of complex **2** from a solution of dichloromethane layered in a 1:1.3 ratio with anhydrous pentane.

A light yellow crystal of (Ph$_3$P)(Ph)Pd(acac) was mounted on a glass fiber and transferred to a Phillips PW1100 diffractometer. All data was collected at room temperature with graphite monochromated Mo-K$_\alpha$ radiation with $2\theta = 23°$ and corrected for Lorentz and polarization effects. Absorption corrections were applied by the empirical method. Unique sets of data with intensities greater than two times the standard deviation were used to solve the structure by the heavy atom (Patterson) method. Refinements were done using least squares refinement. All non-hydrogen atoms were refined anisotropically. For structure solution and refinement the ShelX-97 software package was used[58]. Structure Figures were generated using Ortep-3[59]. Selected crystallographic bond lengths and angles are listed in Tables 2.8 and 2.9 respectively. Crystal data and refinement details are listed in Table 2.18 below. All other crystallographic information is available from Dr. C. Esterhuysen Department of Chemistry, Stellenbosch University, Private Bag X1, 7602 Matieland South Africa.

**Table 2.18 :** Crystal data and structure refinement for complex **2**.

Structure	

Empirical formula	$C_{29}H_{27}O_2PPd$
Formula weight (g.mol^{-1})	544.88
Temperature	293(2) K
Radiation wavelength	Mo Kα, 0.71073 Å
Crystal system, space group	Monoclinic, P 2$_1$/c
Unit cell dimensions	a = 10.255(1) Å α = 90°
	b = 20.509(1) Å β = 111.13°
	c = 12.879(1) Å γ =90°
Volume	2526.6(3) Å^3
Z, Calculated density	4, 1.432 Mg/m^3
Reflections for cell parameters	50
Absorption coefficient	0.821 mm^{-1}
Absorption correction method	None
F(000)	1112
Crystal size	0.375 x 0.35 x 0.275 mm^3
Crystal colour	Light yellow
Diffractometer type	Philips PW1100
Scan type	ω-2θ
Theta range for collection	2.91 to 25.00°
Index ranges	-12 $\leq$ h 11
	0 $\leq$ k $\leq$ 24
	0 $\leq$ l $\leq$ 15
Reflections collected / unique	4436 / 4436 [R(int) = 0.0065]
Refinement method	Full-matrix least-squares on F^2
Data / restraints / parameters	4436 / 0 / 305
Reflections observed [I>2σ(I)]	3423
Goodness-of-fit on F^2	1.178
Final R indices [I>2σ(I)]	R1 = 0.035, wR2 = 0.073
R indices (all data)	R1 = 0.064, wR2 = 0.089
Weighting scheme (calculated)	W=1/[σ^2(Fo^2)=(0.0261P)2]
	where P=(Fo^2+2Fc^2)/3
Maximum shift/esd	0.007
Largest diff. peak and hole	0.377 and −0.344 e.Å^{-3}

2.4.2.3 <u>Synthesis of *complex 3, [(Ph₃P)(Ph)Pd(CH₃S(O)CHC(O)Ph)].*</u>

I) <u>Synthesis of ω-(methylsufinyl)acetophone, CH₃S(O)CH₂C(O)Ph.</u>

a) <u>Synthesis of Ethyl Benzoate.</u>[60]

The preparation of ethyl benzoate is illustrated in Scheme 2.12.

$$Ph-\overset{\overset{\displaystyle O}{\|}}{C}-OH \; + \; CH_3CH_2\text{-}OH \longrightarrow Ph-\overset{\overset{\displaystyle O}{\|}}{C}-OCH_2CH_3$$
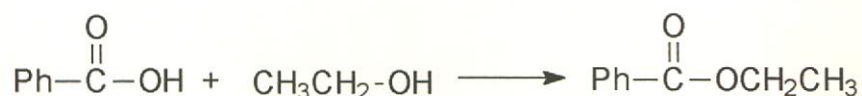
Scheme 2.12 : Synthesis of ethyl benzoate.

A mixture of 30.0g (0.246 mol) of benzoic acid, 80.0g (101ml, 2.50 mol) of absolute methanol and 5.00g (2.70ml) of concentrated sulphuric acid was placed in a 500ml round bottomed flask fitted with a reflux condenser. The mixture was gently refluxed for 5 hours. The reaction mixture was refluxed for a longer period of time to that reported in the literature to increase the overall yield of the synthesis illustrated in Scheme 2.12 above. The excess ethanol was distilled off with the aid of a rotary evaporator. The residue was transferred into a separatory funnel and 10–15ml of carbon tetrachloride was added.
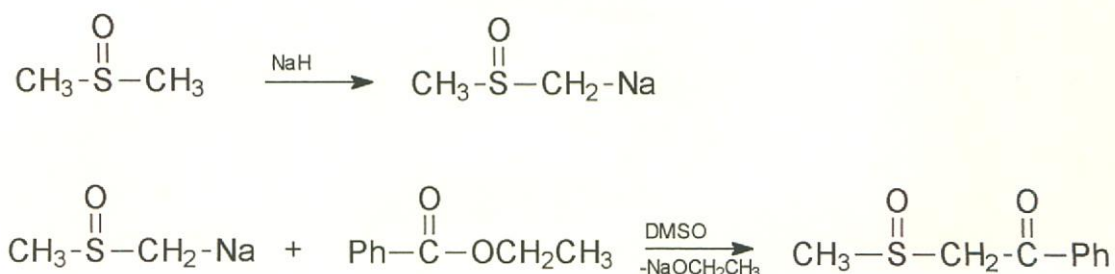
The carbon tetrachloride was added to aid the separation since there is only a comparatively slight difference in the densities of the ester and water. The ester separated sharply and was collected. A concentrated solution of sodium hydrogen carbonate was added to destroy the remaining free acid. The solution was washed with water and dried over anhydrous magnesium sulphate and filtered.

The volatile solvents were removed under reduced pressure and the remaining solution was distilled with the ethyl benzoate fraction being collected at 80-83°C. (6mm Hg).

Yield ethyl benzoate = 96%.

(Yield based on mole benzoic acid used.)

The synthesis of ω-(methylsufinyl)acetophone was completed according to Scheme 2.13 below[61].

$$CH_3-\overset{\overset{\displaystyle O}{\|}}{S}-CH_3 \xrightarrow{\text{NaH}} CH_3-\overset{\overset{\displaystyle O}{\|}}{S}-CH_2-Na$$

$$CH_3-\overset{\overset{\displaystyle O}{\|}}{S}-CH_2-Na \quad + \quad Ph-\overset{\overset{\displaystyle O}{\|}}{C}-OCH_2CH_3 \xrightarrow[\text{-NaOCH}_2\text{CH}_3]{\text{DMSO}} CH_3-\overset{\overset{\displaystyle O}{\|}}{S}-CH_2-\overset{\overset{\displaystyle O}{\|}}{C}-Ph$$

Scheme 2.13 : Preparation of ω-(methylsufinyl)acetophone

The synthesis illustrated above requires anhydrous DMSO in order to allow the formation of the sodium salt of the dimethyl sulphoxide from the sodium hydride.

The DMSO solution was placed over calcium hydride and gently refluxed for 1½ hours followed by distillation onto 4A° molecular sieves under reduced pressure.

b) Synthesis of methylsulfinyl carbanion.

2.00g (8.33×10^{-2} mol) of sodium hydride (±60% mineral oil suspension) was placed in a three-necked round bottomed flask under a nitrogen atmosphere. 10.0 ml of light petroleum ether was added and the resulting suspension was stirred vigorously for several minutes. The sodium hydride was allowed to settle and the remaining solution was removed via syringe. This process was repeated several times to remove the mineral oil. The resulting sodium hydride paste was dried under reduced pressure.

The flask was immediately fitted with a reflux condenser and a rubber septum through which 25-30ml of freshly distilled DMSO was introduced via hypodermic syringe. The mixture was heated to 70-75°C with vigorous stirring until the evolution of H_2 ceases (±45 minutes). Longer reaction time results in

extensive decomposition of the desired product. Extensive decomposition also appears to occur at temperatures higher than 75°C.

The product remaining is a somewhat cloudy pale yellow-grey solution of the sodium salt. The solution was assayed by titration with formanilide using triphenylmethane as indicator.

An equal volume (25ml) of anhydrous THF was added to the solution of the sodium methylsulfinyl carbonyl as prepared above. The resulting mixture was cooled in a NaCl-ice bath. The previously prepared ethyl benzoate (0.5 mole equiv. based on 1 mole equiv. of carbanion) was added to the reaction mixture over a period of several minutes. The ice bath was removed and the reaction mixture was allowed to reach room temperature and stirred for a further 30 minutes.

The reaction mixture was poured into three times its volume of water, acidified with aqueous hydrochloric acid to a pH of 3-4 and extracted three times with chloroform. The combined chloroform extracts were repeatedly washed with water and dried over anhydrous sodium sulphate. The solution was filtered and evaporated to dryness to yield the crude product as a pale yellow crystalline solid. The crude product was then washed with cold ether and filtered to give the pure product.

Yield : 73.2%.

(Yield based on mole methylsulfinyl carbanion initially used).

II) _Synthesis of complex 3. [(Ph₃P)(Ph)Pd(CH₃S(O)CHC(O)Ph)]._

Complex **3** was prepared according Scheme 2.14 below.
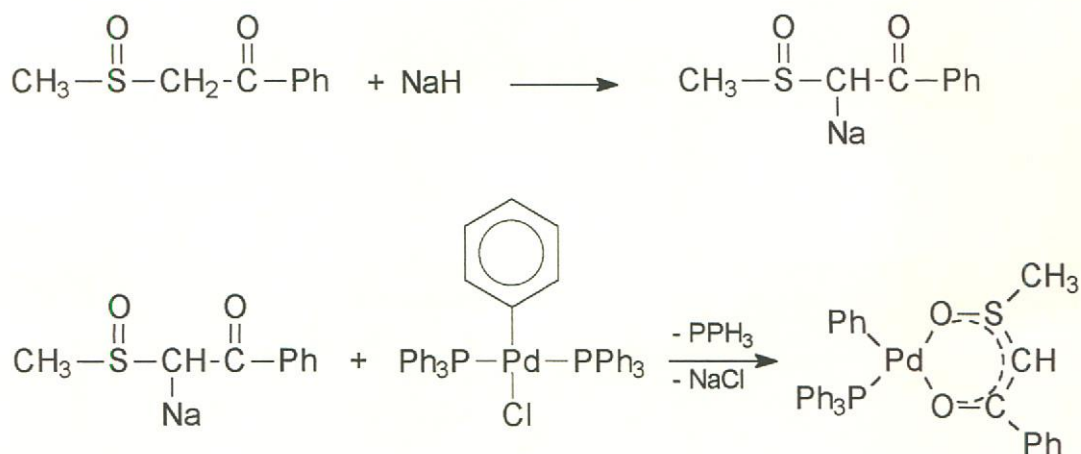
Scheme 2.14 : Preparation of complex **3**.

0.088g (4.8×10^{-4}mol) of ω-(methylsufinyl)acetophone was dissolved in 7.0ml of anhydrous THF. 0.012g (4.8×10^{-4}mol) NaH was slowly added with vigorous stirring and the reaction mixture was stirred for a further 30 minutes.

0.20g (2.7×10^{-4}mol) of [(PPh₃)₂PhPdCl] was dissolved in 7.0ml of anhydrous THF and the ω-(methylsufinyl)acetophone solution was added dropwise over several minutes with vigorous stirring. The solution was left to stir for 36 hours.

After the addition of ω-(methylsufinyl)acetoenone, the reaction solution initially had a milky white colour which gradually became an intense milky yellow as the reaction proceeded during the 36 hours of stirring. The reaction mixture was filtered through an anhydrous celite® packed sinter glass filter and evaporated to dryness under reduced pressure to yield a yellow powder.

Yield = 73%

(yield based on mole ω-(methylsufinyl)acetoenone initially used.)

2.4.2.4 Synthesis of complex 4.

[(Ph₃P)(Ph)Pd(CH₃CH₂O)₂P(O)CHC(O)CH(CH₃)₂)].
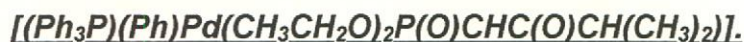
I) Synthesis of Diethyl 1,2-Epoxyalkanephosphonate.

a) Synthesis of Diethyl(Chloromethyl)phosphonate.[62]

The synthesis of diethyl(chloromethyl)phosphonate was carried out according to Scheme 2.15 below.

$$Cl_2P(O)-CH_2-Cl \xrightarrow[-2HCl]{2EtOH} (CH_3CH_2O)_2P(O)-CH_2-Cl$$
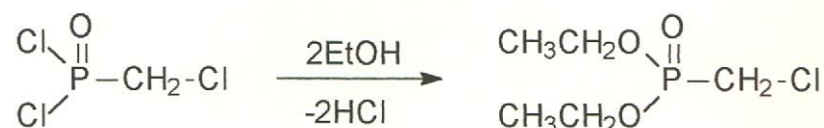
Scheme 2.15 : Synthesis of diethyl(chloromethyl)phosphonate

Chloromethylphosphonate dichloride was slowly added with stirring to absolute ethanol kept at 5°C with a NaCl-ice bath. The mixture was left to stirr overnight (24 hours) and the excess ethanol and HCl were removed at 50°C under reduced pressure. The residue was neutralised with sodium carbonate and extracted with ether. The ether was removed under reduced pressure. Diethyl(chloromethyl)phosphonate was distilled off from the remaining mixture.

Yield = 79% (yield based on mol chloromethylphosphonate initially used).

b.p. 75 – 79°C at 0.75 mmHg. Lit. 86 - 87°C at 2.5 mmHg.

b) Synthesis of 1-diethyl-3-methyl-phosphino-2-butanone. [63]

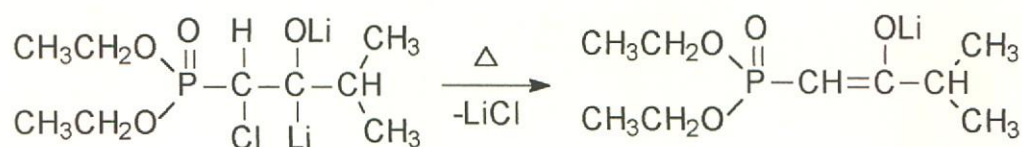The synthesis of 1-diethyl-3-methyl-phosphino-2-butanone was carried out according to Scheme 2.16 below.
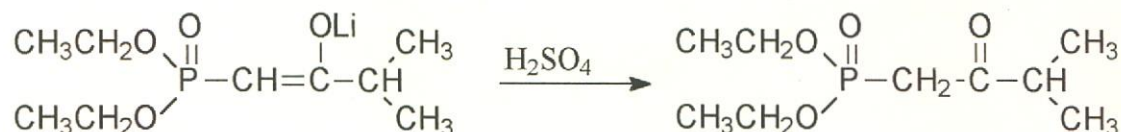
i)

$$(CH_3CH_2O)_2P(O)-CH_2-Cl + BuLi \xrightarrow{-BuH} (CH_3CH_2O)_2P(O)-CH(Li)-Cl$$

ii)

$$CH_3CH_2O \quad \overset{O}{\underset{\parallel}{P}} \overset{Li}{\underset{|}{-CH}} + \underset{CH_3}{\overset{CH_3}{}}CH-\overset{O}{\overset{\parallel}{C}}-H \longrightarrow CH_3CH_2O \quad \overset{O}{\underset{\parallel}{P}} \overset{H}{\underset{|}{-C}} \overset{OLi}{\underset{|}{-C}} \overset{CH_3}{-CH}$$

iii)

$$CH_3CH_2O \quad \overset{O}{\underset{\parallel}{P}} \overset{H}{\underset{|}{-C}} \overset{OLi}{\underset{|}{-C}} \overset{CH_3}{-CH} + LDA \longrightarrow CH_3CH_2O \quad \overset{O}{\underset{\parallel}{P}} \overset{H}{\underset{|}{-C}} \overset{OLi}{\underset{|}{-C}} \overset{CH_3}{-CH}$$

iv)

$$CH_3CH_2O \quad \overset{O}{\underset{\parallel}{P}} \overset{H}{\underset{|}{-C}} \overset{OLi}{\underset{|}{-C}} \overset{CH_3}{-CH} \xrightarrow[-LiCl]{\Delta} CH_3CH_2O \quad \overset{O}{\underset{\parallel}{P}} \overset{OLi}{-CH=C} \overset{CH_3}{-CH}$$

v)

$$CH_3CH_2O \quad \overset{O}{\underset{\parallel}{P}} \overset{OLi}{-CH=C} \overset{CH_3}{-CH} \xrightarrow{H_2SO_4} CH_3CH_2O \quad \overset{O}{\underset{\parallel}{P}} \overset{O}{-CH_2-C} \overset{CH_3}{-CH}$$
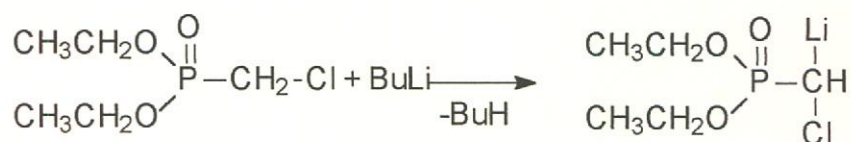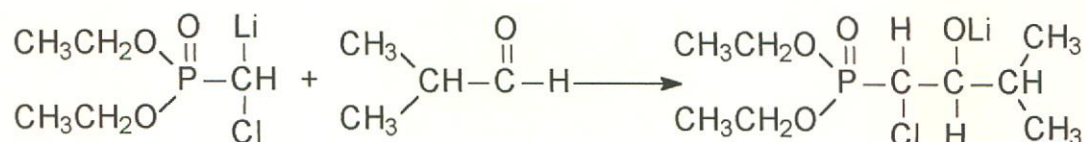
Scheme 2.16 : Synthesis of 1-diethyl-3-methyl-phosphino-2-butanone.

A 1.45 molar solution of n-butyllithium in hexane (0.054 mol + 5%) was placed in a three necked flask equipped with a stirrer, an addition funnel, a low temperature thermometer and a nitrogen inlet tube. An equal volume of THF (±40 ml) was added to the cooled solution. Subsequently, diethyl chloromethanephosphonate (10g, 0.054mol) in THF (10ml) was added dropwise at – 70°C. After ~10 minutes the clear reaction mixture becomes turbid and the isopropyl aldehyde (0.054mol) in THF (10ml) was added while keeping the solution at –70°C. The mixtures slowly became clear. After 30 minutes, previously prepared lithium diisopropylamide (0.054Mol + 5%[xii]) was added at –70°C. (The lithium diisopropylamide was previously prepared by the addition of n-butyllithium to diisopropylamine dissolved in THF at 0°C). Stirring

[xii] The slight excess of LDA (5%), was to compensate for losses due to traces of moisture and oxygen.

was continued for a further 3 hours at –70°C after which the mixture was slowly allowed to warm to room temperature overnight.

At room temperature the mixture was slowly hydrolyzed with 2N H_2SO_4 so that it became neutral and the aqueous solution was further extracted with dichloromethane (3 x 50ml). The combined organic extracts were dried over magnesium sulphate, filtered and the solvent removed under reduced pressure. The pure product was isolated by distillation.

Preparation of lithium diisopropylamide (LDA).
The preparation of LDA was carried out according to Scheme 2.17 below:[64, 65]

Scheme 2.17 : Preparation of lithium diisopropylamide.

4.9mmol butyllithium (1.6M solution) was added to 1.2ml (8.6mmol) of diisopropylamine in 4ml hexane at –20°C. LDA started to precipitate out after a few minutes. After having been warmed to room temperature, the mixture was stirred for a further 15 minutes. The excess diisopropylamine and solvent was removed under reduced pressure. The prepared lithium diisopropylamide was used within a few minutes of synthesis.

II) *Synthesis of complex 4,*

[(PPh₃)(Ph)Pd{(CH₃CH₂O)₂P(O)CHC(O)CH(CH₃)₂}].

The synthesis of complex **4** was carried out according to Scheme 2.18 below.
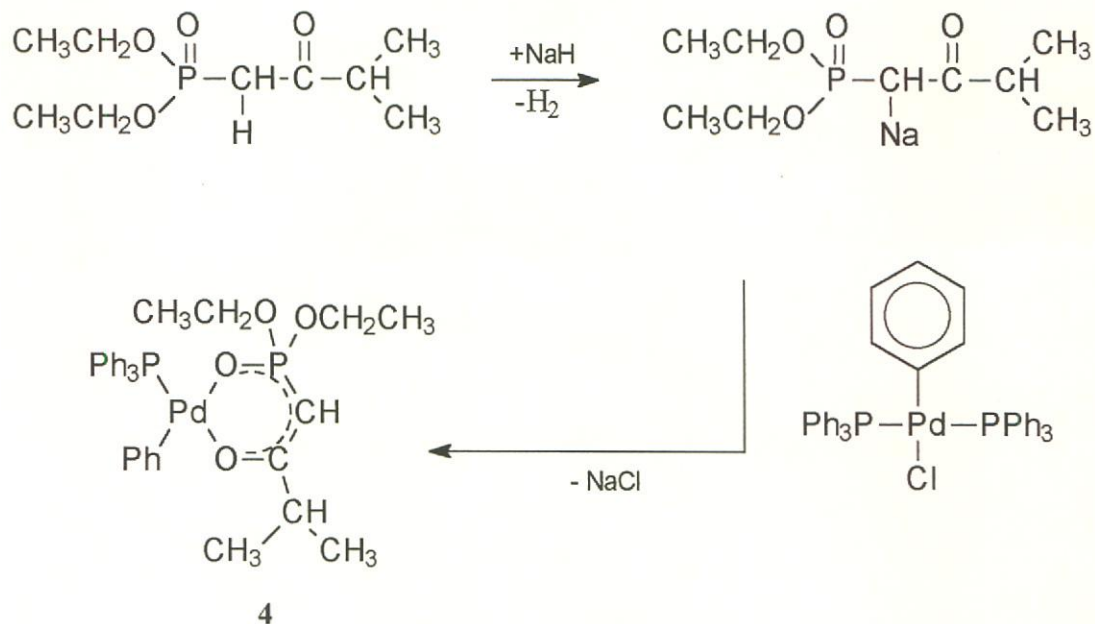
Scheme 2.18 : Synthesis of complex **4**.

4.84×10^{-4} mole (0.108g) of $[(CH_3CH_2O)_2P(O)CH_2C(O)CH(CH_3)_2]$ was dissolved in 40.0ml of anhydrous diethyl ether. A NaH suspension in mineral oil was repeatedly washed with anhydrous pentane and reduced to dryness under reduced pressure to remove the mineral oil. 0.013g (5.3×10^{-4} mole) of the washed NaH was slowly added to the diethyl ether solution. Upon addition of the NaH the evolution of gas was observed. Stirring was continued for 1 hour.

The reaction mixture was reduced to dryness under reduced pressure and re-dissolved in 7ml of anhydrous THF. 0.200g (2.69×10^{-4} mole) of complex **1**, $[(Ph_3P)_2Pd(Ph)(Cl)]$, was dissolved in 7.00ml of anhydrous THF. The THF solution of $Na^+[(CH_3CH_2O)_2P(O)CH_2C(O)CH(CH_3)_2]^-$ that was previously prepared was added dropwise with vigorous stirring over several minutes. The solution was stirred for a further 48 hours. During this reaction time the reaction mixture took on a strong yellow-orange colour and a fine white

precipitate had become evident. The reaction mixture was filtered through an anhydrous celite® packed filter and reduced to dryness to yield a yellow-orange solid.

Yield = 65%

(Yield based on mole [$(CH_3CH_2O)_2P(O)CH_2C(O)CH(CH_3)_2$] initially used).

Melting point of complex **4**.

The melting point was recorded on a standard Büchi 535 apparatus and is uncorrected.

Mp 127.3°-128.6°C (dec)

2.5 *Cited References*

[1] G.T. Morgan, H.W. Moss, *J. Chem. Soc.*, 105, **1914**, 189.

[2] J. P. Fackler Jr., *Prog. Inorg. Chem.*,7, **1966**, 361.

[3] (a) R.C. Mehrotra, R. Bohra, D.P. Gaur, *Metal ß-Diketonates and Allied Derivatives,* Academic Press, New York **1978**.

(b) K.C. Joshi, V.N. Pathak, *Coord. Chem. Rev.*, 22, **1977**, 37.

[4] D. W. Thompson, *J of Chem. Educ.*, 48, **1971**, 79.

[5] D.W. Thompson,*J. of Chem. Educ.*, 48, **1971**, 79.

[6] D.H. Dewer, J.E. Fergusson, P.R. Hentschel, C.J. Wilkins, P.P. Williams, *J. Chem. Soc.*, **1964**, 688.

[7] D.H. Dewer, J.E. Fergusson, P.R. Hentschel, C.J. Wilkins, P.P. Williams, *J. Chem. Soc.*, **1964**, 688.

[8] J.P. Fackler, Jr., *Prog. Inorg. Chem.*, 7, **1966**, 361.

[9] K. Flatau, H. Junge, M. Kuhr, H. Musso, *Angew. Chem.*, 83, **1971**, 239.

[10] *J. Chem. Educ.*, 48, **1971**, 79.

[11] S. Komiya, J. K. Kochi, *J. Am. Chem. Soc.*, 99, **1977**, 3695.

[12] S. Komiya, J. K. Kochi, *J. Am. Chem. Soc.*, 99, **1977**, 3695.

[13] R.S. Nyholm, *Proc. Chem. Soc.*, **1961**, 273.

P.J. Davidson, M.F. Lappert, P. Pearce, *Chem. Rev.*, 76, **1976**, 219.

[14] T.W.G. Solomons, '*Solomon's Organic Chemistry*', 5th Ed., John Wiley & sons, New York, p. 726.

[15] 3D Search and Research using the Cambridge Structural Database.

F.H. Allen, O. Kennard, *Chemical Design Automation News*, **1993**, 8, 31.

IsoStar: A Library Of Information about Nonbonded Interaction, I.J. Bruno, J.C. Cole, J.P.M. Lommerse, R.S. Rowland, R. Taylor, M. Verdonk, *Journal of Computer-Aided Molecular Design*, **1997**, 11-6, 525.

[16] Pak-Hing Leung, G.H. Quek, Huifang Lang, A.M. Liu, K.F. Mok, A.J.P. WhiteD.J. Williams, N.H. Rees, W. McFarlane, *J. Chem. Soc. Dalton Trans.*, **1998**, 1639.

[17] J. Lorberth, S. Wocadlo, W. Massa, *J. Organomet. Chem.*, 480, **1994**, 163.

[18] 3D Search and Research using the Caimbridge Structural Database.

F.H. Allen, O. Kennard, *Chemical Design Automation News*, **1993**, 8, 31.

IsoStar: A Library Of Information about Nonbonded Interaction, I.J. Bruno, J.C. Cole, J.P.M. Lommerse, R.S. Rowland, R. Taylor, M. Verdonk, *Journal of Computer-Aided Molecular Design*, **1997**, 11-6, 525.

[19] E.V. Grigorev, N.S. Yashina, A.A. Prischenko, M.V. Livantsov, V.S. Petrosyan, L. Pelleritot, M.J. Schafer, *Appl. Organomet. Chem.*, 7, **1993**, 353.

[20] J.E. Barclay, G.J. Leigh, A.Houlton, J. Silver, *J. Chem. Soc. Dalton Trans.*, **1988**, 2865.

[21] M. Röper, '*Industrial Applications of Homogeneous Catalysis*', ed. M. Moritreux and M. Petit, D. Reidel, Dordrecht, **1988**, 1.

[22] a) G.K. Anderson, R.J. Cross, *Acc. Chem. Res.,* 17, **1984**, 67.

b) J.J. Alexander, *The Chemistry of the Metal Carbon Bond,* ed. F.R. Hartley, Wiley New York, **1985**, vol. 2, ch. 5.

c) P.E. Garron, R.F. Heck, *J. Am. Chem. Soc.,* 98, **1976**, 4115.

[23] A.M. Bertus, P. Wijkens, J. Boersma, A.L. Spek, G. van Koten, *Rec. Trav. Chim. Pays-Bas,* 110, **1991**, 133.

[24] V. De Felice, V.G. Albano, C. Castellari, M.E. Cucciolito, A. De Renzi, *J. Organomet. Chem.*, 403, **1991**, 269.

[25] T. Saruyama, T. Yamamoto, A. Yamamoto, *Bull. Chem. Soc. Jpn.*, 49, **1976**, 546.

[26] G.K. Anderson, G.J. Lumetta, *Organometallics*, 4, **1985**, 1542.

[27] G.K. Anderson, G.L. Lumetta, *Organometallics*, 4, **1984**, 1542.

[28] A.M. Bertus, P. Wilkens, J. Boersma, A.L. Spek, G. van Koten, *Rec. Trav. Chim. Pays-Bas*, 110, **1991**, 133.

[29] D.P.C. Dekker, C.J. Elsevier, K. Vrieze. P.W.N.M. van Leeuwen, Organometallics, 1992, 11, 1598.

[30] 3D Search and Research using the Cambridge Structural Database. F.H. Allen, O. Kennard, *Chemical Design Automation News*, **1993**, 8, 31 –37. IsoStar: A Library Of Information about Nonbonded Interaction, I.J. Bruno, J.C. Cole, J.P.M. Lommerse, R.S. Rowland, R. Taylor, M. Verdonk, *Journal of Computer-Aided Molecular Design*, **1997**, 11-6, 525-537.

[31] W.A. Herrman, C. Broner, . Priermeier, K. Öfele, *J. Organomet. Chem.*, 481, **1994**, 97.

[32] W.A. Herrman, C. Broner, Priermeier, K. Öfele, *J. Organomet. Chem.*, 481, **1994**, 97.

[33] G.M. Sheldrick, SHELX-97, Program for the determination and refinement of crystal structures, Institut für Anorganische Chemie, Universität Göttingen, Tammanstrasse 4, D-3400, Göttingen, Germany, **1997**.

[34] L.J. Farrugia, ORTEP-3 for Windows, *J. Appl. Crystallogr.*, **1997**, 565.

[35] W.A. Herrmann, C. Broner, Priermeier, K. Öfele, *J. Organomet. Chem.*, 481, **1994**, 97.

[36] C. Thompson, *A structural study of palladium complexes containing hemilable ligands*, Thesis Philosophiae Doctor, Rand Afrikaans University, **2000**, 59.

[37] S. Okeya, S. Ooi, K. Matsumoto, T. Nakamura, S. Kawaguchi, *Bull. Chem. Soc. Jpn*, 54, **1981**, 1085.

[38] S. Okeya, S 'ichiro Ooi, K. Matsumoto, Y Nakamura, S, Kawaguchi, *Bull. Chem. Soc. Jpn*, 54, **1981**, 1085.

[39] B.E. Mann, R. Pietropaola, B. Shaw, *J. Chem. Soc. - Dalton Trans.*, **1973**, 2390.

[40] P. J. McCarthy, A. E. Martell, *Inorg. Chem.*, 6, **1967**, 781.

[41] S. Okeya, S 'ichiro Ooi, K. Matsumoto, Y Nakamura, S, Kawaguchi, *Bull. Chem. Soc. Jpn*, 54, **1981**, 1085.

[42] S. Komiya, J.K. Kochi, *J. Am. Chem. Soc.*, 99, **1977**, 3695.

[43] S. Okeya, S Ooi, K. Matsumoto, Y. Nakamura, S. Kawaguchi, *Bull. Chem. Soc. Jpn.*, 54, **1981**, 1085.

[44] J.P. Collman, *Angew. Chem.*, 4, **1965**, 132.

[45] J.P. Collman, *Angew. Chem.*, 4, **1965**, 132.

[46] Pretch, Clerc, Serbl, Simon, *Tables of Spectral Data for Structure Determination of Organic Compounds 13C-NMR 1H-NMR IR MS UV/VIS*, Chemical Laboratory Practice 2nd Ed., **1983**, 132.

[47] J.E. Huheey, *Inorganic Chemistry*, 2nd ed., Harper International Edition, **1978**, 182.

[48] G.M. Sheldrick, SHELX-97 Program for the determination and refinement of crystal structures, Institut für Anorganische Chemie, Universität Göttingen, Tammanstrasse 4, D-3400, Göttingen, Germany, **1997**.

[49] L.J. Farrugia, ORTEP-3 for Windows, *Journal of Applied Crystallography*, **1997**, 565.

[50] J. Cavell, Hong Jin, Brian W. Skelton, Allan H. White, *J. Chem. Soc. Dalton Trans.*, **1993**, 1973.

[51] D. W. Thompson, *J. Chem. Educ.*, 48, **1971**, 79.

[52] P. Savignac, P. Coutrot, *Synth. Commun.*, **1978**, 682.

[53] J.E. Huheey, *Inorganic Chemistry*, 2nd ed., Harper International Edition, **1978**, 182.

[54] M.F. Lipton, C.M. Soreson, A.C. Sadler, R. H Shapiro, *J. Organomet. Chem., 1980, 186, 155.*

[55] G.M. Sheldrick, SHELX-97 Program for the determination and refinement of crystal structures, Institut für Anorganische Chemie, Universität Göttingen, Tammanstrasse 4, D-3400, Göttingen, Germany, **1997**.

[56] L.J. Farrugia, ORTEP-3 for Windows, *Journal of Applied Crystallography*, **1997**, 565.

[57] P.K. Baker, A.I. Clark, M.G.B. Drew, M.C.Durrant, R.L. Richards; *J. Organomet. Chem.*, 549, **1997,** 193.

[58] G.M. Sheldrick, SHELX-97 Program for the determination and refinement of crystal structures, Institute für Anorganische Chemie, Universität Göttingen, Tammanstrasse 4, D-3400, Göttingen, Germany, **1997**.

[59] L.J. Farrugia, ORTEP-3 for Windows, *J. Appl. Crystallogr.*, **1997**, 565.

[60] *Vogel's Textbook of Practical Organic Chemistry*, 1077.

[61] E. J. Corey, M Chaykovsky, *J. Am. Chem. Soc.*, 87, **1965**, 1345.

[62] *J. Chem. Soc. Perkin Trans. II*, **1972**, 304 – 311.

[63] P. Savignac, P. Coutrot, *Synth. Commun.*, **1978**, 682

[64] P. Savignac, P. Coutrot, *Synth. Commun.*, **1978**, 684.

[65] W. Bauer, D. Seebach, *Helv. Chim. Acta*, 67, **1984**, 1986.

Neutral η^3-hetero Allyl Palladium(II) Complexes.

This chapter is concerned with the preparation and spectroscopic studies of several palladium(II) complexes with η^3-coordinated ligands. The goal of this study was to synthesize these complexes and characterize them by means of melting point, IR spectroscopy, MS, NMR spectroscopy and X-ray crystal structure characterization (where possible).

3.1.1 Introduction

$[(Ph)_2PS_2]^-$, has been used for many years as a ligand in its capacity to facilitate metal complex formation in both organic and inorganic media. Several reviews describe the use of $[(Ph)_2PS_2]^-$ and its derivatives as ligands in organometallic complexes[1, 2].

The Chemistry of phosphorus sulfides:

The study of compounds formed from phosphorus and sulphur in general is very old. The first report of phosphorus sulphides is estimated to have been in about 1740 when A.S. Marggraff described a fused mixture of phosphorus and sulphur.[3] Since then, chemical formulae have been erroneously formulated for many phosphorus-sulphur compounds ranging from P_4S to P_2S_{12}.[4] This continued until A. Stock showed that only three compounds can be obtained from the thermal decomposition of phosphorus and sulphur, namely P_4S_3, P_4S_7 and P_4S_{10}.

At present, all efforts in the synthesizing of novel phosphorus sulphur products can be divided into three categories; -

i)   thermal reactions

ii)   abstraction of sulphur with phosphines

iii)   construction of P-S bonds with sulphur precursors[5].

Due to their potential use in electrochemistry[6], microelectronics,[7] catalysis,[8] ion exchange,[9] sensors,[10] photochemistry[11] etc., research phosphonate chemistry in these circles has flourished. In contrast, research concerning phosphor-1,1-dithio type ligands has been disappointing little.

Four coordinate phosphorus(V) is present in most life-sustaining systems and is also present in many toxic man-made nerve gasses. Despite this almost omnipresence, the study of the dithiophosphinate $[S_2PR_2]^-$ systems as complexing agents for transition metals, with particular reference to palladium, isn't as plentiful as one would expect. Only eight structures are listed on the Cambridge Crystallographic Database where dithiophosphinate has been used as ligand with coordination through both the sulphurs to the central palladium atom.[12] Figure A similar complex was prepared by Narayan et al. in 1998. This structure contained a methyl group in place of the phenyl group of complex **6**. Crystals were not obtained by Narayan et al. and the crystal structure was not solved, only proposed.[13]

There are three reasons for the relative slow development of dithiophosphinate-type ligands as complexing agents with transition metals: -

i)   commercial unavailability despite being the synthesis of these compounds being relatively simple

ii)   inherent reactivity (especially towards hydrolysis)

iii)   relative high toxicity levels.

Deprotonated diphenyl-dithiophosphinic acid $[S_2PPh_2]^-$ can coordinate to virtually all main group and transition metals giving rise to a variety of coordination patterns. The possible contributing resonance structures of the anion are illustrated as in Scheme 3.1 below.

Scheme 3.1 Resonance structures of deprotonated diphenyl-dithiophosphinic acid.

Due to the symmetry present in diphenyl-dithio-phosphinate resonance structure A is as important as structure B. The metal type to which the ligand is coordinating, as well as the oxidation state of the metal determine which resonance structure dominates during complexation. Resonance structures A and B are applicable to complexes where the ligand binds in η^1-fashion with a 'dangling' second sulphur atom.

3.1.2 *Goals and scope of this section of the project.*

Chapter 2 involved palladium(II) complexes comprising of acac⁻-type ligands coordinating directly to the palladium through delocalized bonds forming 6-membered rings. In this chapter, complexes formed by η^3-coordinating ligands bonded directly to palladium are described. Examples of the complexes prepared are illustrated in Figure 3.1 below.

X = S or O

Type 1   Type 2   Type 2

Figure 3.1 Typical complexes discussed in chapter 3.

The complexes illustrated in Figure 3.1 above could exhibit hemilability in the following manner: -
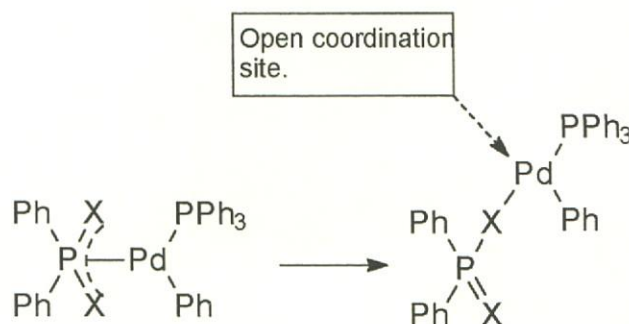
Figure 3.2 : Potential hemilabile activity of complexes to be prepared here.

Due to the symmetrical nature of the ligand, and as a result of the η^3-coordination of the ligand, the ligand could potentially open up and become η^1 coordinated, thereby freeing a coordination site on the palladium to allow the coordination of the substrate species to be activated.

Complexes of type 1, 2 and 3 above both involve a ligand η^3-coordinated to the central palladium atom. These two types of complexes were chosen to investigate the difference in stability that results due to the bulky $-Si(CH_3)_3$ groups that are attached to the nitrogen atoms in type 2 and 3 versus the non-encumbered sulphur and oxygen atoms in complexes of type 1. It was not known whether these complexes would exhibit hemilability.

The main goal of this study was to prepare and characterize complexes of the type illustrated in Figure 3.1 and attempt to obtain crystals for structure characterization. Structure characterization enables the investigation of the metal ligand bonding in these types of complexes and then serves to correlate structural parameters with complex reactivity in catalytic reactions such as carbon monoxide insertion. However, the investigation of the catalytic activity of these types of complexes falls outside the scope of this investigation. Despite employing many crystallization methods, it was difficult to obtain crystals suitable for crystal structure determination.

The general method of preparation of the complexes synthesised in this chapter is very similar to the synthetic route used to prepare the complexes in chapter 2. It involves the reaction of the applicable deprotonated ligand with starting complex **1** to substitute a triphenylphosphine group. Readilly removable sodium chloride is produced as a byproduct (see Scheme 3.2(a), Scheme 3.2(b) and Scheme 3.3 below).

(a)
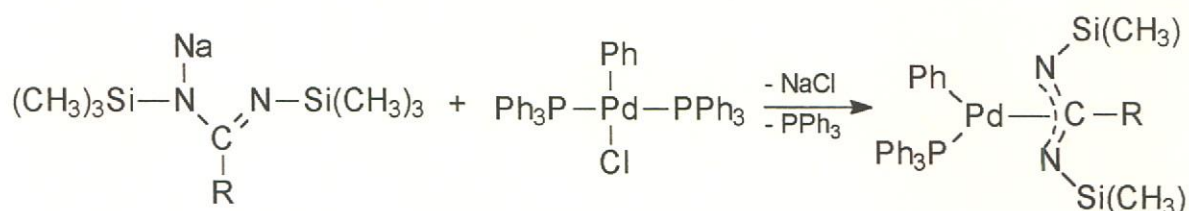
(b)
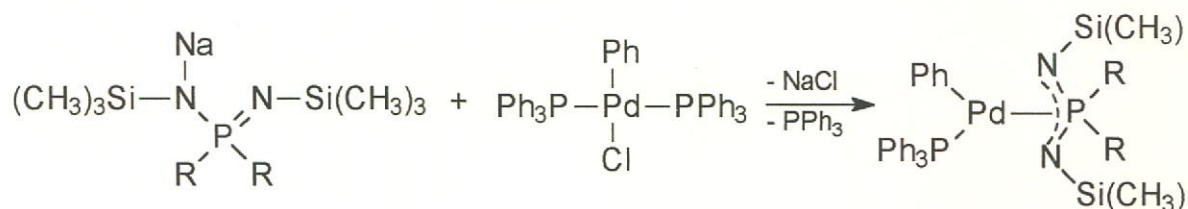
Scheme 3.2 : General reaction used for preparation.

X = S or O
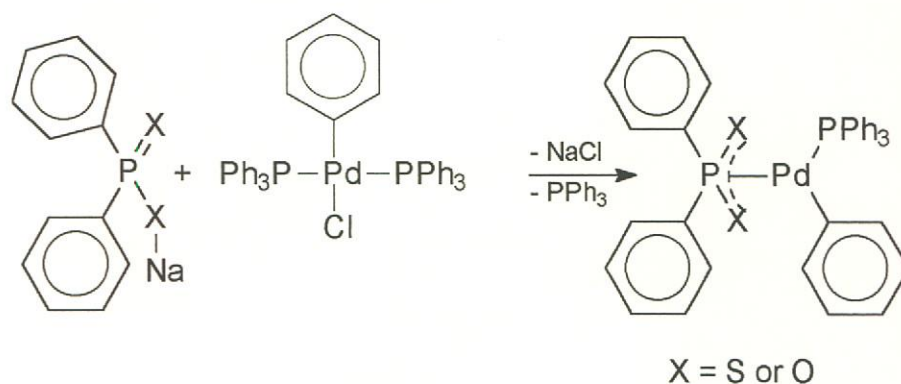
Scheme 3.3 : General reaction used for preparation.

3.2 *Results and discussion.*

3.2.1 Complex 1, *trans*-[(Ph$_3$P)$_2$(Ph)PdCl].

I) Preparation of complex 1, trans-[(Ph$_3$P)$_2$(Ph)PdCl].

Trans-[(Ph$_3$P)$_2$(Ph)PdCl] was synthesised according to the method described by Hermann and his co-workers illustrated in Scheme 3.4 below.[14] It involved the reaction palladium chloride with triphenylphosphine to produce palladium tetrakis triphenylphosphine. The final step of preparation involved an oxidative addition of phenyl chloride to deliver complex 1. The clean product was isolated by crystallization from a 1:1 mixture of anhydrous dichloromethane and pentane.

$$PdCl_2 \xrightarrow{4PPh_3} Pd(PPh_3)_4 \xrightarrow{C_6H_5-Cl} \underset{Cl}{\overset{Ph}{Ph_3P-Pd-PPh_3}}$$

1
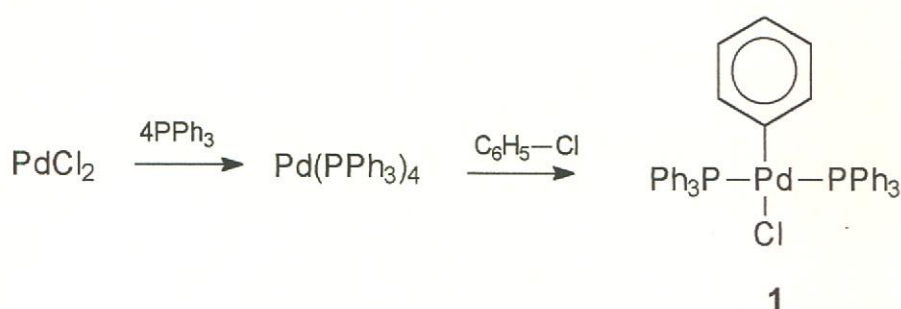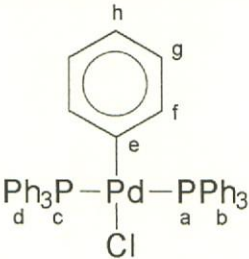
Scheme 3.4 : Preparation of complex **1**.

Trans-[(Ph$_3$P)$_2$(Ph)PdCl] was synthesised according to Scheme 3.3 above and was used as the starting complex for all the neutral palladium complexes prepared in this chapter.

II) NMR Spectroscopic analysis of complex 1, trans-[(Ph$_3$P)$_2$(Ph)PdCl].

The ^{1}H and ^{13}C NMR data for complex **1** are summarized in table 3.1 below. The ^{1}H and ^{13}C for complex **1** are reported for both d^2-dichloromethane and d^6-benzene to enable all proton groups present in the synthesised complexes to be individually assignable.

Starting Complex.

Ph$_3$P—Pd—PPh$_3$
d   c | a   b
       Cl

Solvent : CD$_2$Cl$_2$ (TMS used as internal standard)		Solvent : C$_6$D$_6$ (TMS used as internal standard)	
Proton (δ-values)			
a:	---	---	
b:	7.19 – 7.88 (m, 30H)	6.99 – 7.82 (m, 30H)	
c:	---	---	
d:	7.19 – 7.88 (m, 30H)	6.99 – 7.82 (m, 30H)	
e:	---	---	
f:	6.59 (d, 2H, J_{H-H} = 6.6Hz)[i]	6.91 (d, 2H)	
g:	6.19 (t, 2H)[i]	6.34 (t, 2H)	
h:	6.34 (t, 1H)[i]	6.31 (t, 2H)	
Carbon 13 {^{1}H} (δ-values)			
b:	122.5 – 155.5	122.3 – 137.8	
d:	122.5 – 155.5	122.3 – 137.8	
e:	155.5	156.7	
f, g, h:	122.5 – 155.5	122.3 – 137.8	
Phosphorus 31 {^{1}H} (δ-values)[ii]			
a:	24.41	24.62	
c:	24.41	24.62	

Table 3.1 : ^{1}H and ^{13}C data for complex **1**.

---

[i] Peak assignments done largely on the grounds of signal multiplicity and integration values for the Pd-Ph group. It is virtually impossible to assign specific peaks for the triphenylphosphine groups due to the complex multiplet that these triphenylphosphine groups deliver.

[ii] δ-values are relative to H$_3$PO$_4$ used as an external standard.

III) Single crystal structure determination of complex 1.

Suitable crystals for crystal structure determination were obtained by crystallization of complex **1** from a solution of dichloromethane layered in a 1:1 ratio with pentane.

The crystal structure for complex **1** was solved by the heavy atom (Patterson) method. Illustrations of the single crystal structure and unit cell as well as a detailed discussion of the crystal structure of complex **1** can be found in chapter 2. Selected crystallographic bond lengths and angles are listed in Table 2.3 and Table 2.4 respectively.

3.2.2 Complex 5, $[[\eta^3\text{-}((CH_3)_3SiN)_2C(Ph)Pd(PPh_3)(Ph)]$.

I) Preparation of complex 5, $[\eta^3\text{-}((CH_3)_3SiN)_2C(Ph)Pd(PPh_3)(Ph)]$.

The free ligand, sodium-N'N'-bis(trimethylsilyl)benzaimidinate, was prepared from synthesised hexamethyldisilazine,[15] sodium amide[16] and sodium bis-trimethylsilylamide[17] according to published literature methods as illustrated in Scheme 3.5 below.[18]

$$2(CH_3)_3Si-Cl + 3NH_3 \longrightarrow \begin{array}{c} (CH_3)_3Si \\ \diagdown \\ (CH_3)_3Si \diagup \end{array} N-H + 2NH_4Cl_{(s)}$$

$$2Na + 2NH_3 \longrightarrow 2NaNH_2 + H_2$$

$$\begin{array}{c} (CH_3)_3Si \\ \diagdown \\ (CH_3)_3Si \diagup \end{array} N-H + NaNH_2 \longrightarrow \begin{array}{c} (CH_3)_3Si \\ \diagdown \\ (CH_3)_3Si \diagup \end{array} N-Na + NH_3$$
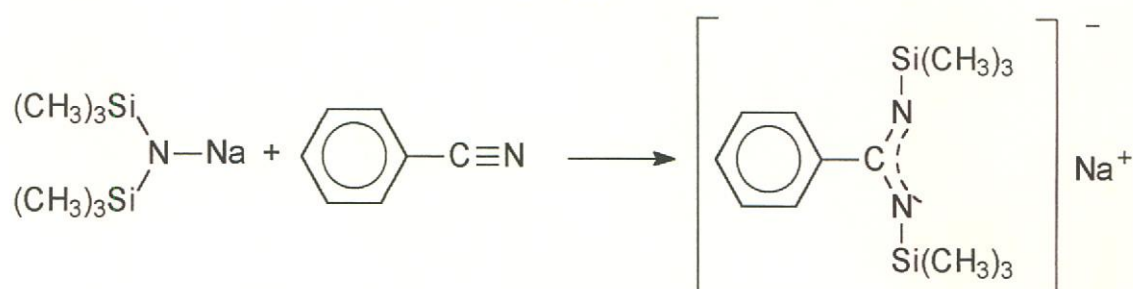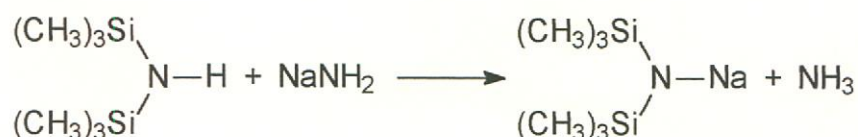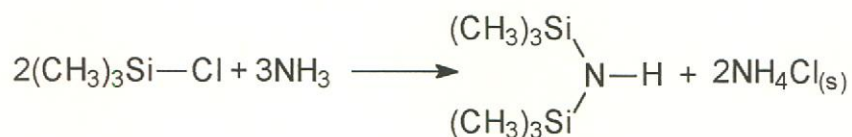
Scheme 3.5 : Preparation of sodium-N'N'-bis(trimethylsilyl)benzamidinate.

Complex **5** was prepared according to Scheme 3.6 below. The free ligand, sodium-N'N'-bis(trimethylsilyl)benzamidinate, was reacted with the starting complex **1**, *trans*-[(Ph₃P)₂(Ph)PdCl], to substitute a triphenylphosphine group. Readily removable sodium chloride is produced as a byproduct.
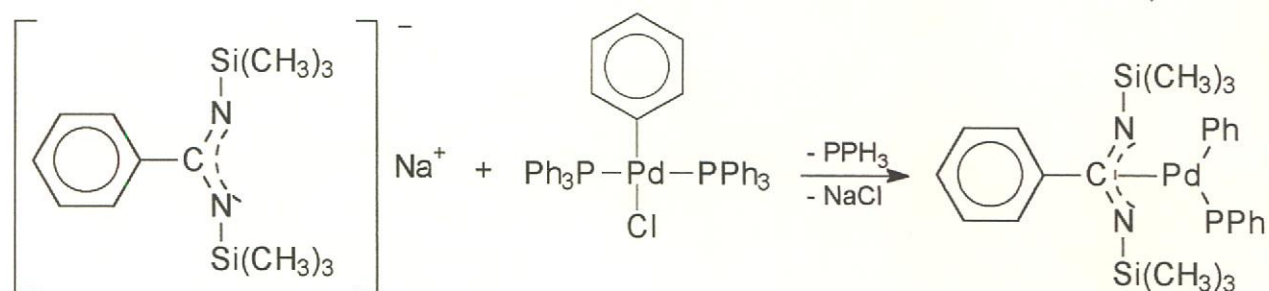
Scheme 3.6 : Preparation of complex **5**.

*II)*NMR spectroscopic analysis of sodium-N'N'-bis(trimethylsilyl)benzamidinate and complex **5**, [η^3-((CH$_3$)$_3$SiN)$_2$C(Ph)Pd(PPh$_3$)(Ph)].

The ^{1}H and ^{13}C NMR data for the free ligand, sodium-N'N'-bis(trimethylsilyl)benzamidinate, is summarised in table 3.2 below. The ^{1}H and ^{13}C data are reported for both d^2-dichloromethane and d^6-benzene to enable all proton signals to be assigned.

Free Ligand

Solvent : CD$_2$Cl$_2$ Temperature (K) : 293	Solvent : C$_6$D$_6$ Temperature (K) : 293
Proton (δ-values)	
a: -0.15 or – 0.13 (m, 18 H) b: -0.15 or – 0.13 (m, 18 H) c: --- d: 6.90 – 7.44 (m , 5H)	-0.427 or -0.27 (s, 9H) -0.427 or -0.27 (s, 9H) --- 6.61 – 7.02 (m, 5H)
Carbon 13 {^{1}H) (δ-values)	
c: Not recorded d: Not recorded d$_{ipso}$: Not recorded	142.6 127.2 – 129.6 132.6

Table 3.2 : ^{1}H and ^{13}C data for sodium-N'N'-bis(trimethylsilyl)benzamidinate

The ^1H and ^{13}C NMR data for complex **5**, are summarized in Table 3.3 below. The ^1H and ^{13}C data are reported for d^6-benzene.

Complex	
	Si(CH$_3$)$_3$ (a) — N — C(d) — Pd — Ph(e), PPh$_3$(f), N — Si(CH$_3$)$_3$ (b), C(c)

Solvent : C$_6$D$_6$
Temperature (K) : 293

Proton (δ-values)	
a:	0.094 or 0.279 (s, 9H)
b:	0.094 or 0.279 (s, 9H)
c:	---
d:	6.60 – 7.68 (m, 25H)[iii]
e:	6.60 – 7.68 (m, 25H)
f:	6.60 – 7.68 (m, 25H)

Carbon 13 {^1H} (δ-values)	
a:	0.313 or 1.917
b:	0.313 or 1.917
c:	173.2
d:	131.5 – 135.2
d$_{ipso}$:	157.1
e:	126.0 – 129.7
e$_{ipso}$:	143.8
f:	126.0 – 129.7
f$_{ipso}$:	137.0 - 137.5

Phosphorus 31 {^1H} (δ-values)[iv]	
f:	29.69 (s)

Table 3.3 ^1H and ^{13}C data for complex **5**.

[iii] It proved to be impossible to unambiguously assign the separate proton NMR signals of the respective phenyl protons due to their obscuring of one another as well as being obscured by the signal produced by the C$_6$D$_6$ NMR solvent.

Since the majority of palladium(II) complexes are square planar, and the triphenylphosphine and phenyl ligands on the palladium are not identical, two signals in both the proton and carbon-13 spectra are observed for the -Si(CH$_3$)$_3$ groups.

There are few NMR 'handles' present in this complex due to the fact that it is mostly comprised of phenyl rings. The signals of these phenyl rings obscure each other in the proton and carbon-13 spectra.

The chemical shift of carbon 'c' has moved downfield by 30.6ppm. This is in support of a η^3-coordination through the N-C-N atoms of the ligand.

A free displaced triphenylphosphine group was resonated at ca. -4.5ppm in the reaction mixture in a 1:1 ratio with the coordinated triphenylphosphine group. This is further support for the formation of the target complex. No hemilabile interaction or exchange was evident with the displaced triphenylphosphine group.

---

iv δ-values are relative to H$_3$PO$_4$ used as an external standard.

3.2.3 Complex 6, [η³-(Ph)₂P(NSi(CH₃)₃)₂]Pd(PPh₃)(Ph)].

*I) Preparation of complex **6**, [η³-(Ph)₂P(NSi(CH₃)₃)₂]Pd(PPh₃)(Ph)].*

The synthesis of $(C_6H_5)_3SiN=P(C_6H_5)_2NHSi(C_6H_5)_3$ was carried out according to methods described by Scherer and Paciorek (Scheme 3.7 below).[19, 20]

$$(CH_3)_3SiCl + NaN_3 \longrightarrow (CH_3)_3SiN_3 + NaCl$$

$$Ph_2PH + (CH_3)_3SiN_3 \longrightarrow Ph_2P{\displaystyle \substack{NSi(CH_3)_3 \\ NSi(CH_3)_3 \\ | \\ H}}$$
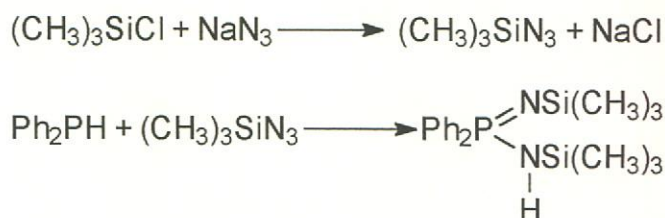
Scheme 3.7 : Formation of $(C_6H_5)_3SiN=P(C_6H_5)_2NHSi(C_6H_5)_3$

The precursor of the free ligand was deprotonated with methyl lithium and reacted with complex **1** to coordinate in a η³ manner by substituting a triphenylphosphine group. Readily removable sodium chloride was produced as a byproduct (Scheme 3.8 below).

$$Ph_2P{\displaystyle \substack{NSiCH_3 \\ NSiCH_3 \\ | \\ H}} + Me-Li \longrightarrow Ph_2P{\displaystyle \substack{NSiCH_3 \\ NSiCH_3 \\ | \\ Li}} + CH_4$$

$$Ph_2P{\displaystyle \substack{NSiCH_3 \\ NSiCH_3 \\ | \\ Li}} + Ph_3P-\underset{\underset{Cl}{|}}{\overset{\overset{Ph}{|}}{Pd}}-PPh_3 \xrightarrow[- NaCl]{- PPh_3} {\displaystyle \substack{Si(CH_3)_3 \\ | \\ Ph\ \ N\ \ \ \ \ \ Ph \\ \diagdown | \diagup \\ P-Pd \\ \diagup | \diagdown \\ Ph\ \ N\ \ \ \ PPh_3 \\ | \\ Si(CH_3)_3}} + LiCl$$

<div align="right">6</div>
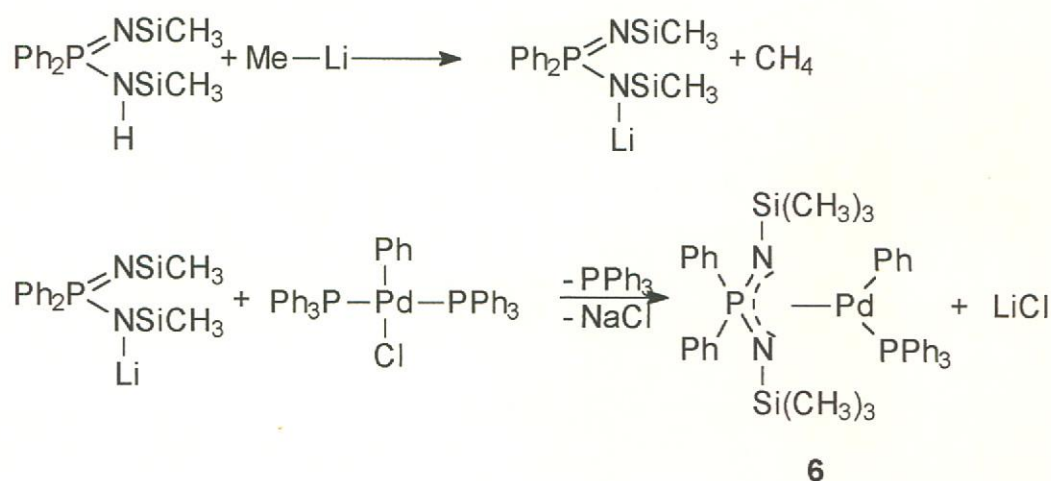
Scheme 3.8 : Formation of complex **6**.

II) Spectroscopic analysis of free ligand, (C₆H₅)₃SiN=P(C₆H₅)₂NHSi(C₆H₅)₃, and complex 6, [η³-(Ph)₂P(NSi(CH₃)₃)₂]Pd(PPh₃)(Ph)].

The ^1H and ^{13}C NMR spectral data for the precursor to the free ligand, $(C_6H_5)_3SiN=P(C_6H_5)_2NHSi(C_6H_5)_3$, are summarized in Table 3.4 below.

Free Ligand	
a Si(CH₃)₃ │ N Ph₂P═ ╱ c d N─H │ e Si(CH₃)₃ b	
Solvent : C₆D₆ Temperature (K) : 293	
Proton (δ-values)	
a, b:	0.11ppm (s, 18H)
c:	7.02 – 7.07ppm and 7.85 – 7.93ppm (m, 10H)
e:	2.97ppm (br s, 1H)
Carbon 13 {¹H) (δ-values)	
a:	-2.1ppm
b:	-2.1ppm
c:	125.1 – 125.9ppm
C$_{ipso}$:	134.3 and 134.9ppm
Phosphorus 31 {¹H } (δ-values) [v]	
d:	21.38ppm

Table 3.4 : NMR spectral data for $(C_6H_5)_3SiN=P(C_6H_5)_2NHSi(C_6H_5)_3$.

[v] δ-values are relative to H_3PO_4 used as an external standard.

The ^{1}H and ^{13}C NMR spectral data for complex **6**, $[\eta^3\text{-}$(Ph)$_2$P(NSi(CH$_3$)$_3$)$_2$]Pd(PPh$_3$)(Ph)], are summarized in Table 3.5 below.

Complex **6**

Solvent : C$_6$D$_6$
Temperature (K) : 293

Proton (δ-values)

a:	0.23 (br s, 18H)
b:	0.23 (br s, 18H)
c:	7.68 – 8.06 (m, 10)
f:	6.96 – 7.08 (m, 20H)
g:	6.96 – 7.08 (m, 20H)

Carbon 13 {^{1}H) (δ-values)

a, b:	0.7ppm
c:	131.2 – 136.7
f:	121.7 – 129.6
g:	121.7 – 129.6

Phosphorus 31 {^{1}H} (δ-values) [vi]

d:	21.88
g:	28.38

Table 3.5. : NMR spectral data for $[\eta^3\text{-}$(Ph)$_2$P(NSi(CH$_3$)$_3$)$_2$]Pd(PPh$_3$)Ph].

Since the complex is primarily comprised of phenyl rings. This results in a number of proton and carbon signals that obscure one another and cannot be assigned unambiguously to a specific proton or carbon group.

[vi] δ-values are relative to H$_3$PO$_4$ used as an external standard.

Very small differences exist in the NMR spectra of the initial ligand precursor and the coordinated complex. This is due to the opposing effects that occur upon deprotonation of the ligand and complexation of the deprotonated ligand with the palladium metal. Deprotonation of the ligand precursor causes an electron density increase on the ligand and an expected upfield shift is expected.   Coordination of the deprotonated free ligand precursor to the palladium causes a downfield shift of 3.97ppm in the phosphorus-31 spectrum for phosphorus atom g. This downfield shift for phosphorus atom g is comparable to the downfield shift of 5.07ppm that was observed for the analogous phosphorus atom in complex **5**.

A free displaced triphenylphosphine group was present at ca. -4.5ppm. in a 1:1 ratio with the coordinated triphenylphosphine group. This is further support that the target complex has been synthesised and the necessary displacement of the original group had occurred as predicted. No exchange was evident with the displaced triphenylphosphine group.

Complex **6** was unstable despite the inert anhydrous conditions. Various methods of crystallization were attempted but decomposition occurred. Crystals suitable for crystal structure determination were not obtained. Steric hindrance and thermodynamic motion of the trimethylsilyl groups of the ligand adjacent to the triphenylphosphine group could contribute to the instability of the complex.

3.2.4 Complex 7, [η^3-(Ph)$_2$PS$_2$][Pd(PPh$_3$)(Ph)].

I) Preparation of complex 7, [η^3-(Ph)$_2$PS$_2$][Pd(PPh$_3$)(Ph)] .

Diphenyl-dithio-phosphinic acid was prepared according to literature methods illustrated in Scheme 3.9 below[21].

$$4C_6H_6 + P_2S_5 \xrightarrow{AlCl_3} 2(C_6H_5)_2\overset{\displaystyle S}{\overset{\|}{P}}{-}SH + H_2S$$
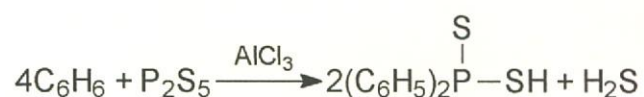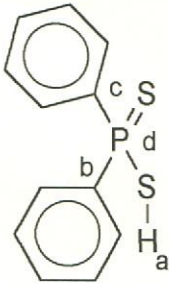
Scheme 3.9 : Preparation of diphenyl-dithio-phosphinic acid.

Diphenyl-dithio-phosphinic acid was subsequently deprotonated with sodium carbonate and the resulting sodium salt reacted with complex **1**. $[(Ph)_2PS_2]^-$ became η^3-coordinated to the palladium by substituting a triphenylphosphine group in complex **1**. Readily removable sodium chloride was produced as a byproduct (Scheme 3.10).
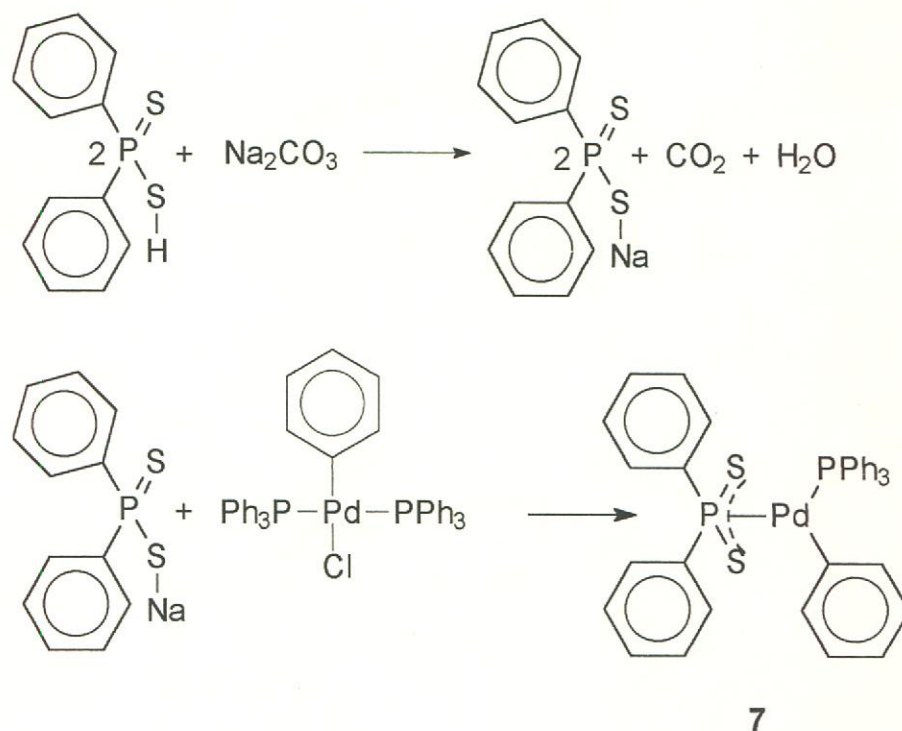
Scheme 3.10 : Preparation of complex **7**.

*II) NMR spectroscopic analysis of the precursor to the free ligand, [(Ph)$_2$PS$_2$H], and complex **7**, [η^3-(Ph)$_2$PS$_2$][Pd(PPh$_3$)(Ph)].*

Free Ligand
Solvent : C$_6$D$_6$ (TMS internal Standard) Temperature : 293K
Proton (δ-values)
a: 2.46 ppm (br s, 1H) b: 6.95 – 7.94ppm (m, 10 H)[vii] c: 6.95 – 7.94ppm (m, 10 H)
Phosphorus31 {^{1}H} (δ-values) [viii]
d: 55.31ppm (s)

Table 3.6 : NMR spectral data for the precursor to the free ligand [(Ph)$_2$PS$_2$H].

The phenyl rings of [(Ph)$_2$PS$_2$H] are in slightly different electronic environments due to the presence of the proton on one of the sulphur atoms thereby preventing the molecule from being symmetrical. This delivers a complex multiplet for the phenyl rings in the NMR spectrum.

[vii] Signal partially obscured by C$_6$D$_6$ signal.

[viii] δ-values are relative to H$_3$PO$_4$ used as an external standard.

Complex **7**.	
Solvent : $CDCl_3$ Temperature : 293K	

Proton (δ-values)

a:	7.21 – 7.44 (m, 21H)[ix]
d:	7.01 – 7.05 (complex m, 2H)[x]
e, f:	6.66 – 6.68 (complex m, 3H)[v]
i:	7.83 – 7.91 (complex m, 4H)
j, k:	7.21 – 7.44 (m, 21H)[xi]
m:	7.83 – 7.91 (complex m, 4H)
n, o:	7.21 – 7.44 (m, 21H)[vi]

Carbon 13 {^{1}H} (δ-values)

a_{ipso}:	136.0 (d, $J_{C\text{-}P}$ = 4.1Hz)
a_{ortho}	134.4 (d, $J_{C\text{-}P}$ = 11.7Hz)
a_{meta}	128.3 (d, $J_{C\text{-}P}$ = 13.1Hz)
a_{para}	128.1 (d, $J_{C\text{-}P}$ = 7.9Hz)
c:	130.6
d:	131.0
e:	127.4
f:	122.7
h:	130.2 (d, $J_{C\text{-}P}$ = 2.4Hz) or 131.2 (d, $J_{C\text{-}P}$ = 3.1Hz)
i:	130.0 (d, $J_{C\text{-}P}$ = 11.7Hz)
j:	128.2 (d, $J_{C\text{-}P}$ = 10.3Hz)
k:	130.4
l:	130.2 (d, $JC\text{-}P$ = 2.4Hz) or 131.2 (d, $J_{C\text{-}P}$ = 3.1Hz)
m:	130.0 (d, $J_{C\text{-}P}$ = 11.7Hz)
n:	128.2 (d, $J_{C\text{-}P}$ = 10.3Hz)
o:	130.4

Phosphorus 31 {^{1}H} (δ-values) [xii]

b:	30.12 (d, 1P) (J = 6.8Hz)
g:	77.29 (d, 1P) (J = 7.3Hz)

Table 3.7 : NMR spectral data for complex **7**.

[ix] The signal is made up of signals from both the triphenylphosphine group as well as signals from the meta- and para-protons from the two phenyl groups of the [(Ph)$_2$PS$_2$H] ligand.

[x] The endo- and exo-protons of this phenyl group are not equivalent due to the different adjacent groups (triphenylphosphine and ligand). As a result, these protons give a complex signal with the endo- and exo-proton signals obscuring each other.

[xi] The signal region includes signals from the two triphenylphosphine groups as well as being obscured by the signal from the d-chloroform (CDCl$_3$).

[xii] δ-values are relative to H$_3$PO$_4$ used as an external standard.

Again, as with previous complexes discussed in this chapter, there are few 'handles' present in this complex due to the fact that it is mostly comprised of phenyl rings. In the ^{1}H NMR spectra, the signals from the phenyl groups obscure each other and it proves to be virtually impossible to unambiguously assign the respective peaks to the individual groups.

Very small differences exist in the NMR spectra of the initial ligand precursor and the coordinated complex. The NMR shifts that are evident in the spectra from the free ligand to precursor are due to the opposing effects that occur upon deprotonation of the ligand and complexation of the deprotonated ligand to the palladium metal. Deprotonation of the ligand precursor causes an electron density increase. As a result of coordination of the deprotonated ligand precursor to the palladium, a downfield shift is expected. Both phosphorus atoms b and g in complex **7** experience an overall downfield shift of and 5.50ppm and 21.98ppm respectively in the phosphorus-31 spectrum. This downfield shift of phosphorus atom b is comparable to the magnitude of downfield shift that was observed for complex **5** (5.07ppm).

When the reaction mixture of complex **7** is analysed, an exchange is observed between the coordinated and substituted triphenylphosphine groups. The exchange kinetics of this exchange was studied qualitatively by means of variable temperature ^{31}P NMR spectroscopy as described later.

Figure 3.3 shows a typical room temperature ^{31}P{^{1}H} NMR spectra of the crystals of complex **7** dissolved in CD_2Cl_2. The two-bond P-P coupling can clearly be seen in this spectrum. This phosphorus-phosphorus coupling is not evident in the ^{31}P spectrum of the reaction mixture even when analysed at low temperatures (Figure 3.4). This is due to the fact that the phosphorus signals in the reaction mixture are broader than the phosphorus signals in the spectra of the crystals. The phosphorus signals of the reaction mixture are broader, even at −90°C, due to the exchange of the coordinated triphenylphosphine group with the substituted triphenylphosphine group, (Figure 3.3 and Figure 3.4 below).
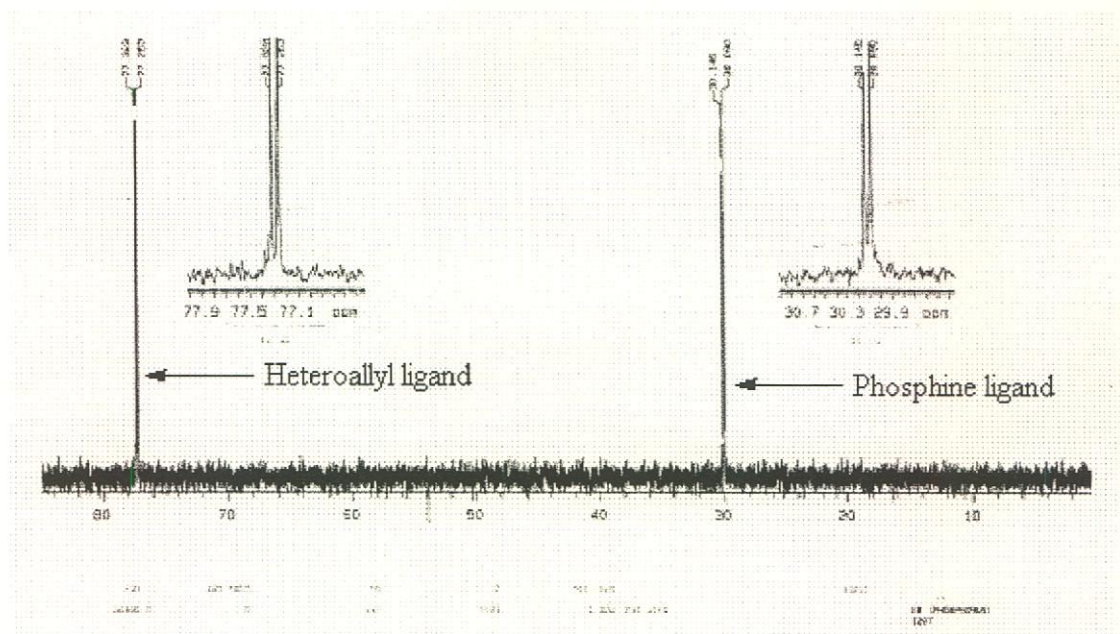
Figure 3.3 : Room temperature $^{31}P\{^1H\}$ NMR spectrum of isolated crystals of complex **7** dissolved in CD_2Cl_2.
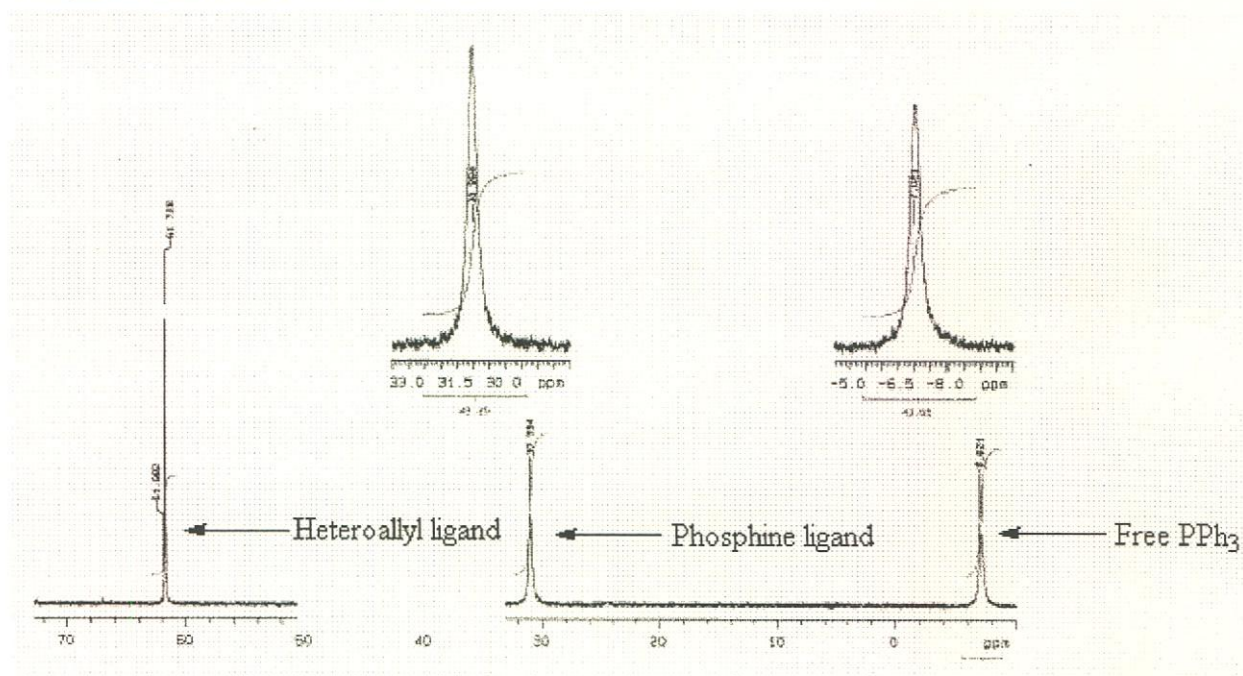
Figure 3.4 : A –90°C temperature $^{31}P\{^1H\}$ NMR spectrum of the reaction mixture before crystallization of complex **7**.

III) *Variable temperature NMR study of complex 7*, $[\eta^3-(Ph)_2PS_2][Pd(PPh_3)(Ph)]$.

Introduction

Nuclear magnetic resonance (NMR) spectroscopy has long been known as an extremely powerful tool in the study of the dynamic behavior of non-ridged organometallic compounds.[22] Due to the relatively slow response rate of this technique, the slow rates of exchange, rearrangement and intramolecular reactions are especially suited for study by means of variable temperature NMR spectroscopy.

The suitability of any spectroscopic method to the study of any dynamic behavior depends on the response time of that specific technique to molecular movement.[23] This time scale is loosely related to the reciprocal of the frequency of electromagnetic radiation utilized by the technique in question. When measured on this scale, it can be seen from the table below that NMR spectroscopy is a relatively slow technique when compared to other available techniques such as IR spectroscopy and UV-visible spectroscopy. Table 3.8 below gives a detailed comparison of these techniques relative to one other.

Technique	Approx. Time Scale (s)
Electron diffraction	10^{-20}
Neutron diffraction	10^{-18}
X-ray diffraction[xiii]	10^{-18}
Ultraviolet	10^{-15}
Visible	10^{-14}
Infrared-Raman	10^{-13}
Electron spin resonance[xiv]	10^{-14} to 10^{-8}
Nuclear magnetic resonance[xii]	10^{-1} to 10^{-9}
Quadrupole resonance[xii]	10^{-1} to 10^{-8}
Mössbauer (iron)	10^{-7}
Molecular beam	10^{-20}
Experimental separation of isomers	$> 10^{2}$

Table 3.8 : Time scale for structural techniques

This means that NMR spectroscopy is responsive to relatively slow rates of change such as those involved in molecular rearrangements and intramolecular reactions. Comparatively fast techniques such as IR- or UV-visible spectroscopy will show 'static' species despite dynamic behavior being present. NMR will reveal either a static species or time averaged signals depending on the rate of the particular dynamic behavior involved. These dynamic processes are usually temperature dependent and can thus be controlled, allowing one to move from a slow exchange (separate well-defined signals) to the fast exchange which delivers time-averaged signals. It can thus be said that signal shape, as well as the particular chemical shift of these signals, are temperature dependent for NMR spectra.

Variable temperature NMR studies allow one to examine the effects of temperature on specific reaction equilibria, allowing the calculation of

---

[xiii] Individual measurements of this duration are collected over a long time span and multiple measurements are collected to give a final structure. A time-averaged signal is thus the net result.
[xiv] Time scale sensitivity is defined by the specific chemical system under investigation.

approximate ΔG° (Gibbs standard free energy) and E_a (activation energy) values.[24]

The dynamic reaction, which is observed for complex **7**, is one in which a non-coordinated triphenylphosphine group exchanges with a triphenylphosphine group that is coordinated to the palladium (Scheme 3.11). This exchange is obviously only observed in the reaction mixture, which contains the non-coordinated triphenylphosphine.

The deprotonated diphenyl-dithio-phosphinic acid ligand remains η^3-coordinated at all times. This exchange between the triphenylphosphine groups can be easily observed in the $^{31}P\{^1H\}$ spectra. It is difficult to see this exchange in the ^1H NMR spectra due to the fact that the non-coordinated triphenylphosphine group signals are similar in ppm shift value to those of the coordinated triphenylphosphine group (7.01 –7.44ppm). No hemilability was observed for the bidentate ligand.
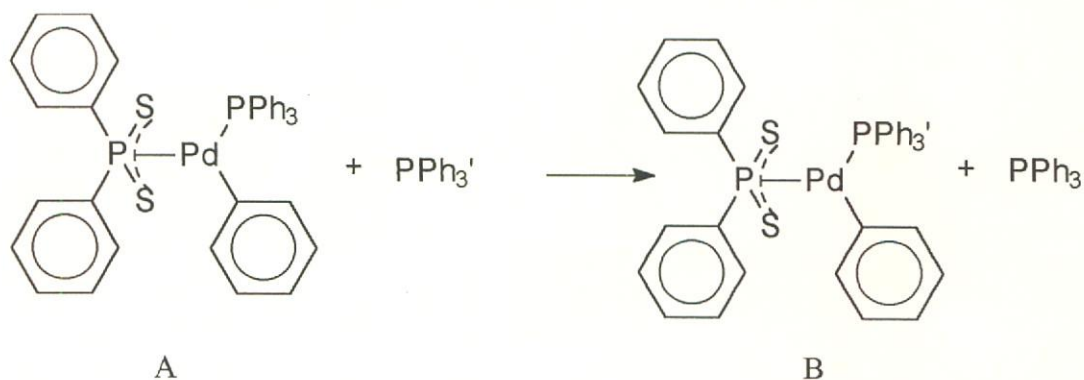
Scheme 3.11 : Exchange between the uncoordinated and coordinated triphenylphosphine groups.

Since each relevant species involved in the exchange illustrated in Scheme 3.11 above, exhibited sufficiently different chemical shifts in the $^{31}P\{^1H\}$ NMR spectra at the slow exchange limit, the equilibrium constant, K, and the rate constant, k, could be determined. Calculations to determine ΔG° and E_a could also be carried out. These values are approximation only.

As the concentration of nuclei measured in $^{31}P\{^{1}H\}$ NMR spectra is directly proportional to the integrated signal intensities, the equilibrium constant, K, for the exchange reaction at a specific temperature was calculated according to the following equations: -

$$A \rightarrow B \qquad \text{...equation 1.}$$

$$K = \frac{[A]}{[B]} \qquad \text{...equation 2}$$

The Gibbs standard free energy, ΔG°, is given by equation (3) below. The ΔG° values of the exchange reaction was determined by the slope of ln K plotted against $\frac{1}{T}$ according to equation (4) below which is derived from equation (3).

Equation (4) is of the form, y = m.x, with the slope being equal to $-\dfrac{\Delta G^{\circ}}{R}$ with R = 8.314 J.K^{-1}.mol^{-1}.

$$\Delta G^{\circ} = -RT \ln K \qquad \text{...equation 3}$$

$$\ln K = -\frac{\Delta G^{\circ}}{R} \cdot \frac{1}{T} \qquad \text{...equation 4}$$

The activation energy, E_a, values for the equilibria were calculated from equation (6), which is derived from the Arrhenius equation (5), The rate constants (k) at a specific temperature were determined by applying the following formula which is defined for slow exchange reactions:[25]

$$k = \pi(h - h_o)$$

where h = the peak width at half height in the NMR spectrum at the specific temperature (T).

h_o = is the peak width at half height with no exchange taking place. For these reactions studied by $^{31}P\{^{1}H\}$ spectroscopic techniques at 121 MHz, h_o was estimated as 1.5Hz.[26]

$$E_a = -RT \ln k \qquad \text{...equation 5}$$

$$\ln k = \frac{E_a}{R} \cdot \frac{1}{T} \qquad \text{...equation 6}$$

This method of studying dynamic systems has been successfully applied in our research group to similar compounds.[27]

Variable temperature NMR study of complex 7, results and discussion.

The equilibrium illustrated in Scheme 3.11 was monitored very successfully with variable temperature (VT) ^{31}P{^{1}H}, NMR techniques in two different solvents. The resonances of the ^{31}P {^{1}H} NMR at the various temperatures in both d_6-benzene and d_2-dichloromethane are shown in Figure 3.4 and Figure 3.5 respectively. These resonances show the time-averaged signals of the two species involved in the equilibrium.

At room temperature the signals are very broad and poorly defined. This is more accentuated in the spectra measured in d_2-dichloromethane. It is evident from the comparison of the spectra in the two different solvents that the exchange is much faster in d_2-dichloromethane. Upon cooling, the signals become sharper and more defined in both solvents. At the poorly defined signals closer to room temperature, the experimental error for the calculation of k and K for the determination of E_a and ΔG^o becomes greater.

The variable temperature ^{1}H NMR spectra yielded very little useful information as the signals from the respective phenyl groups obscure each other and it is virtually impossible to unambiguously distinguish between the signals of the phenyl- and coordinated triphenylphosphine groups from the free triphenylphosphine groups. For this reason the ^{1}H NMR spectra are not included in the calculations or shown here.

Figure 3.4 below is the ^{31}P{^{1}H} resonances in benzene of the phosphine ligand and the uncoordinated triphenylphosphine group that are exchanging with each other. The signals are given at room temperature (20°C), 0°C and at 10° intervals down to –60°C.
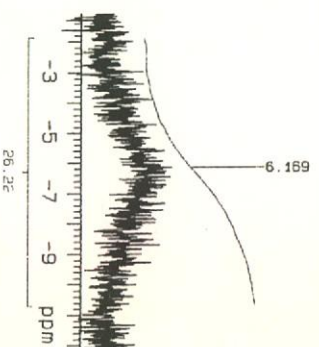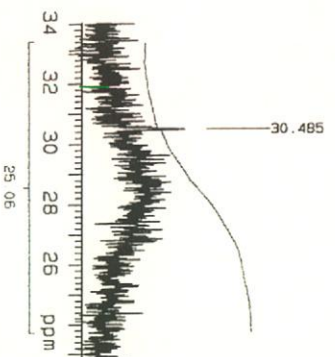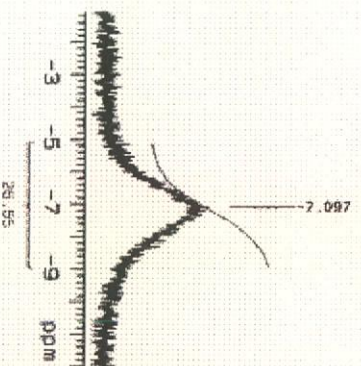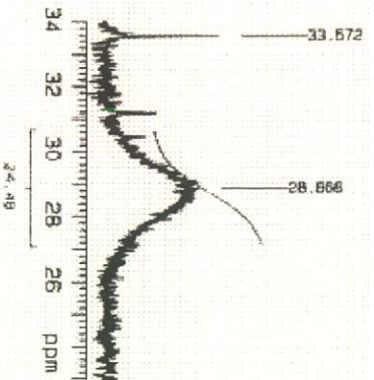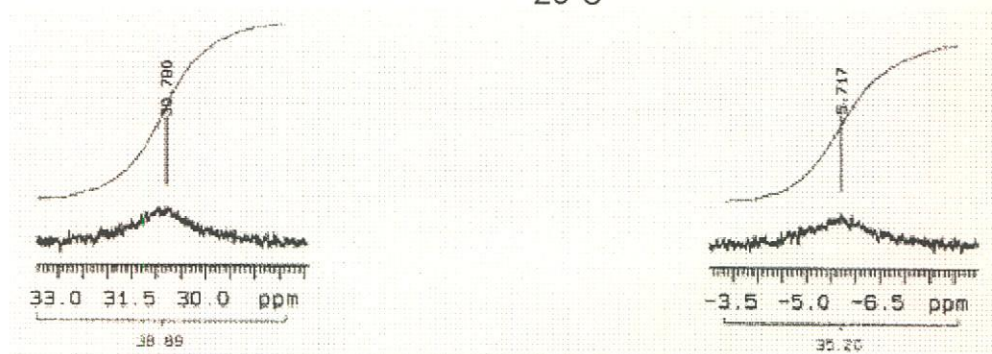
Room temp 20°C

0°C

-10°C

-20°C
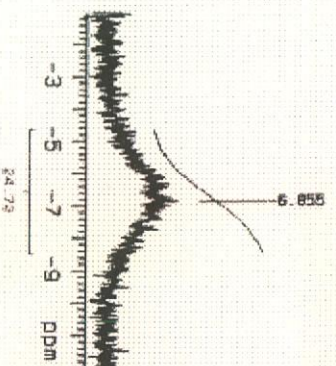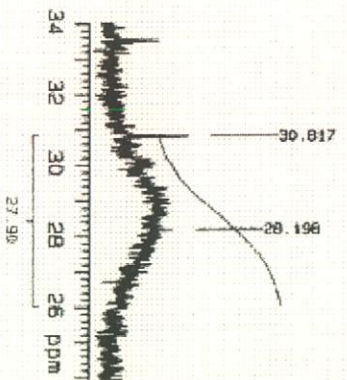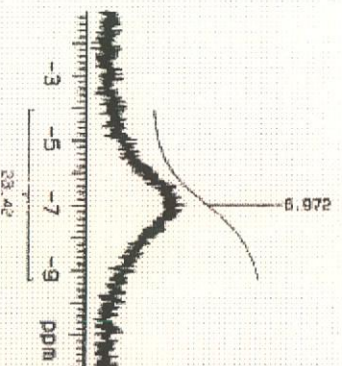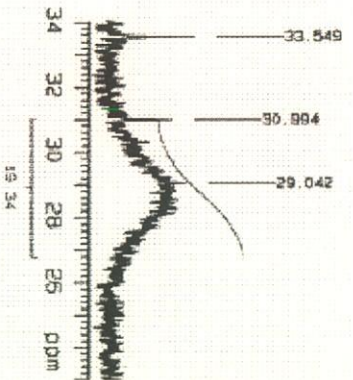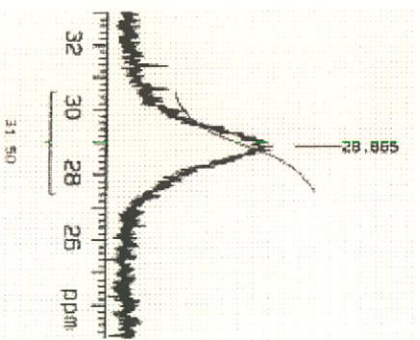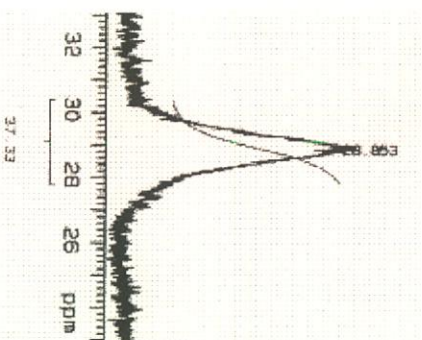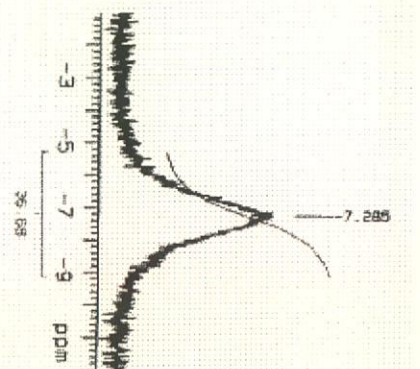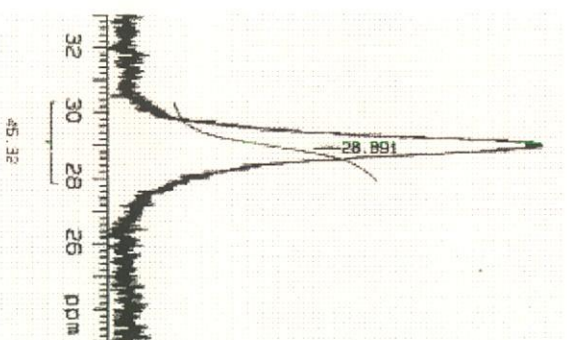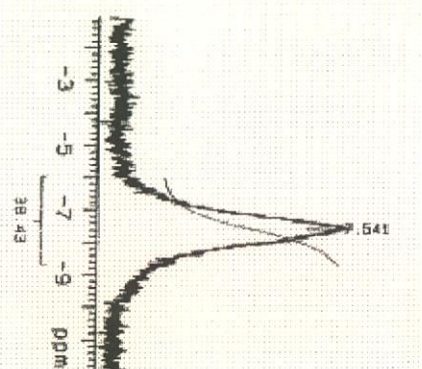
-60°C
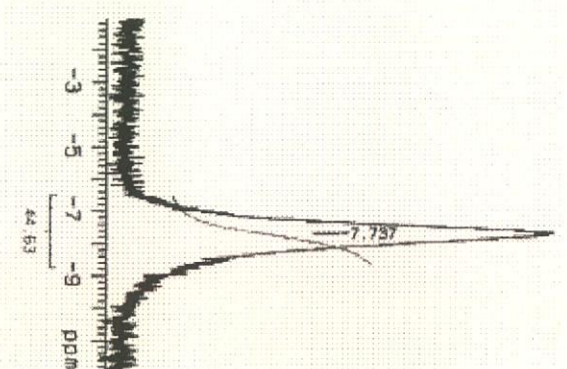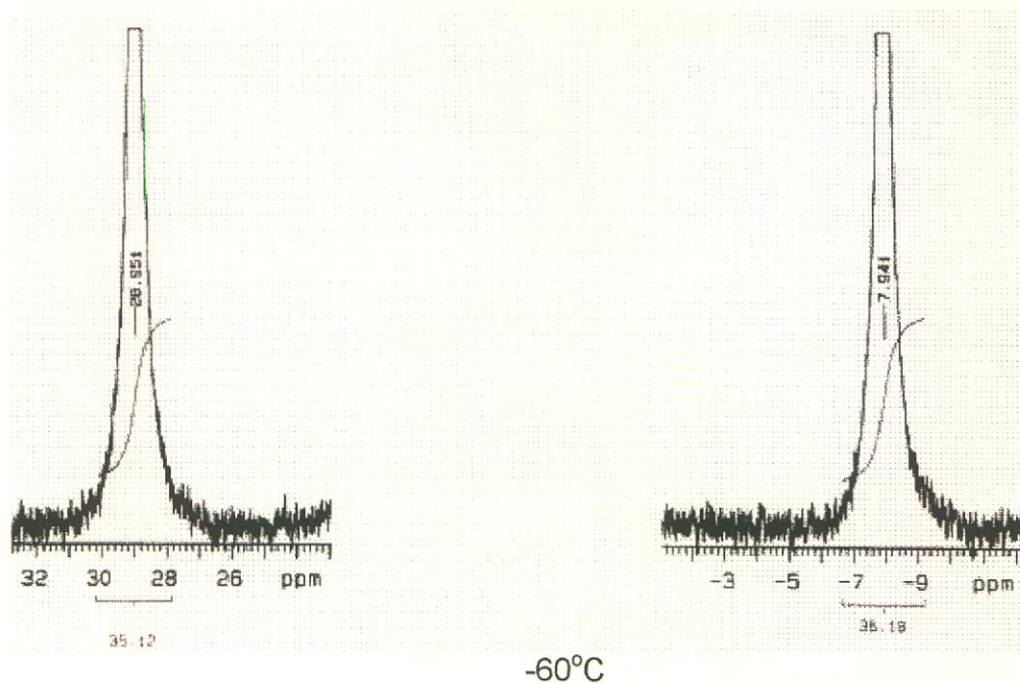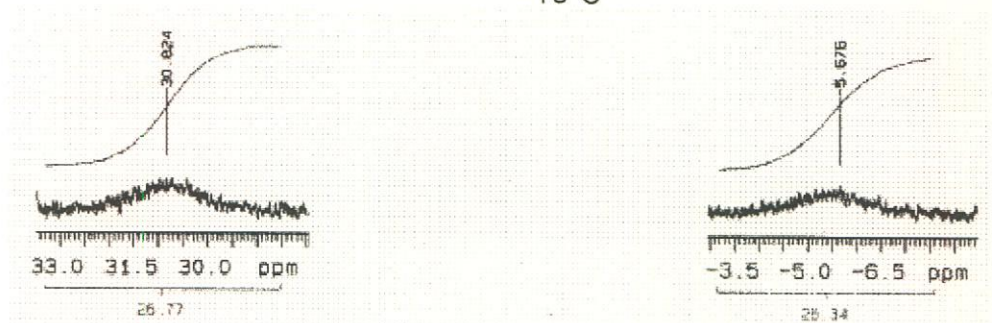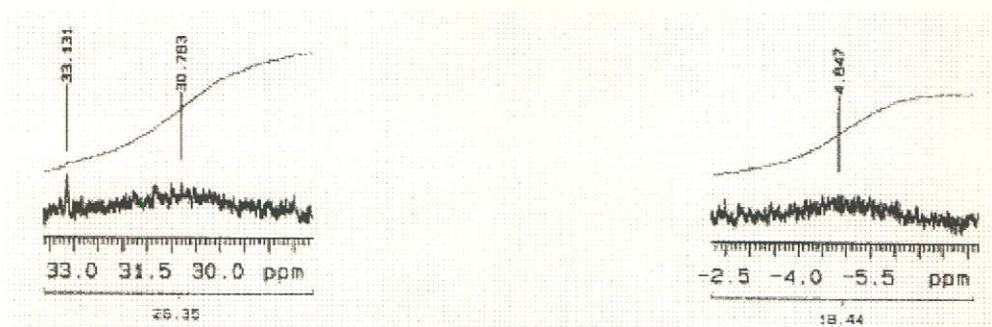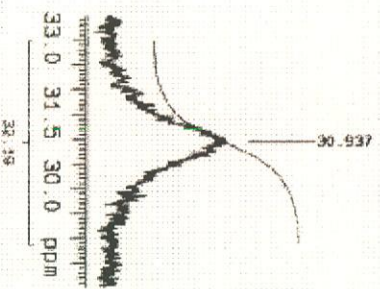
Figure 3.4 : Resonances of the phosphine ligand and exchanging triphenylphosphine group in d_6-benzene.

Figure 3.5 below is the $^{31}P\{^1H\}$ resonance of the phosphine ligand in dichloromethane and the uncoordianted triphenylphosphine group that are exchanging with each other. The signals are given at room temperature (20°C), 0°C and at 10° intervals down to –90°C.
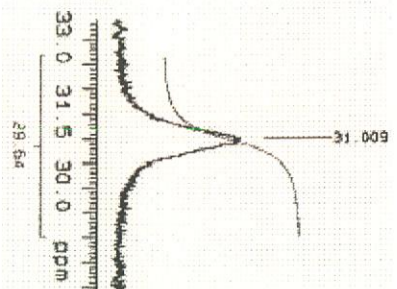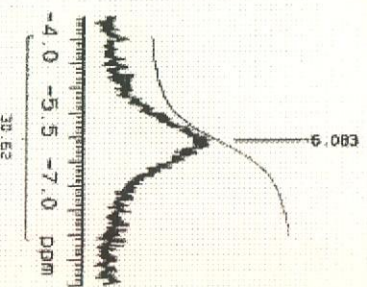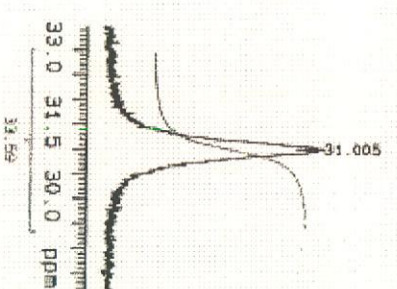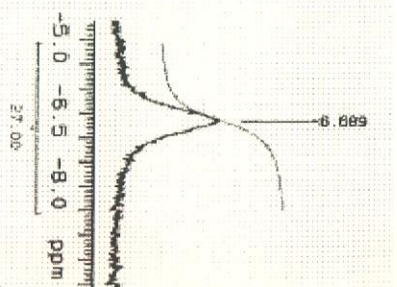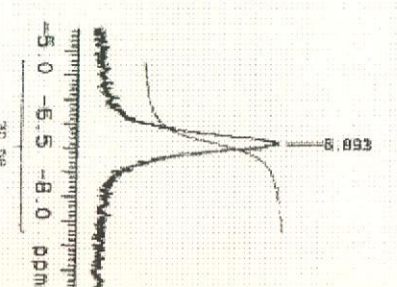

Room Temperature 20°C

0°C

-10°C

-20°C

-30°C

-40°C
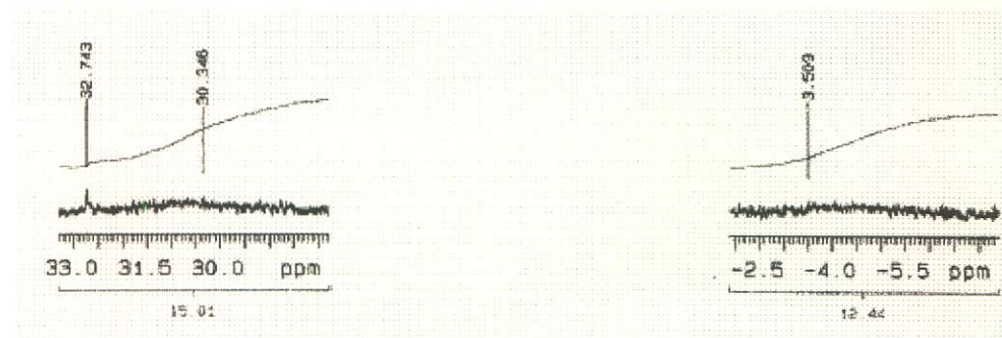
-90°C
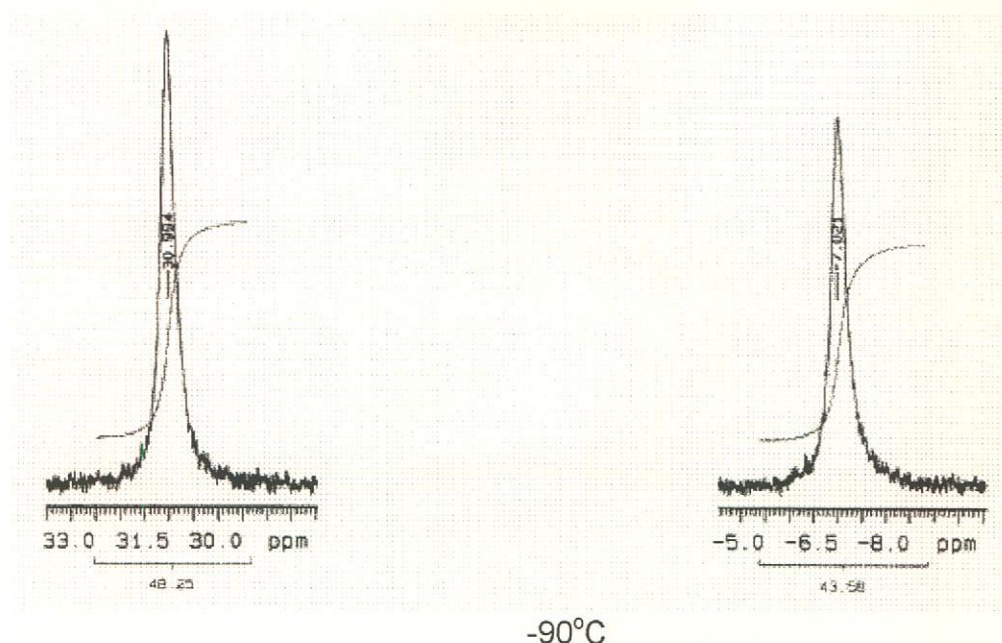
Figure 3.5 : Resonances of the phosphine ligand and exchanging triphenylphosphine group in d_2-dichloromethane.

T(°C)	T(K)	1/T(K)	k(A)[a]	ln k(A)	k(B)[a]	ln k(B)
20	293.15	0.0034	b	b	b	b
0	273.15	0.0037	778	6.7	778	6.7
-10	263.15	0.0038	721	6.6	675	6.5
-20	253.15	0.004	606	6.4	721	6.6
-30	243.15	0.0041	461	6.1	549	6.3
-40	233.15	0.0043	492	6.2	453	6.1
-50	223.15	0.0045	377	5.9	415	6.0
-70	203.15	0.0049	243	5.5	224	5.4
-80	193.15	0.0052	205	5.3	224	5.4
-90	183.15	0.0055	243	5.5	148	5.0

Table 3.9 : Measured approximate rate constant data for the calculation of E_a of complex **7** in CD_2Cl_2.

[a] Determined by $k = \pi(h - h_0)$ where

h = peak width at half height and

$h_0 = 1.5Hz$[28]

[b] Resolution of NMR too low to measure accurate width at half height.

Dichloromethane

Figure with axes "ln k" (vertical) and "1/T (1/K)" (horizontal).

Annotations on plot:
$y = -0.174x + 6.8946$
$R^2 = 0.9286$

$y = -0.2092x + 7.0493$
$R^2 = 0.9263$

Legend: Complex — Free PPh3 — Linear (Complex) - - - Linear (Free PPh3)

Figure 3.6 : Arrhenius plot for calculating the E_a of complex **7** in CD_2Cl_2.

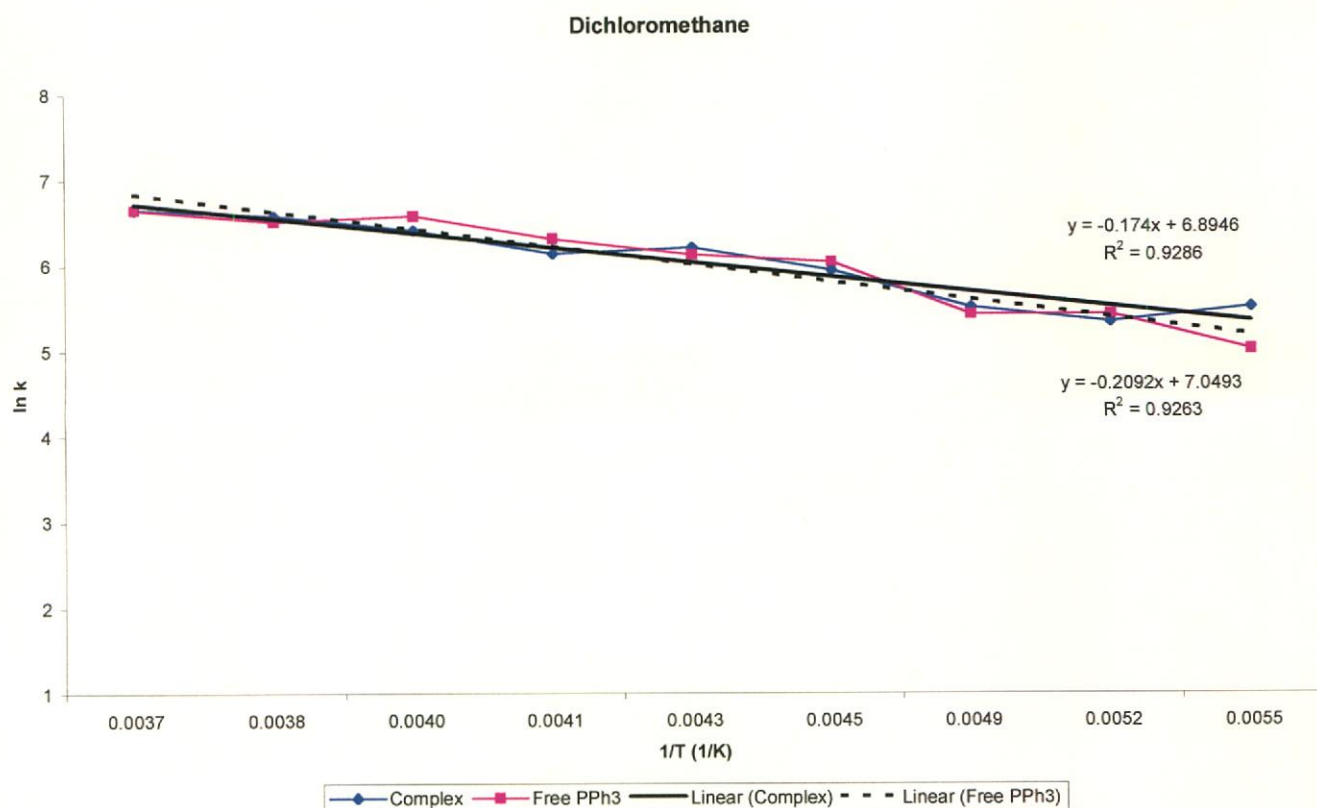| T($^{\circ}$C)	T(K)	1/T(K)	k(A)[a]	ln k(A)	k(B)[a]	ln k(B)
20	293.15	0.0034	1358	7.2	1637	7.4
0	273.15	0.0037	1175	7.1	1045	7.0
-10	263.15	0.0038	1050	7.0	855	6.8
-20	253.15	0.004	778	6.7	682	6.5
-30	243.15	0.0041	530	6.3	537	6.3
-40	233.15	0.0043	442	6.1	446	6.1
-50	223.15	0.0045	392	6.0	308	5.7
-60	213.15	0.0047	320	5.8	358	5.9

Table 3.10 : Measured approximate rate constant data for the calculation of E_a of complex **7** in C_6D_6.

[a] Determined by $k = \pi(h - h_0)$ where

h = peak width at half height and

h_0 = 1.5Hz

Benzene

$y = -0.2213x + 7.4957$
$R^2 = 0.9793$

$y = -0.2255x + 7.4681$
$R^2 = 0.9521$

Complex ─■─ Free PPh3 ──── Linear (Complex) ‑ ‑ ‑ Linear (Free PPh3)
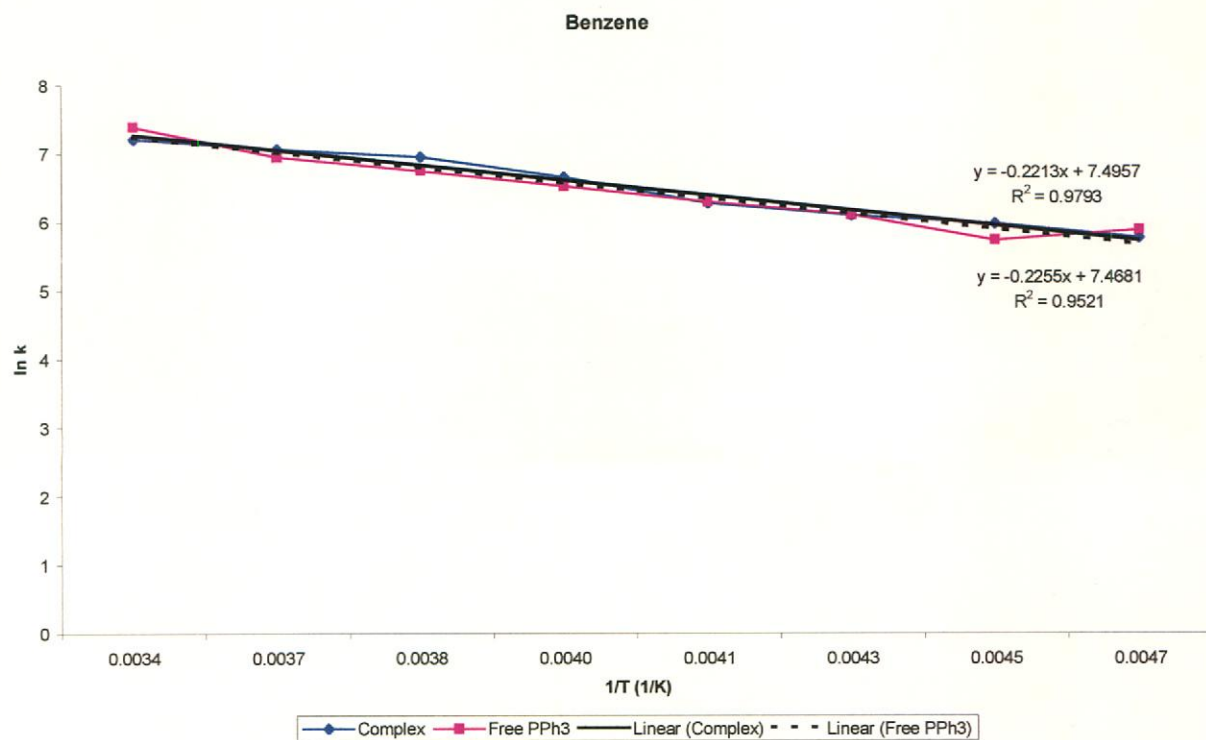
Figure 3.7 : Arrhenius plot for calculating the E_a of complex **7** in C_6D_6.

$T(^oC)$	T(K)	1/T(K)	Integration Value for species A	Integration value for spesies B	K^a	ln K
20	293.15	0.0034	25.06	26.22	1.05	0.05
0	273.15	0.0037	27.90	24.72	0.89	-0.12
-10	263.15	0.0038	19.34	23.42	1.21	0.19
-20	253.15	0.004	24.48	26.55	1.08	0.08
-30	243.15	0.0041	31.50	36.68	1.16	0.15
-40	233.15	0.0043	37.33	38.43	1.03	0.03
-50	223.15	0.0045	45.32	44.63	0.98	-0.02
-60	213.15	0.0047	35.12	36.18	1.03	0.03

Table 3.11 : Equilibrium constant data for the calculation of ΔG^o of complex **7** in C_6D_6.

T(^{o}C)	T(K)	1/T(K)	Integration value for species A	Integration value for species A	K^a	ln K
20	293.15	0.0034	14.89	13.01	0.87	-0.14
0	273.15	0.0037	26.80	18.60	0.69	-0.37
-10	263.15	0.0038	22.01	24.31	1.10	0.10
-20	253.15	0.004	26.77	35.34	1.32	0.28
-30	243.15	0.0041	38.89	35.20	0.90	-0.10
-40	233.15	0.0043	29.35	27.30	0.93	-0.07
-50	223.15	0.0045	32.19	30.62	0.95	-0.05
-70	203.15	0.0049	29.64	27.00	0.91	-0.09
-80	193.15	0.0052	33.59	30.56	0.91	-0.09
-90	183.15	0.0055	48.25	43.58	0.90	-0.10

Table 3.12 : Equilibrium constant data for the calculation of ΔG^o of complex **7** in CD_2Cl_2.
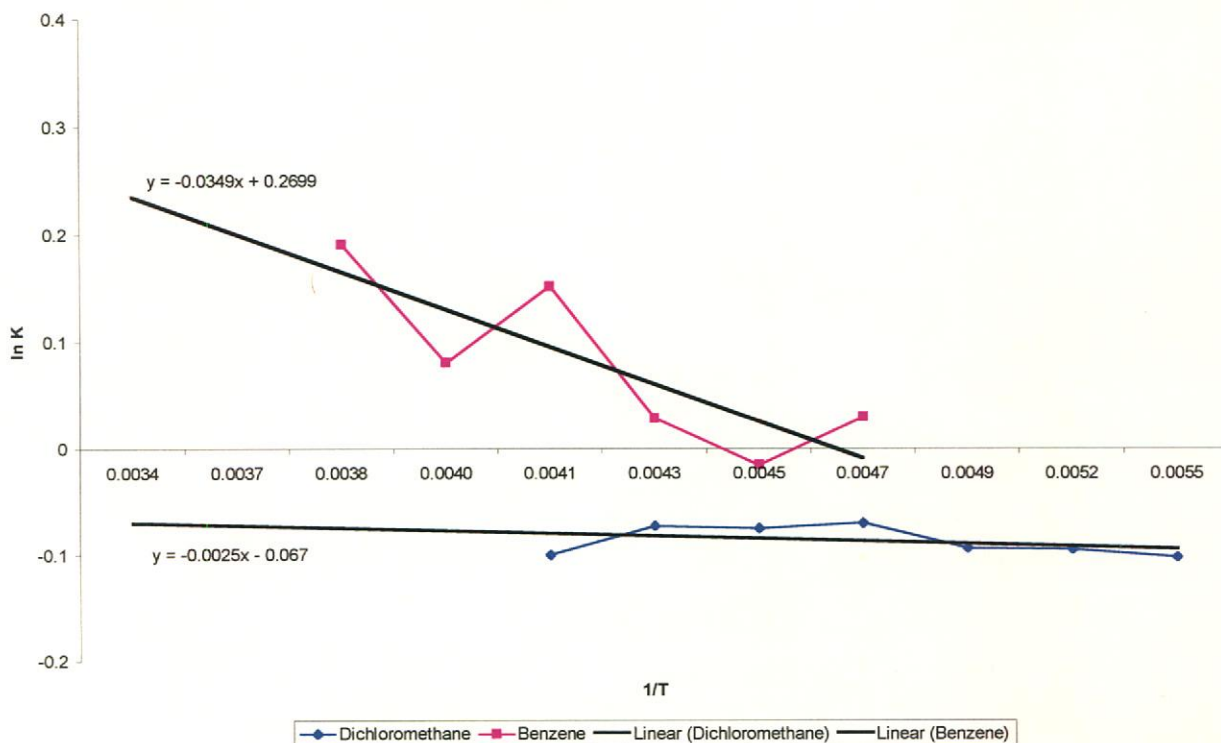
Figure 3.8 : Plot to calculate ΔG^o values for complex **7** in d_6-benzene and d_2-dichloromethane.

Solvent	Species	E_a (k.J.mol^{-1})	ΔG° (x10^{-2} k.J.mol^{-1})
d_6-Benzene	A	1.84	---
d_6-Benzene	B	1.880	---
d_2-Dichloromethane	A	1.45	---
d_2-Dichloromethane	B	1.74	---
d_6-Benzene	A & B	---	29.02
d_2-Dichloromethane	A & B	---	2.09

Table 3.13 : Summary of calculated E_a and ΔG° values of complex **7** in both d_6-Benzene and d_2-Dichloromethane.

It is evident in Figure 3.8 above, that there is a large deviation in both solvents from the linear line shape expected. This deviation from linearity is due to several factors. Firstly, the relaxation time of a free triphenylphosphine group differs from that of a coordinated triphenylphosphine group. This in itself can lead to a relatively large deviation from the required 1:1 integration ratio in the ^{31}P{^{1}H} NMR spectrum. Although there is a deviation from the 1:1 ratio in these spectra, the deviation is within acceptable experimental limits.

Secondly, the broadness of the peaks becomes so large close to room temperature that it becomes very difficult to clearly define and integrate the applicable peaks. It thus becomes difficult to clearly define the applicable integration region. This is more accentuated in the spectra obtained in d_2-dichloromethane.

Due to these strong deviations from linearity close to room temperature, the first four data points of the d_2-dichloromethane data series, and the first two data points in the d_6-benzene series of ln K vs. 1/T, were excluded from calculation of ΔG° (Figure 3.8).

Complex **7** has a square planar geometry as shown by single x-ray crystal structure analysis. Square planar d_8-transition metal complexes are known to almost exclusively undergo associative ligand substitution reactions by means of two parallel pathways.[29] It is known that the 4p$_z$ orbitals are not heavily utilized in metal-ligand σ-bonding and are therefore available for the addition

of a fifth ligand to the square planar coordination sphere.[30] Based on these arguments, the following substitution-elimination mechanism is proposed in Scheme 3.12 below for the equilibrium between complex **7** and the free triphenylphosphine group: -
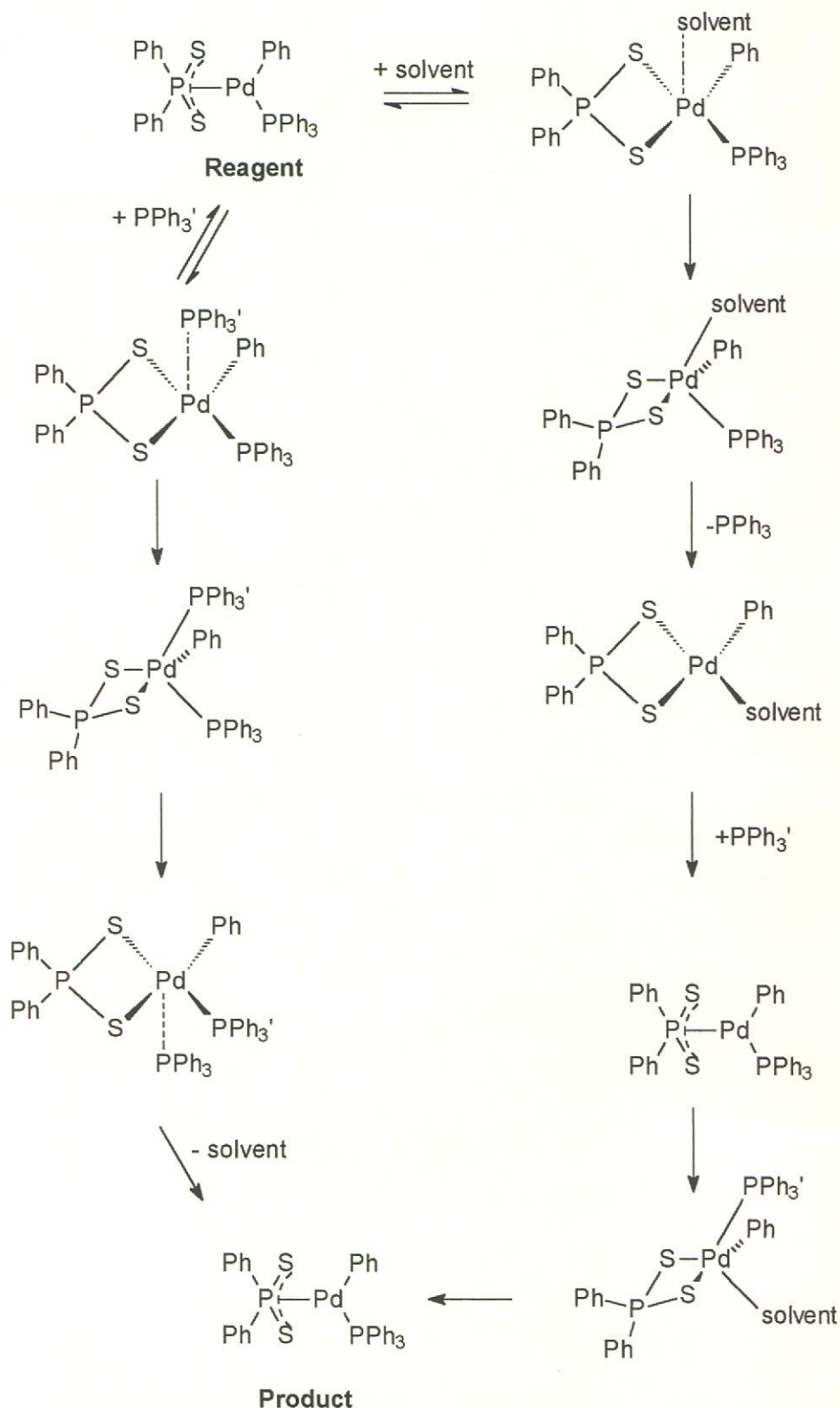

Figure 3.9 : Proposed substitution-elimination mechanism for complex **7**.

In the first pathway, the PPh$_3$ attacks the palladium complex and the reaction passes through a five coordinate transition state and intermediate that has a trigonal bipyramidal structure. The second pathway also involves the formation of a trigonal bipyramidal transition state, except the solvent is the entering group.

It can be seen that the calculated rate constants for the interchanging of the two triphenylphosphine groups differ greatly in the two different solvent systems analysed. The interchanging of the triphenylphosphine groups in the two different solvent systems was observed and monitored as described above, but a more in-depth investigation is required in order to be able to fully explain the observed solvent effect on a quantitative scale. In summary, the exchange illustrated in scheme 3.12 above occurs faster in benzene than in dichloromethane.

IV) _Mass spectrum for complex **7**, [η^3-(Ph)$_2$PS$_2$][Pd(PPh$_3$)(Ph)]._

The fragmentation pattern for complex **7** is illustrated in Scheme 3.14 below. Relative intensities are given in parenthesis. The molecular ion of complex **7** was observed at m/z 695. Subsequent fragmentation occurs along two pathways. One route, like many of the complexes in chapter 2, involves the immediate and total loss of the ligand followed by the further fragmentation of the original palladium-phenyl-triphenylphosphine section of the complex. The second route of fragmentation is, however, more complex. It involves the initial loss of a phenyl group followed by a further loss of sulphur. This fragmentation route then further splits into two parallel pathways, each of which is characterised by relatively high intensities of the ions formed.
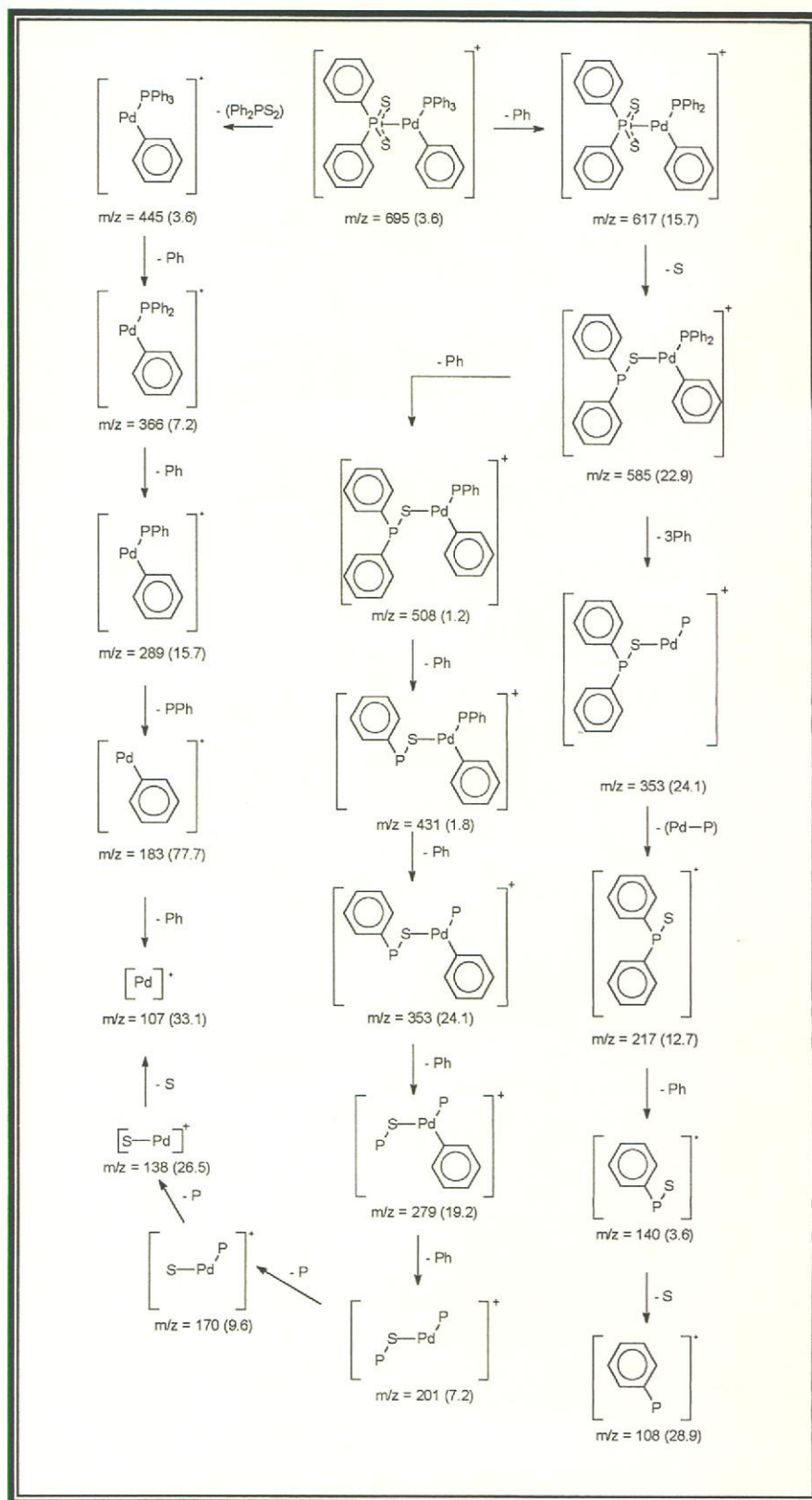
Scheme 3.14 : Mass spectrum fragmentation patterns for complex **7**.

[Relative intensities are given in parenthesis]

V) *Thermogravimetric analysis of the free ligand, diphenyl-dithio-phosphinic acid, and complex **7**.*

The thermal decomposition of the free ligand precursor, diphenyl-dithio-phosphinic acid, and that of complex **7** were studied to compare the thermal stability of the ligand precursor versus the complex as well as to investigate the possible existence of stable intermediates. In the available literature of similar complexes and ligands no indication of thermogravimetric analysis was found. In this manner the differences in the thermal decomposition curves that occur as a result of the complexation of the free ligand to the palladium starting complex could be highlighted.

Figure 3.9 is a graphic representation of the temperature program used to follow the thermal decomposition of ligand **7**. The program involved a $0 - 700^{\circ}C$-temperature range. Initially the temperature was increased from $0 - 30^{\circ}C$ at a rate of $5^{\circ}C$ min^{-1} and maintained at $30^{\circ}C$ for 6 minutes followed by a further $5^{\circ}C$ min^{-1} temperature increase to $700^{\circ}C$.
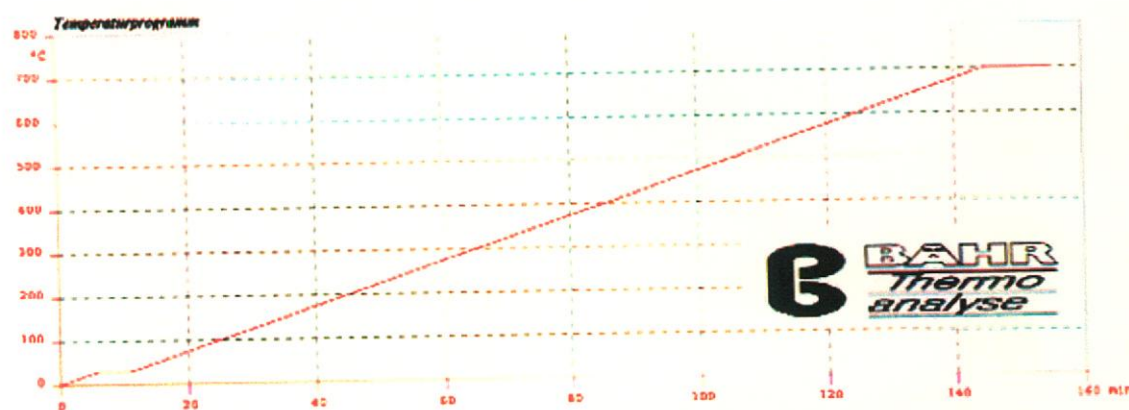

Figure 3.9 : Thermogravimetric analysis temperature program

Figure 3.10 below is a plot of TG and dif. TG versus temperature for ligand **7** while Figure 3.11 is a plot of DTA and TG versus time for the thermogravimetric decomposition analysis of ligand **7**.
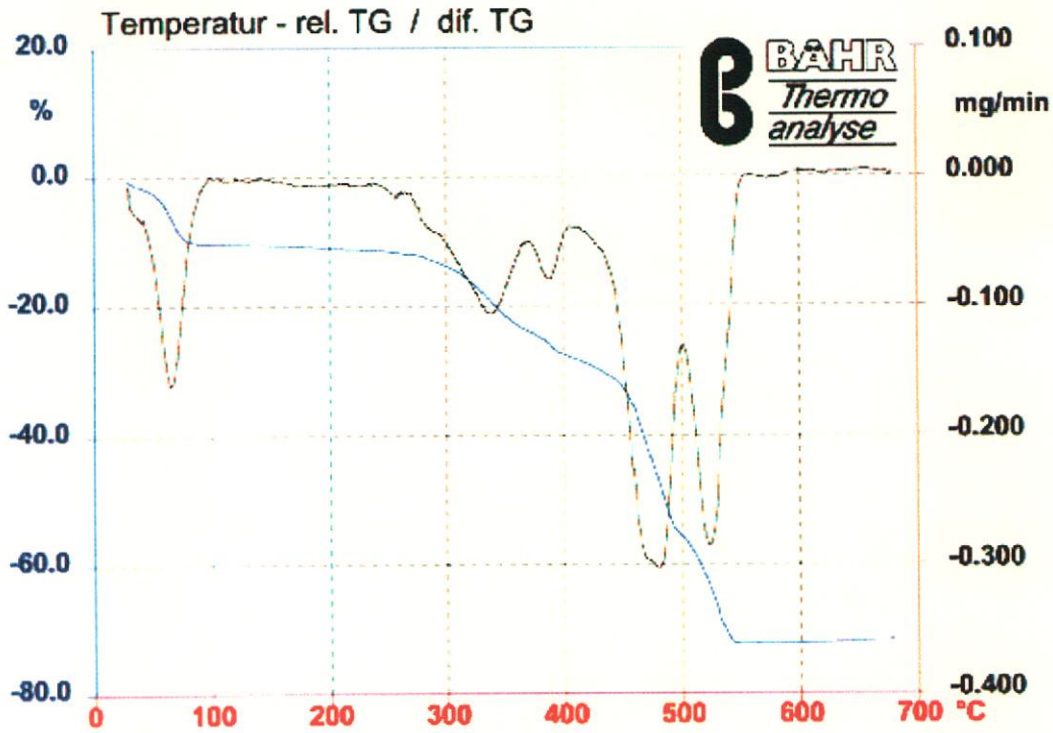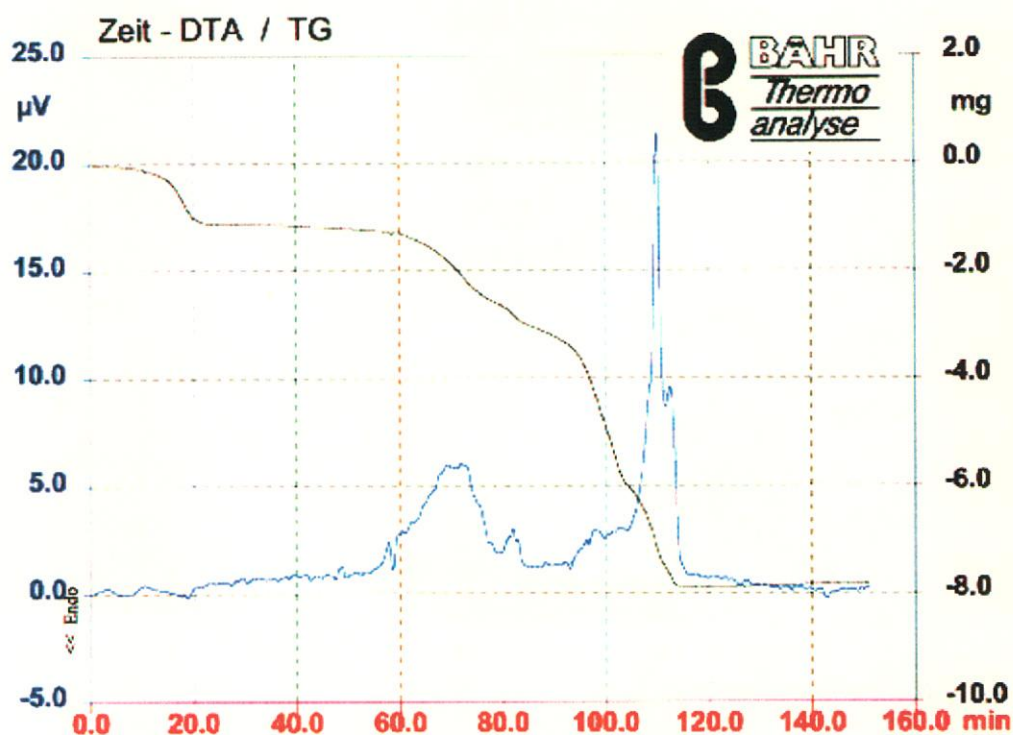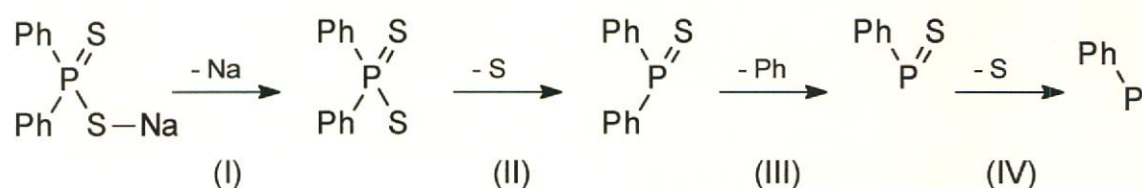

Figure 3.10 : TG and DTG versus temperature plot of the thermogravimetric decomposition analysis of ligand **7**.

Figure 3.11 : DTA and TG versus time plot of the thermogravimetric decomposition analysis of ligand **7**.

Scheme 3.15 illustrated below is a suggested decomposition route of ligand **7**. It involves four main decomposition steps.

Scheme 3.15 : Thermal decomposition of ligand **7**.

The decomposition process starts at 30°C and ends at 540°C. Step 1 in Scheme 3.15 above occurs at ~ 30°C, step 2 at ~270°C, step 3 at ~442°C and the final step at ~500°C. The four steps are well separated from one another. The plateaus that are evident in the integration curve in Figure 3.11 above indicate the existence of intermediates. The final P-Ph species formed appears to be thermally stable up to 700°C.

Figure 3.12 below is a plot of TG and dif. TG versus temperature while Figure 3.13 is a plot of DTA and TG versus time for the thermal decomposition of complex **7**.
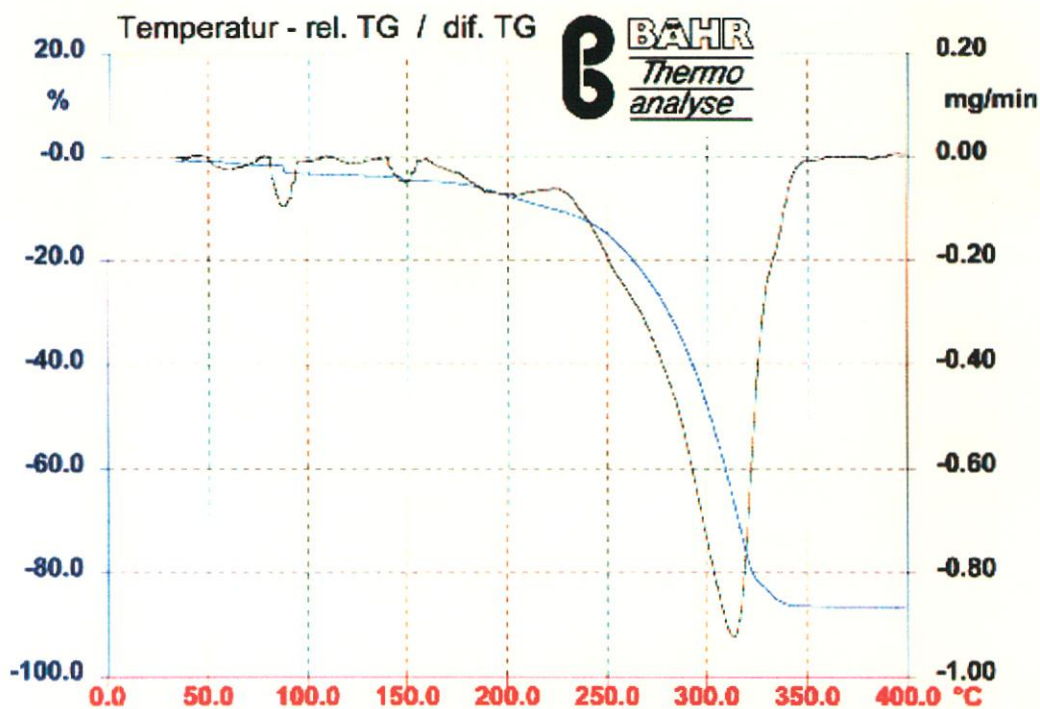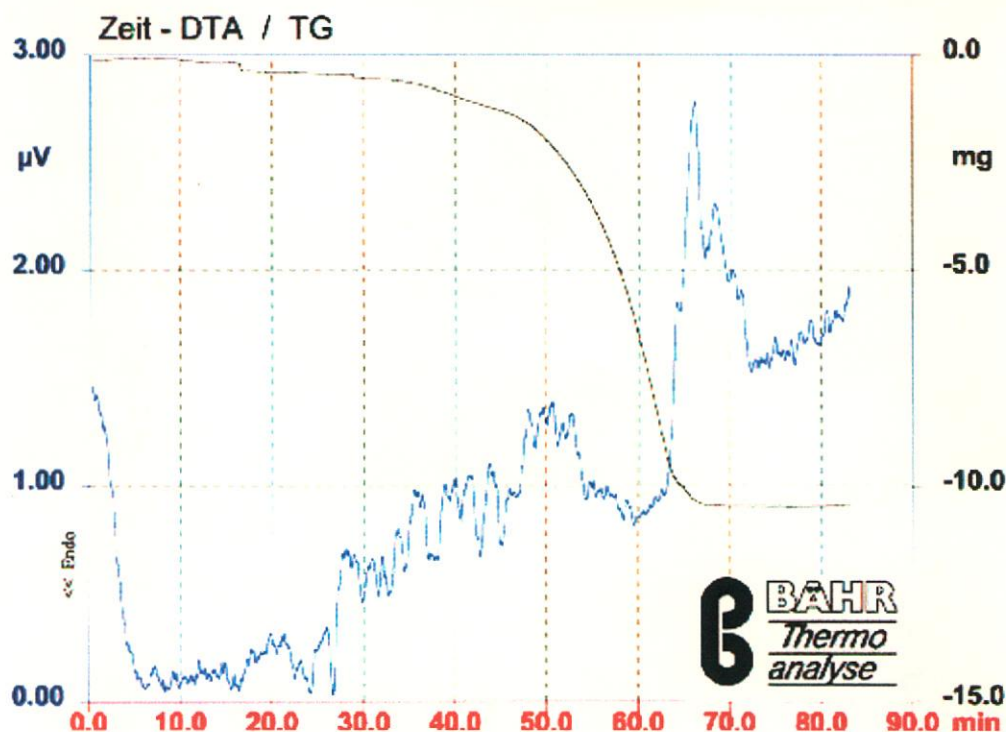

Figure 3.12 : TG and DTG versus temperature plot of the thermogravimetric decomposition analysis of complex **7**.

Figure 3.13 : DTA and TG versus time plot of the thermogravimetric decomposition analysis of complex **7**.

Complex **7** does not give distinct decomposition steps but rather a gradual continuous decomposition curve in the region of 200°C – 340°C. All the organic material of complex **7** is lost within this range leaving pure Pd that is stable to temperatures of 400°C. No similarities of the thermal decomposition trends were visible between that of the free ligand precursor (see Figure 3.10 and Figure 3.11) versus complex **7** (see Figure 3.12 and Figure 3.13).

VI) *Single crystal structure determination of complex* **7** *without solvent interaction.*

Single crystals of complex **7** were obtained by crystallization from two different solvent systems. This gave crystals with two different space groups.

A single colourless crystal of complex **7** was mounted on a glass fiber and transferred to Siemens SMART system CCD area detector diffractometer. All data were collected at room temperature with graphite monochromated Mo-K$_\alpha$ radiation. The empirical (SADABS) method of absorption correction was

applied. Unique sets of data with intensities greater than two times the standard deviation were used to solve the structure by the heavy atom (Patterson) method. Refinements were done using least squares refinement. All non-hydrogen atoms were refined anisotropically. For structure solution and refinement the ShelX-97 software package was used.[31] Structure figures were generated using Ortep-3. [32]

Selected crystallographic bond lengths and angles are listed in Table 3.14. All other crystallographic information is available from Dr. C. Esterhuysen Department of Chemistry University of Stellenbosch, Private Bag X1, 7602 Matieland South Africa.

Selected bond lengths(Å)		Bond angles(^{o})	
Pd1-C 31	2.006 (4)	C31-Pd-P2	87.5 (1)
Pd1-P1	2.956 (1)	C31-Pd-S2	90.7 (1)
Pd1-P2	2.254 (1)	C31-Pd1- S1	172.8 (1)
Pd1-S1	2.457 (1)	P2-Pd1-S1	99.1 (4)
Pd1-S2	2.403 (1)	P2-Pd1-S2	171.1 (4)
S1-P1	2.011 (1)	S2-Pd1-S1	83.3 (3)
S2-P1	2.014 (1)	S2-P1-S1	106.8 (6)
P1-C111	1.810 (4)	C31-Pd1-P1	132.5 (1)
P1-C121	1.812 (4)	P2-Pd1-P1	137.0 (3)
P2-C211	1.815 (4)	S2-Pd1-P1	42.6 (3)
P2-C231	1.821 (4)	S1-Pd1-P1	42.3 (3)
P2-C221	1.826 (4)	P1-S1-Pd1	82.2 (4)
		P1-S2-Pd1	83.5 (4)
		C111-P1-S1	111.3 (1)
		C121-P1-S1	112.4 (1)

Table 3.14 : Selected bond lengths (Å) and angles (^{o}) with e.s.d's. in parenthesis for complex **7**, without solvent interaction.
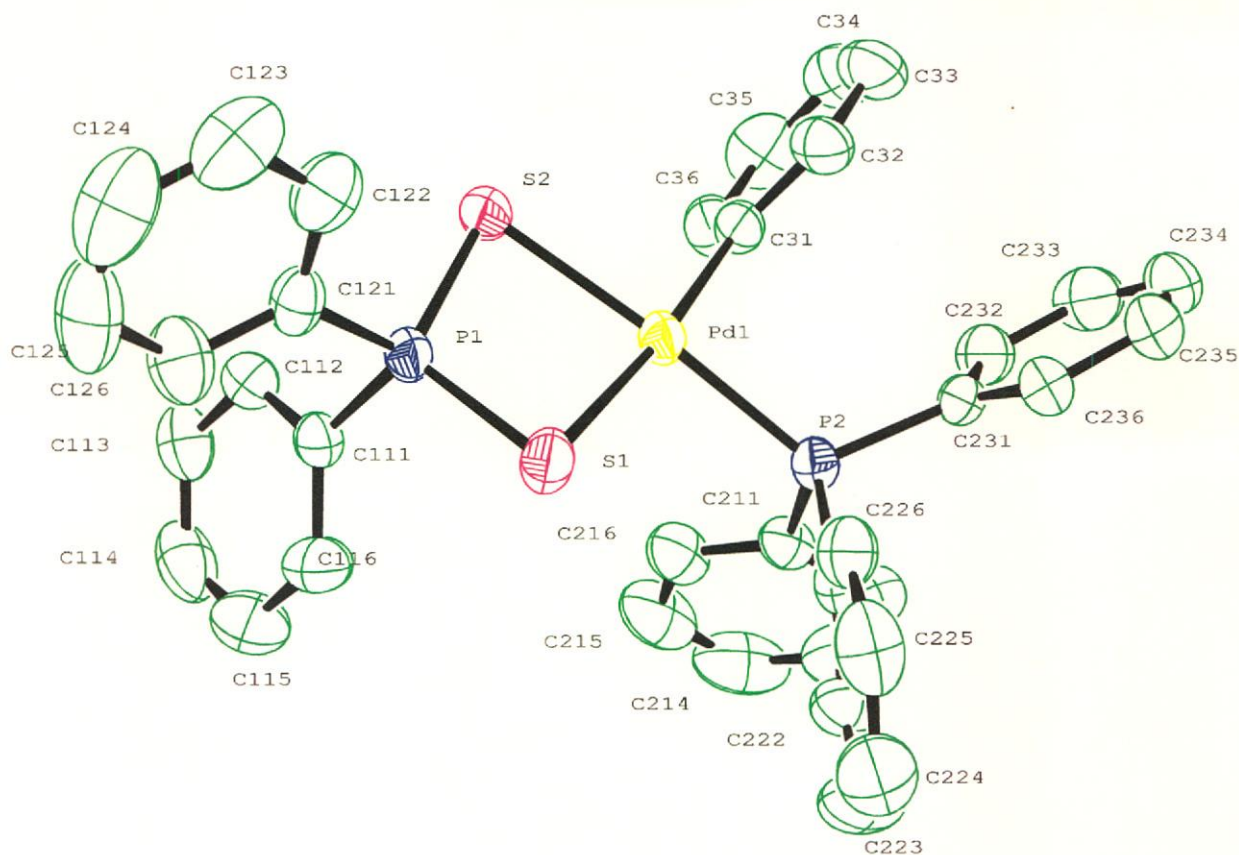
Figure 3.14 : Ortep-3 plot of molecular structure of complex **7** at 50% ellipsoid probability and showing the numbering scheme used.[33] Hydrogen Atoms have been excluded to make viewing easier.

VII) *Discussion of the structure and bonding in complex **7** (without solvent interaction).*

Bond angles and bond lengths for complex **7** are reported in Table 3.14 above. The crystal structure illustrated in Figure 3.14 above will be discussed with respect to the data listed in Table 3.14

As can be seen from the Cambridge Crystallographic Structural Database (CCSD), most organo-palladium complexes are square planar. In the ideal molecule the four atoms surrounding the palladium will lie at right angles to one another in the plane of the palladium. The average deviation from the ideal bond angles around the palladium with a square planar configuration was found to be 5.85° with the maximum being 9.07°. The average angle of deviation was calculated by taking the absolute value of the difference

between the experimental angle and the ideal angle (180° or 90°) and taking the average of the four resulting values while the maximum was the largest of the six numbers. The root mean square (RMS)[xv] of complex **7** was 0.111Å while the maximum deviation from planarity was 0.133Å. This maximum deviation from planarity for complex **7** is significantly greater than that of the palladium starting complex **1** (complex **1**, 0.026Å). The planarity of complex **7** is lost to compensate for the deviation in the bond angles around the palladium. Due to the bending of the complex, the phosphorus atom (P1) is sitting 0.5Å above the plane allowing it to come within 3Å of the palladium atom.

The plane containing the palladium atom and the sulphur atoms S1 and S2 is twisted by 10° with respect to the plane containing the Pd1, P2 and C31 atoms and by 23° compared to the plane containing the P1, S1 and S2 atoms.

The palladium-sulphur (Pd1-S1, Pd1-S2) and phosphorus-sulphur (S1-P1, S2-P1) bond lengths similar, within 0.05Å. The palladium-sulphur-phosphorus (Pd1-S1-P1 and Pd1-S2-P1) bond angles are also identical.

VIII) Discussion of the structure and bonding in complex 7' with solvent interaction.

Orange single crystals of complex **7'** were obtained by crystallization from a 1:1 THF:benzene solution. The space group and unit cell of the crystals of complex **7'** is different from that of **7**. THF crystallized in a 1:1 ratio with the complex.

The data for these crystals was collected with a Siemens SMART system CCD area detector diffractometer under the same conditions. The crystal structure was solved in the same manner as complex **7**.


[xv] RMS deviation $= \left[\dfrac{1}{N} \sum \left(x_i - \overline{x} \right)^2 \right]^{\frac{1}{2}}$, N = number of observations, x_i = value of observation i and $\overline{x}$ = mean

Selected bond lengths and angles are listed in Table 3.15 below. The structure of complex **7** with solvent interaction is illustrated in Figure 3.15. All other crystallographic information is available from Dr. C. Esterhuysen Department of Chemistry, Stellenbosch University, Private Bag X1, 7602 Matieland South Africa.

Selected bond lengths(Å)		Bond angles(°)	
Pd1-C31	2.016 (7)	C31-Pd1-P2	88.52 (19)
Pd1-P1	2.99	C31-Pd1-S2	170.33 (18)
Pd1-P2	2.2637 (18)	C31-Pd1-S1	87.50 (19)
Pd1-S1	2.381 (2)	P2-Pd1-S1	176.01 (7)
Pd1-S2	2.501 (2)	P2-Pd1-S2	100.37 (7)
S1-P1	2.009 (3)	S2-Pd1-S1	83.60 (7)
S2-P1	2.002 (3)	S2-P1-S1	108.46 (11)
P1-C111	1.808 (7)	P1-S1-Pd1	85.43 (9)
P1-C121	1.816 (8)	P1-S2-Pd1	82.43 (9)
P2-C211	1.834 (7)	C111-P1-S2	112.9 (3)
P2-C231	1.820 (7)	C121-P1-S1	111.0 (2)
P2-C221	1.841 (7)	C111-P1-S1	110.1 (3)

Table 3.15 : Selected bond lengths (Å) and angles (°) with e.s.d's. in parenthesis for complex **7'**.
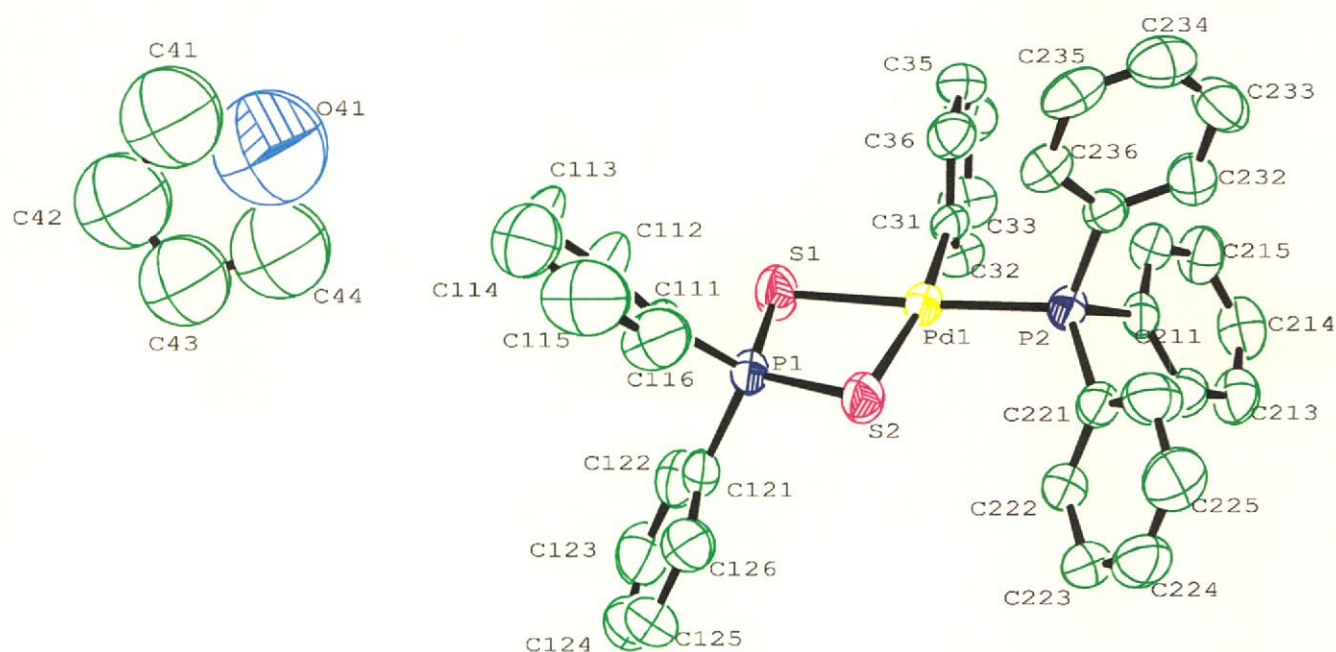
Figure 3.15 Ortep-3 plot of the molecular structure of complex **7'** at 50% ellipsoid probability, showing solvent interaction and the numbering scheme used.[34] Hydrogen Atoms have been omitted for clarity.

Bond angles and bond lengths for complex **7** are reported in Table 3.15. The crystal structure is illustrated in Figure 3.15.

As with the structure of complex **7**, there is a deviation from planarity within this structure as well as a deviation from the ideal bond angles around the palladium atom (Table 3.15). The average deviation from the ideal square bond planar bond angles around the palladium was found to be 5.74° with the maximum being 10.38°. The root mean square deviation (RMS) is 0.035Å while the maximum deviation from planarity is 0.047Å. These values were calculated in the same manner as before.

This constraint to planarity as compared to when there is no solvent interaction affects the palladium sulphur bond lengths significantly with the Pd-S1 bond [2.381(2) Å] being 0.120Å shorter than the Pd-S2 bond [2.501(2) Å]. This constraint to planarity also appears to contribute to the slight difference in

the palladium-sulphur-phosphorus bond angles (Pd-S1-P1 and Pd1-S2-P1) which differ by 3°.

IX). *Direct comparison between the crystal structures of complex 7 with and without solvent interaction.*

Before a direct comparison is made of the two crystal structures, it must be borne in mind that the following data is characteristic of phosphorus-sulphur bond lengths and angles[35]: -

Bond type	Bond length and bond angle
P-S bond length	2.1Å
P=S bond length	1.9Å
S-P-S bond angle	93° – 94°
S-P=S bond angle	116.1° – 116.4°

Table 3.16 : Characteristic bond lengths and bond angles of phosphorus sulphur bonds.

As can be seen from the table above, the P-S bond lengths in both the crystal structure of **7** and the crystal structure of **7'** compare well with the trends of similar bond types published in the literature.

The two tables below summarize the distinct differences between the two crystal structures of complex **7** (with and without solvent interaction). The tables include bond lengths and bond angles that are the most distinct. These bond angles and bond lengths listed below are not the only bond lengths and bond angles that differ between the two structures. For a more detailed comparison consult Table 3.14 and Table 3.15.

Bond Lengths (Å)	Structure 7	Structure 7'
Pd1-P1	2.96 (1)	2.99 (1)
Pd1-S1	2. 457 (1)	2.381 (2)
Pd1-S2	2.403 (1)	2.501 (2)

Table 3.17 : Comparison of bond lengths between the two different crystal structures of complex **7** and **7'**.

Bond Angles	Structure 7	Structure 7'
P2-Pd1-S1	99.07 (4)	100.37 (7)
P2-Pd1-S2	171.08 (4)	176.01 (7)

Table 3.18 : Comparison of bond angles between the two different crystal structures of complex **7** and **7'**.

The most important differences between the two crystal structures can be summarized as follows: -

☞ There is a distinct and significant deviation from square planar geometry of the central palladium atom in **7** while the structure **7'** conforms closer to the classic square planar conformation of palladium (II) complexes.

☞ In the crystal structure of **7**, the palladium sulphur bond lengths (Pd1-S1, Pd1-S2) and the sulphur phosphorus (S1-P1, S2-P1) bond lengths are similar in length while in the crystal structure of **7'**, there is a small yet noticeable difference in the palladium sulphur bond lengths. The sulphur phosphorus bond lengths in the second structure however remain similar to each other.

The planarity of the Pd-S-P-S 4-membered rings in both **7** and **7'** differ. As a result of the aforementioned 4-membered ring in **7** being 'bent', the phosphorus and palladium atoms are close enough to allow a Pd-P1 interaction (2.96(1) Å). This Pd-P1 interaction is not evident in **7'** (2.99 (1)Å).

These differences that are highlighted above become visibly evident when the packing of the molecules within the unit cell of each structure are compared. The crystal system in **7** is monoclinic while in **7'** it is triclinic. In the case of **7'**, the molecules pack in strings alternating with solvent molecules. The steric influence of the solvent molecules constrains the Pd-S-P-S2 plane to be flat and parallel to one another. However, in the case of **7** the ligand is able to buckle to relieve the strain in the 4-membered ring that is aggravated by the bulky triphenylphosphine group. The molecules pack together in an interlocking network.

Figures 3.16 and 3.17 below show the different crystal packing of **7** compared to **7'**.
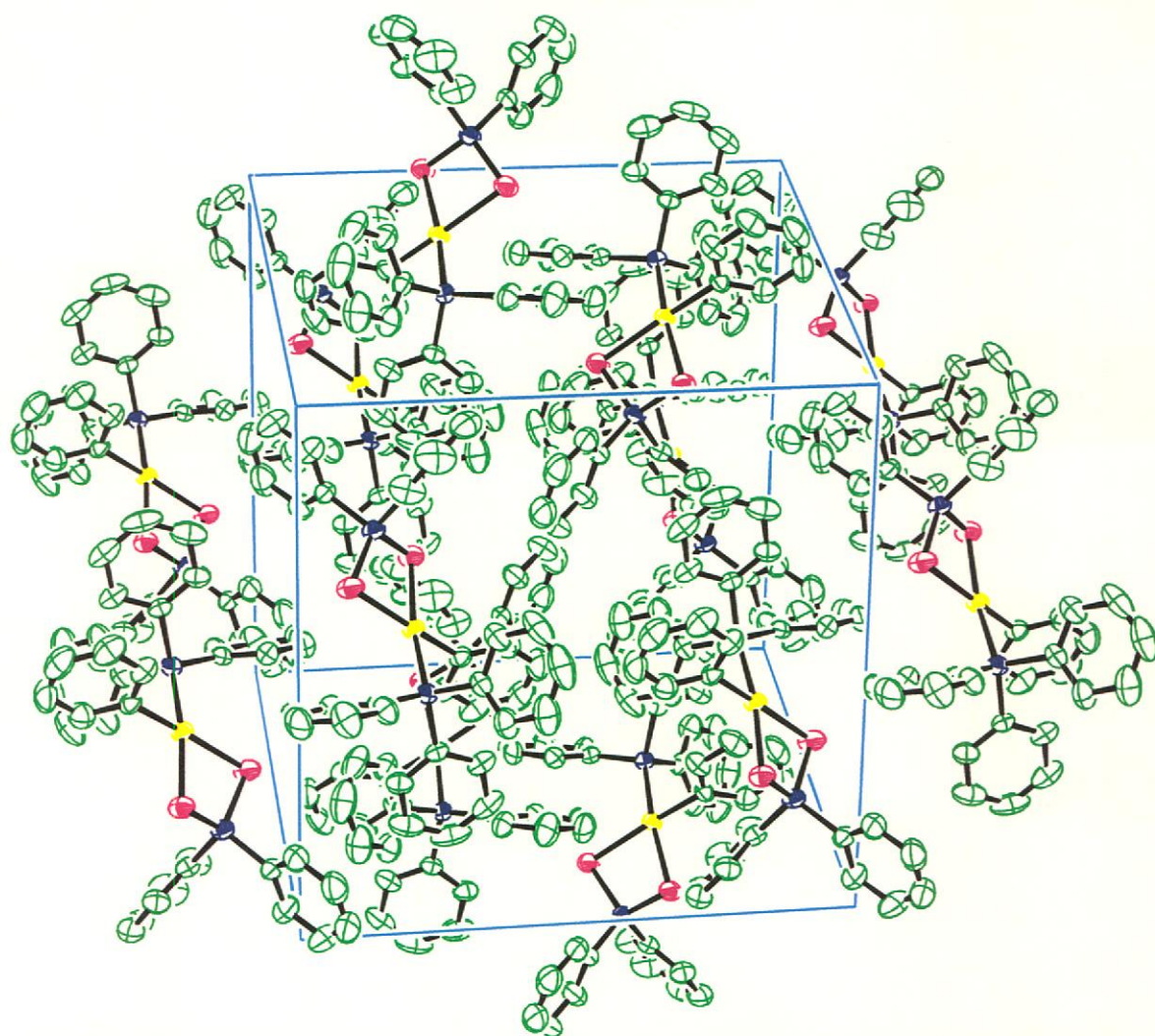
Figure 3.16 : Ortep-3 plot of the unit cell of complex **7** at 50% ellipsoid probability with no solvent interaction.[36] Hydrogen atoms have been omitted for clarity.
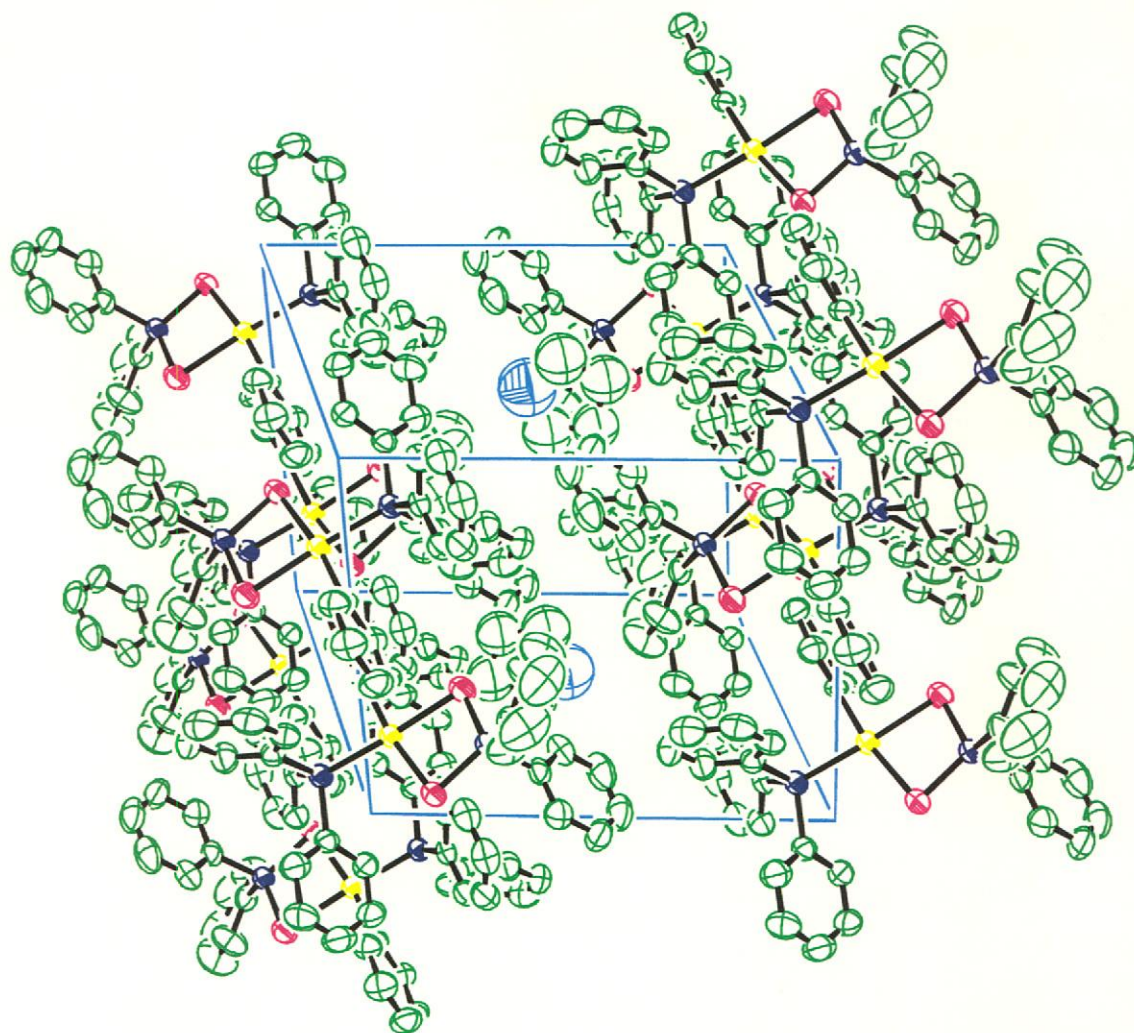
Figure 3.17 : Ortep-3 plot of the unit cell of complex **7'** at 50% ellipsoid probability.[37] Hydrogen atoms have been omitted for clarity.

3.3 *Experimental*

3.3.1 Materials

Solvents:

High spectroscopic grade solvents were used and were pre-dried over 4Å molecular sieves for at least 48 hours prior to use. All solvents were freshly distilled under nitrogen and used immediately.

Diethyl ether, tetrahydroforan (THF), benzene and hexane were distilled under nitrogen over sodium with the formation of a benzophenone ketyl as indicator. Dichloromethane was distilled over calcium hydried under nitrogen. All alcohols were distilled over magnesium shavings under nitrogen or argon. Alkyl lithium reagents were standardized by literature methods[38].

All deuterated solvents, dichloromethane (d_2-CD_2Cl_2) and benzene (d_6-C_6D_6), that were used in the spectroscopic investigations for the complexes and ligands in this series were purchased from Aldrich. All these solvents were stored over 4Å molecular sieves under an inert atmosphere in order to keep them free from moisture and oxygen.

3.3.2 *Physical Methods.*

A. General:

Unless otherwise noted, all reactions and manipulations were carried out under an inert atmosphere with a positive gas flow of argon or nitrogen using standard vacuum line and Schlenk techniques. Solutions were stirred magnetically with Teflon coated stirrer bars. Room temperature refers to 22-24°C. Glassware was oven dried at ±120°C, assembled while hot and cooled under vacuum.

B. Instrumentation:

➤ *Melting points: -*

Melting points were determined on a standard Büchi 535 apparatus and are uncorrected.

➢ *Mass Spectroscopy*

MS spectra were obtained by one of the following techniques: -

- FAB-MS (Fast Atom Bombardment Mass Spectra) spectra were recorded on a Micromass DG 70/70E double focussing mass spectrometer coupled to an Ion Tech fast atom bombardment unit using Xenon gas as bombardment atoms.

- Standard MS Spectra were obtained by means of the electron impact mass spectrometry technique on an AMD INTECTRA GmbH 604 double focusing mass spectrometer.

➢ *Infra Red Spectroscopy*

Infra red spectral data was obtained using the following two instruments: -

- Perkin Elmer FT1600 series (4000 to 600cm^{-1}) with samples prepared as films between NaCl plates using hexachloro-1,3-butadien or as standard liquid cell solutions in anhydrous dichloromethane with 16 scans with 4cm^{-1} resolution.

- Perkin Elmer 841 IR spectrometer (4000 to 600cm^{-1}) with samples prepared as films between NaCl plates using hexachloro-1,3-butadien.

➢ *Nuclear Magnetic Resonance Spectroscopy*

- ^1H, $^{13}C\{^1H\}$, $^{31}P\{^1H\}$ NMR data were recorded on a Varian VXR 300 FT spectrometer at.

NMR data is expressed as parts per million (ppm) downfield from the internal (TMS) or external standard used. The respective nuclei were recorded under the following parameters: -

Nucleus	*Frequency*	*Standard*
^1H	300 MHz	$(CH_3)_4Si$ as internal standard
$^{13}C\{^1H\}$	75 MHz	$(CH_3)_4Si$ as internal standard
APT $\{^1H\}$	75 MHz	$(CH_3)_4Si$ as internal standard
$^{31}P\{^1H\}$	121 MHz	85% H_3PO_4 as external standard

Table 3.21 : NMR spectroscopy parameters used.

➢ *X-ray crystallography:*

Crystals that were suitable for use in diffraction intensity measurements at room temperature were mounted on a glass fiber using fast adhesive. Crystal structure data collection and correction procedures were carried out on an Phillips PW1100 diffractometer or a Siemens SMART system diffractometer. All systematic absences were consistent with the space groups assigned in each case. The positions of the hydrogens in each case were calculated by assuming idealized geometries.
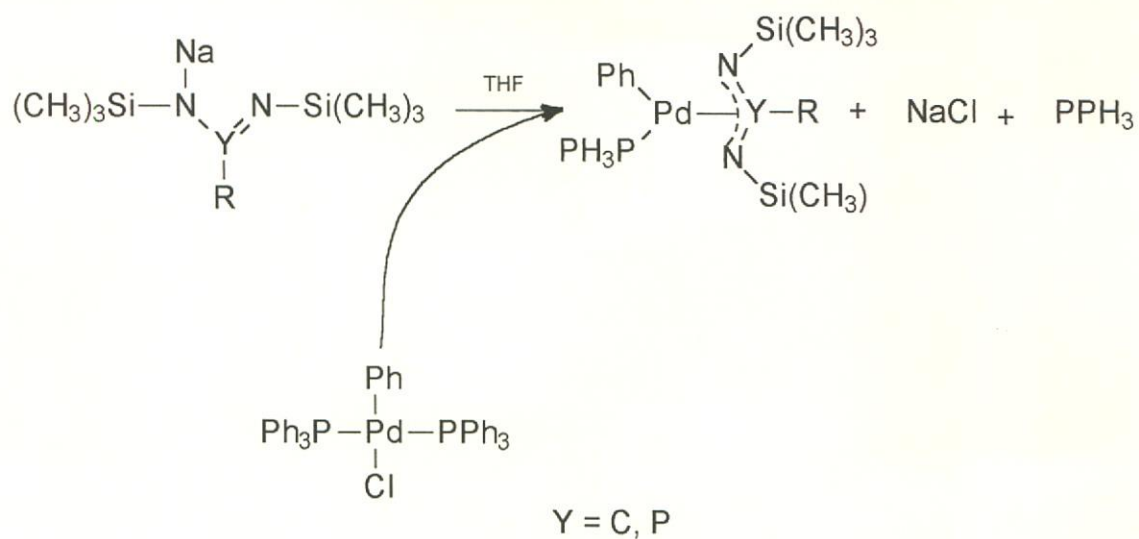
C. General preparation of starting materials and ligands:

Several of the starting materials and the ligands were synthesized from literature and have been referenced accordingly. However, almost all of the literature methods that have been used to synthesise the ligands have been modified to varying degrees since these literature methods most often refer to different target complexes than those prepared here. For this reason, detailed methods of preparation have been given for all the ligands and starting materials used in this chapter.

D. General Preparation of Complexes.
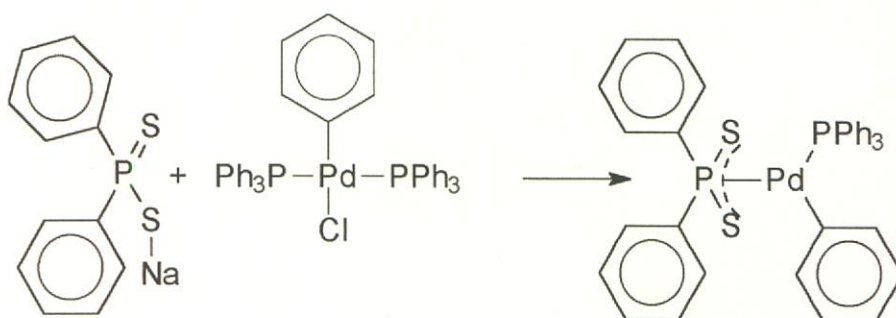
In the preparation of the complexes synthesised here, standard Schlenk techniques were employed throughout. All solvents were dried and purified by standard methods. All other reagents, unless otherwise stated in the relevant sections, were used as received.

The general methods of preparation of the complexes in this series were according to Scheme 3.13 and Scheme 3.14 below: -

$$(CH_3)_3Si-N \overset{\overset{\displaystyle Na}{|}}{\underset{\underset{\displaystyle R}{\overset{\displaystyle |}{Y}}}{}} N-Si(CH_3)_3 \quad \xrightarrow{\text{THF}} \quad \underset{PH_3P}{\overset{Ph}{\diagdown}} Pd \overset{\overset{\displaystyle N-Si(CH_3)_3}{\parallel}}{\underset{\underset{\displaystyle Si(CH_3)}{N}}{Y-R}} \quad + \quad NaCl \quad + \quad PPH_3$$

$$Ph_3P-\overset{\overset{\displaystyle Ph}{|}}{\underset{\underset{\displaystyle Cl}{|}}{Pd}}-PPh_3$$

$$Y = C, P$$

Scheme 3.13

Scheme 3.14

3.3.2.1 <u>Preparation of complex 5, [[η^3-((CH₃)₃SiN)₂C(Ph)Pd(PPh₃)(Ph)]</u>.

i) Synthesis of hexamethyldisilazine, ((CH₃)₃Si)₂NH.

Hexamethyldisilazine was synthesised according to the reaction illustrated below[39].

$$2(CH_3)_3Si—Cl + 3NH_3 \longrightarrow \begin{array}{c}(CH_3)_3Si\\ \\(CH_3)_3Si\end{array}N—H + 2NH_4Cl_{(s)}$$
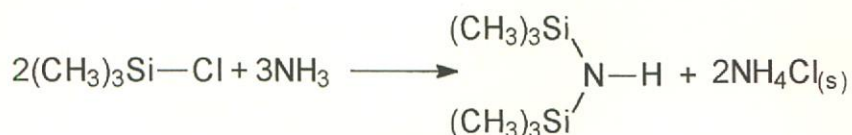
Reaction 3.1 : Synthesis of hexamethyldisilazine.

Trimethylchlorosilane (1 mol, 109g) was dissolved in 500ml of anhydrous ether in a 1 liter round bottomed flask. The flask was fitted with an efficient reflux condenser bearing a side arm fitted with a gas inlet tube through which ammonia gas was bubbled[xvi].

Upon the introduction of ammonia, a white precipitate of ammonium chloride formed almost immediately. The solution was brought to reflux temperature and the slow introduction of ammonia was maintained for six hours.

After six hours, the precipitate was allowed to settle and the ethereal solution was decanted and filtered. The precipitate was washed with 3x50ml of ether. The ethereal extracts were concentrated on a Buchi rotovap. The concentrated solution was then transferred to flame dried distillation apparatus and distilled under vacuum. The pure product, hexamethyldisilazine, was collected at 118°C at 6mm Hg.

Yield : 10.5%

(Yield based on mole trimethylchlorosilane used.)

ii) Synthesis of NaNH₂.

NaNH₂ was synthesised according to reaction 2 illustrated below[40]: -

---

[xvi] *Note: An effective reflux condenser must be used to avoid the neck of the reflux condenser becoming blocked by the ammonium chloride that forms during the refluxing process.*

$$2Na + 2NH_3 \longrightarrow 2NaNH_2 + H_2$$

Reaction 2 : Synthesis of $NaNH_2$.

Ammonia gas was liquefied in the following manner: -
A 1 litre three-necked round bottomed flask was fitted to a mechanical stirrer, 1 one-way bubbler and a gas inlet tap that was connected to a pre-cooler trap. The pre-cooling trap was cooled to -30°C and the reaction flask was cooled to -80°C. A slow stream of ammonia gas was allowed to flow through the system causing the ammonia gas to condense. Once ±500ml of liquid ammonia was collected, the ammonia gas flow was terminated and the system was flushed with nitrogen.

Iron nitrate ($Fe(NO_3)_3.9H_2O$), 0.250g, and sodium metal, 25.00g, was added to the liquid ammonia. The sodium metal lumps were previously rinsed with anhydrous pentane to remove the mineral oil. Innitially the ammonia solution turned blue, but once all the sodium was dissolved and had formed NH_2Na, the solution had a light gray appearance.

After the reaction was deemed to be complete (visual inspection), the solution was allowed to reach room temperature and the liquid ammonia was allowed to evaporate and escape through the oil bubbler over night.

iii) Synthesis of sodium bis-trimethylsilylamide, $((CH_3)_3Si)_2N-Na$.
Sodium bis-trimethylsilylamide was synthesised according to the reaction illustrated below[41].
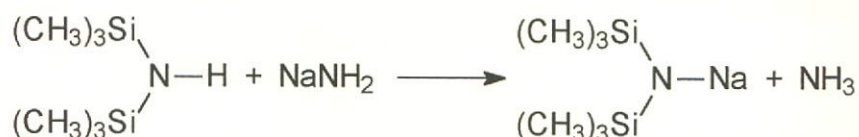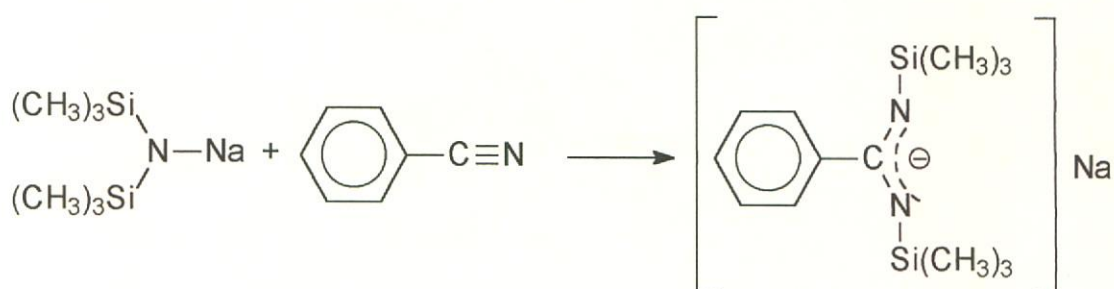

Reaction 3 : Synthesis of sodium bis-trimethylsilylamide.

The previously synthesised hexamethyldisilazine, 10.00g, was added to 24.60ml of benzene and 2.160g of $NaNH_2$ thereby creating a 30% $NaNH_2$/benzene solution. The solution was gently brought to reflux temperature and refluxed for 4 – 5 hours. The solution was allowed to cool to room temperature and evaporated to dryness under reduced pressure to yield a white salt.

iv) Synthesis of sodium-N'N'-bis(trimethylsilyl)benzamidinate.
Sodium-N'N'-bis(trimethylsilyl)benzamidinate was synthesised based on known literature methods[42] as illustrated in reaction 4 below: -

Reaction 4 : Synthesis of sodium-N'N'-bis(trimethylsilyl)benzamidinate.

Sodium bis-trimethylsilylamide, 1.834g, was dissolved in ±10 ml of anhydrous ether. Benzonitrile, 1.02ml, was added to the mixture and stirred vigorously for 24 hours. The solvent was removed under reduced pressure to yield a white salt.

Yield: 2.664g (9.299x10^{-3} mol), 92.9%
(Yield based on mole sodium bis-trimethylsilylamide used.)

*v) Synthesis of complex **5**, [η^3-((CH$_3$)$_3$SiN)$_2$C(Ph)Pd(PPh$_3$)(Ph)].*
Complex **5** was prepared according to scheme 3.15 illustrated below: -
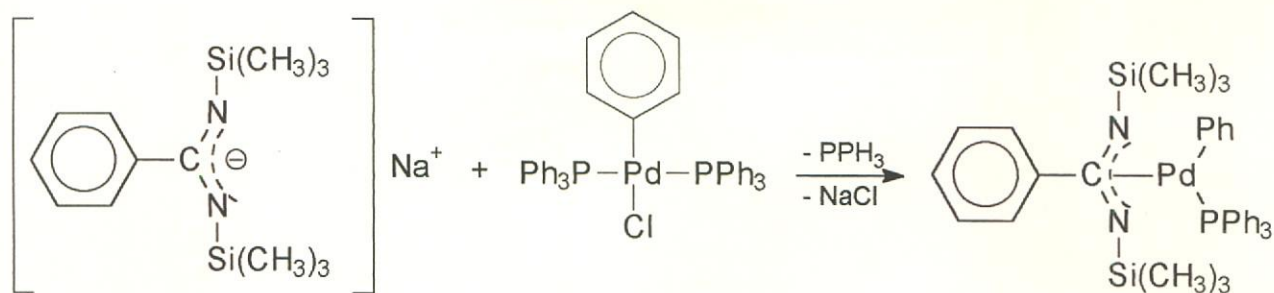
Scheme 3.15 : Preparation of complex **5**.

Sodium-N'N'-bis(trimethylsilyl)benzamidinate, 4.842 x 10^{-4}mol (0.139g, 1.8 equiv.) was dissolved in 7.5ml of THF and added dropwise to 2.689 x 10^{-4}mol (0.200g) of $(Ph_3P)_2Pd(Ph)(Cl)$ previously dissolved in 7.5ml of anhydrous THF. The reaction mixture was allowed to stir for 48 hours. At this time, a very fine precipitate was evident. The reaction mixture was then filtered through a celite packed filter and reduced to dryness under reduced pressure.

Yield = 68%

(Yield based on mole sodium-N'N'-bis(trimethylsilyl)benzamidinate initially used.)

3.3.2.2 Preparation of complex 6, $[\eta^3\text{-}(Ph)_2P(NSi(CH_3)_3)_2]Pd(PPh_3)(Ph)$

i) Synthesis of $(CH_3)_3SiN=P(Ph)_2\text{-}NHSi(CH_3)_3$.

The synthesis of the ligand used in the preparation of complex **6** was carried out according to scheme 3.15 which is based on a literature known method for the synthesis of $(C_6H_5)_3SiN=P(C_6H_5)_2NHSi(C_6H_5)_3$[43, 44]: -

$$(CH_3)_3SiCl + NaN_3 \longrightarrow (CH_3)_3SiN_3 + NaCl$$
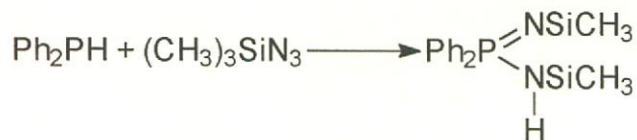
Scheme 3.16 : Synthesis of $(CH_3)_3SiN=P(Ph)_2\text{-}NHSi(CH_3)_3$.

Synthesis of trimethylsilylazide (CH₃)₃SiN₃: -

NaN_3, 16.2g, was dissolved in 70ml of anhydrous pyridine and refluxed under an inert atmosphere for 8 hours. The pyridine was previously prepared by refluxing it over CaH. The $(CH_3)_3SiN_3$ was then isolated by fractional distillation.

Synthesis of (CH₃)₃SiN=P(Ph)₂-NHSi(CH₃)₃

Ph_2PH, 0.582g (3.126×10^{-3} mol), and 0.971g (8.430×10^{-3} mol) of $(CH_3)_3SiN_3$ were heated under an inert atmosphere to 110 –115°C for 90 hours in a Schlenk tube fitted with a bubbler system. After the heating period the reaction mixture was washed with anhydrous ether and crystallized from anhydrous hexane.

Yield = 69%

(Yield based on mol Ph_2PH used.

Literature reported yield = 71%)

ii) Synthesis of complex 6, [(η³-(Ph)₂P(NSi(CH₃)₃)₂)Pd(PPh₃)(Ph)].

The synthesis of complex **6** was carried out according to scheme 3.18: -
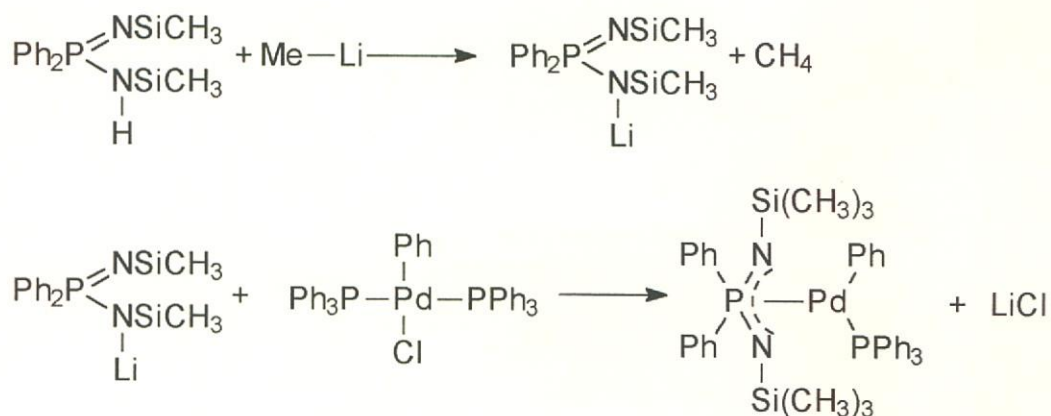
Scheme 3.18 : Preparation of complex **6**.

The deprotonation of the ligand in the first step in scheme 3.18 above was carried out according to a known literature method[45]. 5.5g (15.2mmol) of $(CH_3)_3SiN=P(Ph)_2-NHSi(CH_3)_3$ was dissolved in 20ml of anhydrous ether.

15.23mmol of methyl lithium in 9ml of anhydrous ether was added dropwise to the solution and the reaction mixture was stirred for a further 2 hours. The solvent was then removed under reduced pressure.

The lithium salt, 0.186g, prepared in scheme 3.18 above was dissolved in ±7ml anhydrous THF and added dropwise to 0.200g of $(Ph_3P)_2(Ph)PdCl$ dissolved in ±7ml anhydrous THF. The reaction mixture was vigorously stirred at room temperature for a further 2 days. The reaction mixture was filtered though an anhydrous celite packed filter and the solvent was removed under reduced pressure to yield a yellow powder.
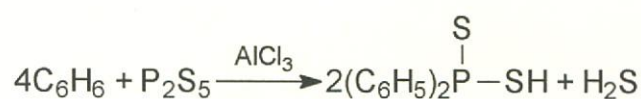
Yield = 89%

(Yield based on mole $(CH_3)_3SiN=P(Ph)_2-NSi(CH_3)_3Li$ initially used.)

3.3.2.3 Preparation of complex 7, [η^3-(Ph)$_2$PS$_2$][Pd(PPh$_3$)(Ph)].

i)Synthesis of diphenyl-dithio-phosphinic acid.

The synthesis of diphenyl-dithio-phosphinic acid used to prepare complex **7** was carried out according to known literature methods and is illustrated below[46].

$$4C_6H_6 + P_2S_5 \xrightarrow{AlCl_3} 2(C_6H_5)_2\overset{\displaystyle S}{\overset{\displaystyle \|}{P}}-SH + H_2S$$

Scheme 3.19 : Preparation of diphenyl-dithio-phosphinic acid.

A reaction mixture of 468g (6 mol) of benzene and 189g (0.85mol) phosphor-(V)-sulphide is heated to 65°C and stirred for 4 hours with the addition of 457g (3.4 mol) aluminiumchloride over this time period. While the aluminiumchloride is being added, the temperature of the reaction mixture was brought to 90°C and maintained at this temperature for a further 10 hours. The reaction mixture was allowed to cool to room temperature followed by further cooling to 0°C in an ice bath for several hours. The cold solution is extracted with

benzene. The combined extracts are reduced to dryness under reduced pressure to yield the product in a high degree of purity.

Dissolving the product in a 10% sodium hydroxide solution, acidifying it and extracting it with benzene further purified the raw product. The benzene was removed under reduced pressure and the product was re-crystallized from isopropanol.
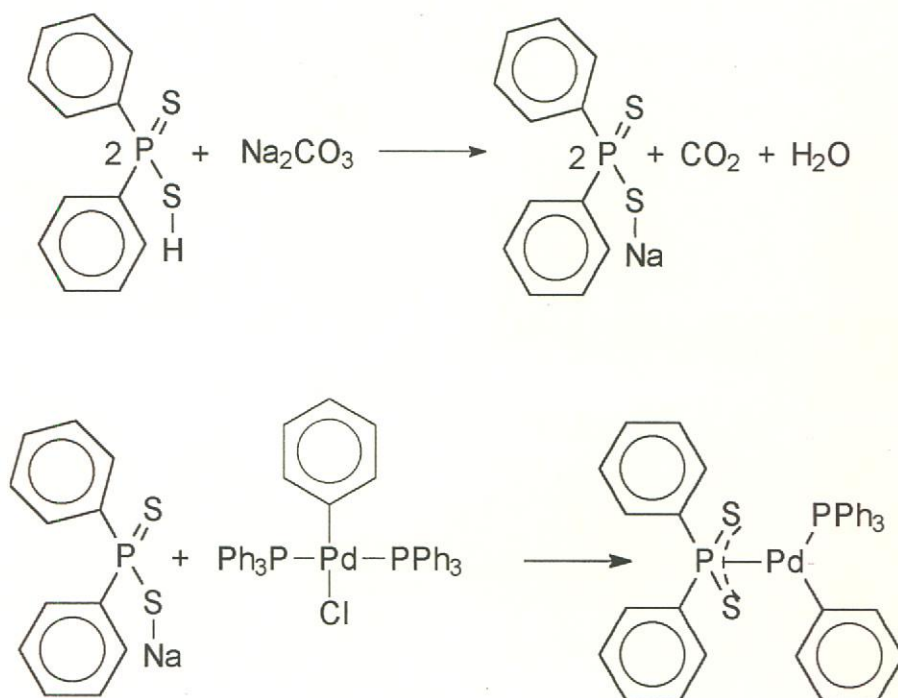
Yield = 51%

(Yield based on mole phosphorus(V)sulphide initially used.)

Literature reported yield = 54%

*ii) Synthesis of complex **7**, [η³-(Ph)₂PS₂]Pd(PPh₃)(Ph).*

[η³-(Ph)₂PS₂]Pd(Ph₃)(Ph) was synthesised according to the following reaction scheme:

Scheme 3.20 : Synthesis of complex **7**, [η³-(Ph)₂PS₂]Pd(PPh₃)(Ph).

Diphenyl-dithio-phosphinic acid, 0.1212g (4.845 x 10-4 mol), was dissolved in 10ml of methanol and 2ml of THF. 0.025g of sodium carbonate (Na_2CO_3) was added and the mixture was stirred for one hour. The solution was then evaporated to dryness to deliver a white salt product that was placed under high vacuum for several hours to ensure all the water formed was removed.

The sodium salt was dissolved in 7ml of anhydrous THF and added dropwise to 0.2g (2.689×10^{-4}mol) of $(PPh_3)_2Pd(Ph)(Cl)$ and stirred vigorously for 36 hours. The reaction mixture developed a yellow colour during this period. The solution was filtered through an anhydrous celite packed sinter glass filter and evaporated to dryness.

Once the product was confirmed by NMR analysis to be in high yield, the reaction mixture was further purified by crystallization. Two crystallization solutions were attempted, namely 1:1 THF pentane and 1:1 benzene pentane which yielded two different crystal systems with one showing unexpected solvent effects.

Yield: 58%,
(Yield based on mole $(Ph)_2PS_2H$ used.)

iii) Molecular structure determination of complex 7.

Suitable crystals for crystal structure determination were obtained by crystallization of complex **7** from a solution of dichloromethane layered in a 1:1 ratio with pentane as well as from a solution of THF layered in a 1:1 ratio with pentane. These two crystallization methods delivered two different crystal systems, one with THF interaction one without any solvent interaction.
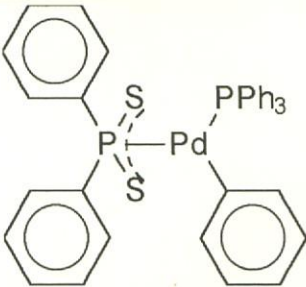
An orange crystal of $(Ph)_2PS_2Pd(PPh_3)(Ph)$.THF and a colourless crystal of $(Ph)_2PS_2Pd(PPh_3)(Ph)$ were mounted on a glass fiber and transferred to a Siemens SMART system diffractometer. All data was collected at room temperature with graphite monochromated Mo-K_α radiation and corrected for Lorentz and polarization effects. Absorption corrections were applied by the

empirical method. Unique sets of data with intensities greater than two times the standard deviation were used to solve the structure by the heavy atom (Patterson) method. Refinements were done using least squares refinement. All non-hydrogen atoms were refined anisotropically. For structure solution and refinement the ShelX-97 software package was used[47]. Structure Figures were generated using Ortep-3.[48]

Selected crystallographic bond lengths and angles for both crystals are listed in tables 3.16 and 3.17 respectively. All other crystallographic information is available from Dr. C. Esterhuysen Department of Chemistry, Stellenbosch University, Private Bag X1, 7602 Matieland South Africa.

Structure	

Empirical formula	$C_{36}H_{30}P_2PdS_2$
Formula weight (g.mol^{-1})	695.06
Temperature	293(2) K
Radiation wavelength	Mo Kα, 0.71073 Å
Crystal system, space group	Monoclinic, P 2_1/c
Unit cell dimensions	a = 12.9199 (6) Å α = 90.00 $^\circ$
	b = 16.2919 (8) Å β = 103.777(1)$^\circ$
	c = 15.9092 (8) Å γ =90.00°
Volume	3252.4 (3) Å^3
Z, Calculated density	4, 1.419 Mg/m^3
Reflections for cell parameters	16692
Absorption coefficient	0.821 mm^{-1}
Absorption correction method	Empirical (SADABS)
F(000)	1416
Crystal size	0.38 x 0.32 x 0.25 mm^3
Crystal colour	Colourless
Diffractometer type	Siemens SMART system
Scan type	Area detector
Theta range for data collection	1.82 to 25.00°
Index ranges	-15 $\leq$ h 13
	-19 $\leq$ k $\leq$ 19
	-15 $\leq$ l $\leq$ 18
Reflections collected / unique	16692 / 5664 [R(int) = 0.0539]
Refinement method	Full-matrix least-squares on F^2
Data / restraints / parameters	5664 / 0 / 492
Reflections observed [I>2σ(I)]	4282
Goodness-of-fit on F^2	1.103
Final R indices [I>2σ(I)]	R1 = 0.0463, wR2 = 0.0692
R indices (all data)	R1 = 0.0742, wR2 = 0.0759
Weighting scheme (calculated)	W=1/[σ^2(Fo^2)=(0.038P)^2 + 2.9006P]
	where P=(Fo^2+2Fc^2)/3
Maximum shift/esd	0.052
Largest diff. peak and hole	0.355 and −0.421 e.Å^{-3}

Table 3.22 : Crystal data and structure refinement for complex **7** with no solvent interaction.

Structure	
Empirical formula	$C_{36}H_{30}P_2PdS_2 \cdot THF$
Formula weight (g.mol^{-1})	765.15
Temperature	293(2) K
Radiation wavelength	Mo Kα, 0.71073 Å
Crystal system, space group	Triclinic, P 1
Unit cell dimensions	a = 10.9884 (6) Å α = 88.534 (1)$^\circ$
	b = 13.2742 (7) Å β = 83.825 (1)$^\circ$
	c = 13.4552 (7) Å γ =71.356 (1)$^\circ$
Volume	1848.74 (17) Å^3
Z, Calculated density	2, 1.375 Mg/m^3
Reflections for cell parameters	9866
Absorption coefficient	0.731 mm^{-1}
Absorption correction method	Empirical (SADABS)
F(000)	784
Crystal size	0.35 x 0.35 x 0.25 mm^3
Crystal colour	Orange
Diffractometer type	Siemens SMART system
Scan type	Area detector
Theta range for data collection	1.52 to 25.00°
Index ranges	-13 $\leq$ h 13
	-15 $\leq$ k $\leq$ 15
	-15 $\leq$ l $\leq$ 12
Reflections collected / unique	9866 / 6239 [R(int) = 0.0532]
Refinement method	Full-matrix least-squares on F^2
Data / restraints / parameters	6239 / 0 / 422
Reflections observed [I>2σ(I)]	5439
Goodness-of-fit on F^2	1.115
Final R indices [I>2σ(I)]	R1 = 0.0731, wR2 = 0.1761
R indices (all data)	R1 = 0.0851, wR2 = 0.1862
Weighting scheme (calculated)	$W=1/[\sigma^2(F_o^2)=(0.0662P)^2 + 8.6715P]$
	where $P=(F_o^2+2F_c^2)/3$
Maximum shift/esd	0.036
Largest diff. peak and hole	02.904 and −0.606 e.Å^{-3}

Table 3.23 : Crystal data and structure refinement for complex **7** with solvent interaction.

3.4 Cited References.

[1] I. Haiduc, D.B. Sowerby, S Lu, *Polyhedron*, 14, **1995**, 3389

[2] I. Haiduc, D.B. Sowerby, *Polyhedron*, 15, **1995**, 2469

[3] A.S. Marggraff, *Miscellanea Berlinensia*, 6, **1740**, 54

[4] H. Hofman, M. Becke-Goehring, *Topics in Phosphorus Chemistry*, E.J. Griffith, M. Grayson eds., Interscience Publishers, New York, vol. 8, **1976**, 193

[5] M.E. Jason, *Inorg. Chem.*, 36, **1997**, 2641

[6] R.W. Murray, *Acc. Chem. Res.*, 13, **1980**, 135

[7] G.G. Roberts, *Adv. Phys.*, 34, **1985**, 475

[8] S. Cheng, G. Peng, A. Clearfield, *Ind. Eng. Chem. Prod. Res. Dev.*, 23, **1984**, 2

[9] a) A. Clearfield, *New Developments in Ion Exchange Materials*, M. Abe, T. Kataoka, T. Suzuki Eds., Kodansha Ltd., Tokoyo, **1991**

b) J.D. Wang, A. Clearfield, G. Peng, *Mater. Chem. Phys.*, 35, **1993**, 208

[10] G. Alberti, M. Casciola, R. Palombari, *Solid State Ionics*, 61, **1993**, 241

[11] a) L.A. Vermeulen, M.E. Thompson, *Nature* 358, **1992**, 656

b) L.A. Vermeulen, J.L. Snover, L.S. Sapochak, M.E. Thompson, *J. Am. Chem. Soc.*, 115, **1993**, 11767

[12] 3D Search and Research using the Caimbridge Structural Database.

F.H. Allen, O. Kennard, *Chemical Design Automation News*, **1993**, 8, 31 –37

IsoStar: A Library Of Information about Nonbonded Interaction, I.J. Bruno, J.C. Cole, J.P.M. Lommerse, R.S. Rowland, R. Taylor, M. Verdonk, *Jouranl of Computer-Aided Molecular Design*, **1997**, 11-6, 525-537.

[13] Narayan, Sanjay, Jain, K. Vimal, S. Chaudhury, *J. Organomet. Chem.*, **1997**, 530(1-2), 101-105.

[14] W.A. Herrman, C. Broner, . Priermeier, K. Öfele, *J. Organomet. Chem.*, 481, **1994**, 97.

[15] R.O. Sauer, *J. Am. Chem. Soc.*, 66, **1944**, 1707.

[16] Brauer, *Handbuch der Präparativen Anorganischen Chemie,* Bd. I, Ed. R. Steudel, P.W. Schenk, 449.

[17] A.R. Sanger, *Inorganic Nuclear Chemistry Letters*, 9, **1973**, 351.

[18] M. Wedler, F. Knösel, M. Noltemeyer, F.T. Edelman, *J. Organomet. Chem.* 388, **1990**, 21.

[19] O.J. Scherer, G. Schieder, *Che. Ber.,* 101, **1968**, 4184.

[20] K.L. Paciorek, R. H. Kratzer, *J. Org. Chem.*, 31, **1966**, 2426.

[21] Houben-Weyl, *Methoden Der Organischen Chemie*, Vierde Auflage, Herausgegeben von Eugen Müller, K. Sasse : Phosphinsäuren und deren Derivate, 272.

[22] W. Kemp, *NMR in Chemistry – A multinuclear introduction*, **1986**, McMillian Education Ltd., London, 158.

[23] K. Vrieze, *Dynamic Nuclear Magnetic Spectroscopy*, L.A. Jackman, F.A. Cotton, Eds., Academic Press, New York, **1975**, 441.

[24] K.G. Orrell, *Coord. Chem. Rev.*, 96, **1989**, 1.

[25] R.J. Abraham, J. Fisher, P. Loftus, *Introduction to NMR Spectroscopy,* Wiley, New York, **1992**, 21.

[26] W.H. Meyer, R. Brüll. H.G. Raubenheimer, C. Thompson, G.J. Kruger, *J. Organomet. Chem.,* 553, **1998**, 83

[27] W.H. Meyer, R. Brüll. H.G. Raubenheimer, C. Thompson, G.J. Kruger, *J. Organomet. Chem.,* 553, **1998**, 83

[28] W.H. Meyer, R. Brüll, H.G Raubenheimer, C. Thompson, G.J. Kruger, *J. Organomet. Chem.,,* 553, **1998,** 83.

[29] K.F. Purcell, J.C. Kotz, *Inorg. Chem.*, **1977**, W.B. Saunders Company, London, 697.

[30] K.F. Purcell, J.C. Kotz, *Inorg. Chem.*, **1977**, W.B. Saunders Company, London, 694.

[31] Sheldrick, G.; *SHELX-97 Program for Crystal structure Determination and Refinement*; Institut fur Anorganische Chemie der Universität, Tammanstrasse 4, D-3400 Göttingen, Germany.

[32] Ortep-3 for windows; L.J. Farrugia; *J. Appl. Crystallogr.*, **1997**, 565.

[33] Ortep-3 for windows; L.J. Farrugia; *J. Appl. Crystallogr.*, **1997**, 565.

[34] Ortep-3 for windows; L.J. Farrugia; *J. Appl. Crystallogr.*; **1997**, 565.

[35] W.E. Van Zyl, *Low Nuclearity complexes of Gold, Copper and Iron with organophosphor-1,1-dithiolato type ligands: Synthesis, Structure, Reactivity, and luminescence Properties*, PhD Thesis submition **1989**, 36

[36] Ortep-3 for windows; L.J. Farrugia; *J. Appl. Crystallogr.*; **1997**, 565.

[37] Ortep-3 for windows; L.J. Farrugia; *J. Appl. Crystallogr.*; **1997**, 565.

[38] M.F. Lipton, C.M. Soreson, A.C. Sadler, R. H Shapiro, *J. Organometal. Chem.,l* **1980**, *186, 155.*

[39] R.O. Sauer, *J. Am. Chem. Soc.*, 66, **1944**, 1707.

[40] Brauer, *Handbuch der Präparativen Anorganischen Chemie,* Bd. I, Ed. R. Steudel, P.W. Schenk, 449.

[41] A.R. Sanger, *Inorganic Nuclear Chemistry Letters*, 9, **1973**, 351.

[42] M. Wedler, F. Knösel, M. Noltemeyer, F.T. Edelman, *J. Organometal. Chem.,* 388, **1990**, 21.

[43] O.J. Scherer, G. Schieder, *Che. Ber.,*101, **1968**, 4184.

[44] K.L. Paciorek, R. H. Kratzer, *J. Org. Chem.*, 31, **1966**, 2426.

[45] H. Schmidbaur, K. Schwirten, H. Pickel, *Chem. Ber.*, 102, **1969**, 564

[46] Houben-Weyl, *Methoden Der Organischen Chemie*, Vierde Auflage, Herausgegeben von Eugen Müller, K. Sasse : Phosphinsäuren und deren Derivate, 272.

[47] G.M. Sheldrick, SHELX-97 Program for the determination and refinement of crystal structures, Institute für Anorganische Chemie, Universität Göttingen, Tammans t rasse 4, D-3400, Göttingen, Deutschland, **1997**.

[48] L.J. Farrugia, ORTEP-3 for Windows, *J. Appl. Crystallogr.*, **1997**, 565.

η^3-Allyl Palladium(II) Complexes Belonging to a Family of Potential Catalytic Precursors

This chapter is concerned with the preparation and spectroscopic characterization of several η^3-hetero allyl palladium(II) bimetallic complexes with tellurium(II) containing ligands. The goal of this study was to synthesize and characterize these complexes by means of melting point, IR, MS (where possible), NMR spectroscopy and X-ray crystal structure determination.

4.1 Introduction.

Although the first examples of metal complexes of selleno- (R_2Se) and telluro-ether (R_2Te) were reported around the beginning of the 20th century, but detailed studies of the their chemistry date only from the late 1970's. The neglect of the study of these complexes stemmed from a variety of causes. The reasons included the wide held view that seleno- (R_2Se) and telluro-ethers were weak donors with poor coordination chemistry except to soft (class B) metals and, even in these cases, they were believed to be little different from their thioether analogues. Being largely commercially unavailable, a reputation for being toxic and extremely malodorous compounds along with the apparent lack of applications, account for the very limited interest and late development of research into tellurium chemistry in general.

There has however recently been a growth in the interest of tellurium chemistry that can be attributed to a number of factors. One being the fact that tellurium has isotopes of half-integral spin with a reasonably high natural abundance. Coupled with modern multinuclear FT NMR instrumentation, this

provides a sensitive spectroscopic probe. In contrast, sulphur has only an insensitive quadrupolar nucleus in ^{33}S (I= 3/2 0.76%, Rp = 1.71 x 10 $^{-5}$).

Practical applications of metal telluroether complexes (or of mixtures of metal halides or alkyls and R_2Te) include various types of chemical vapour deposition processes for thin-film fabrication of new electronic materials such as group II-VI semiconductors.

Although several complexes of R_2Te ligands are reported in the older literature,[1] reported data were often limited to a single melting point. Only in the last 20 years has a reasonable body of spectroscopic data been collected. However, the available data are still much more limited and fragmented than that of other group 15 or 16 donor ligands. Structural data with less than 15 structures were reported at the time one of the latest reviews on tellurium chemistry appeared.[2]

A short overview of recent palladium-tellurium chemistry.
This section was included to give a brief overview of the tellurium chemistry in general so as to illustrate to the reader the bigger picture of tellurium chemistry in general along with its associated limitations and difficulties. It is hope that by doing this it will be possible for the reader to see how the ligands and complexes synthesised in this chapter fit into the greater scheme of tellurium-palladium chemistry.

Tellurium's interaction with palladium is very often reported along with that of tellurium-platinum complexes. Palladium(II) and platinum(II) telluroether complexes were amongst the earliest examples reported. A recent re-examination of the $[ML_2X_2]$ (M = Pd or Pt; L = $TeMe_2$, $TePh_2$, TeMePh; X = Cl, Br or I) by ^{125}Te and ^{195}Pt spectroscopy showed that in CH_2Cl_2 solution both the *cis* and *trans* isomers were present for all complexes except for the $[Pd(TePh_2)_2X_2]$. The structure of *trans*-$[Pt(TeMePh)I_2]$ has been determined.[3] Complexes of this unsymmetrical telluroether can exist in RR/SS or RS/SR enantiomeric forms, which interconvert by pyramidal inversion at the tellurium center. In the crystal studied the RR/SS form was present.

Ditelluroethers have recently been prepared and only a limited amount of their chemistry has been explored. The largest number of complexes using these types of ligands have been for palladium and platinum as central metals. The first examples were the yellow or orange $[M(RTe(CH_2)_3TeR)X_2]$ (R = Me, Ph; X = Cl, Br, I) complexes. Comparison of the ^{125}Te NMR chemical shifts ($\delta_{complex}$ - $\delta_{free\ ligand}$) in the complexes of the five and six membered chelate ring complexes, reveal large high-frequency shifts in the former which are characteristic of this ring size.

Palladium(II) and platinum(II) complexes $[M(L-L)X_2]$ (X = Cl, Br) have been prepared with long chain telluroethers $(p\text{-}EtOC_6H_4)Te(CH_2)_nTe(p\text{-}EtOC_6H_4)$ (n=6-10). The complexes with n = 6 are insoluble in common solvents and are probably ligand bridged polymers. The other complexes appear to be a mixture of isomers, although the systems are not understood in detail.[4]

A considerable number of complexes of telluroether-type ligands have been reported, mostly with palladium(II), platinum(II) and mercury(II). In view of the often-complicated coordination chemistry of hybrid ligands, it is unfortunate that, with three exceptions, the structures are based on spectroscopic rather than crystallographic data.

The reactions of the sodium salts of 2-R-telluroethanols (R = 4-MeOC$_6$H$_4$ or 4-EtOC$_6$H$_4$) with palladium(II), platinum(II) or mercury(II) give complexes $[\{M(RTeCH_2CH_2O)Cl\}_2]$ which are formulated as halide bridged dimers on the bases of IR, ^1H and ^{13}C NMR data.[5] Halide-bridged dimeric complexes also appear to be formed by the (2-hydroxy-5-methylphenyl)aryltellurides (aryl = 4-MeOC$_6$H$_4$, 4-EtOC$_6$H$_4$ or Ph) with palladium(II), platinum(II) or mercury(II) chlorides, with the ligands acting as chelating mono-anions, via the deprotonated phenol function and the tellurium.[6] Complexes of telluroacetic acid, $RTeCH_2CO_2H$ (R = Ph, 4-MeOC$_6$H$_4$, 4-EtOC$_6$H$_6$)[7], and tellurobenzoic acids $[o\text{-}(4\text{-}EtOC_6H_4Te)C_6H_4CO_2H]$[8] have been described. The complexes of

RTeCH$_2$CH$_2$SMe (R = 4-MeOC$_6$H$_4$, 4-EtOC$_6$H$_4$) of type [M(L-L)Cl$_2$] (M = Pd, Pt) are square planar with TeSCl$_2$ donor sets.[9]

A variety of tellurium-nitrogen donor ligands have been studied. The structures of the telluroethylamine complexes were suggested to involve coordination via both nitrogen and tellurium.[10] In palladium(II) and platinum(II) complexes, the ligands behave as N^Te chelates giving planar [M(N^Te)Cl$_2$] complexes.[11] The ligand used in these complexes is illustrated in figure 4.1 below.
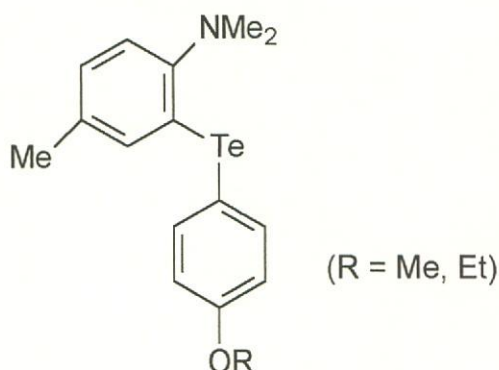
Figure 4.1 : An example of an N^Te chelate ligand.

Although not directly applicable to the work covered in this project some interesting observations have been reported for the potentially tridentate ligand illustrated in Figure 4.2 below. The characteristics observed for complexes with this ligand are worth noting here as they illustrate the dynamic and often unexpected behavior of tellurium ligands in both the solid and liquid phase.
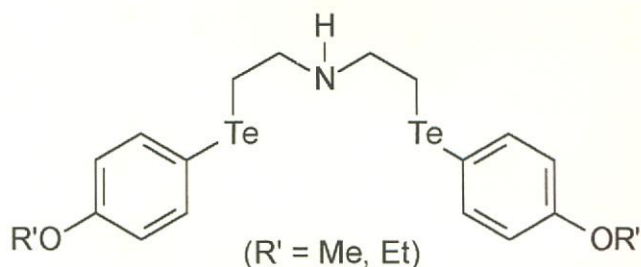

Figure 4.2 : An example of a tridentate ligand containing tellurium(II)

The palladium(II) and platinum(II) complexes [M(Te^N^Te)Cl$_2$] are monomeric and non-electrolytes in chloroform, but exhibit varying conductivity in more polar solvents.[12] The structures are suggested to be five coordinate with Te$_2$NCl$_2$ donor sets. Since neither tellurium nor nitrogen are known to favour five-coordination for these two metal centers, an alternative possibility is that they are planar (TeNCl$_2$), with fast exchange between free and bound tellurium groups in solution, coupled with some ionisation (and partial formation of a Te$_2$NCl donor set) in polar solvents. An X-ray study coupled with [125]Te and [195]Pt NMR studies in solution could provide some interesting results.

Crystal structure studies of tellurium complexes.

When the complex chemistry of tellurium is reviewed, the lack or scarcity of solved X-ray crystal structures is a prominent feature of note. Based on a structural search of the Cambridge Crystallographic Database,[13] there are twenty known structures containing palladium-tellurium bonds of which only seven contain telluroether moieties as donor atoms. These seven structures can further be broken down into the following groups: -

- Three with monodentate ligands
- Three with bidentate ligands
- 1 containing a heteronuclear bidentate (Te^N) ligand. See Figure 4.3 below.
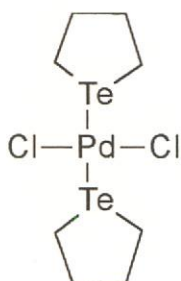
Monodentate telluroether
type ligand.
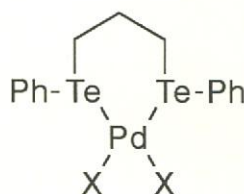
Bidentate telluroether
type ligand.
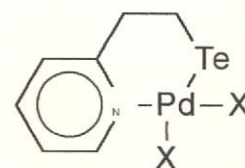
Heteronuclear bidentate
telluroether type ligand

Figure 4.3 : Examples of known telluroether structures.[14,15,16]

The other four known bidentate crystal structures of palladium with heteronuclear bidentate tellurium ligands all have carborane structures.

The limited number of crystal structures that are known for palladium complexes with tellurium-coordinated ligands, reflect two characteristics of this field: -

- The relatively late development of this metal complex-type of chemistry.
- The inherent general unstable nature of these types of complexes (both neutral and cationic.

The crystals of palladium-tellurium complexes that have been obtained by members of our research group and that could be solved by X-ray diffraction studies, were only obtained in extremely low yields along with a high degree of decomposition of the remaining product. The crystals obtained were very air and moisture sensitive and extremely unstable. This resulted in relatively poor R factors for the crystal data. Unfortunately all attempts made in the present work to obtain crystals suitable for crystal structure analysis failed.

NMR spectroscopic summery of Tellurium-125.

Early NMR spectroscopic studies for tellurium-125 relied upon indirect double resonance methods, but with the advent of modern multinuclear FT instruments, direct observation is straightforward. Although organotellurium chemistry is a field of rapidly growing interest with many diverse applications, the ligand properties of organotellurium species still lags well behind those of its selenium and sulfur analogues and is mainly restricted to R_2Te or RTe^- type species.[17]

Coupled to this limited literature reported tellurium NMR spectroscopic data, it must also be mentioned that the literature data of $^{13}C\{^1H\}$ chemical shifts of the tellurium compounds is also rather sparse. However, a reported trend in uncoordinated tellurium compounds is that the ^{13}C chemical shifts of the (allyl)Te groups appeared at a lower δ than TMS (-15 to −24ppm). This is a general effect observed for ^{13}C atoms bonded to heavy atoms, including

iodine and lead, and is similarly as due to electron spin-orbit interactions in the heavy atoms.[18]

Even with ^1H decoupling, Te-C coupling, J_{Te-C}, is reported as being difficult to measure accurately but is in the region of 30–40 Hz.

The essential properties of ^{125}Te for NMR spectroscopic analysis are as follows: -

Spin	Natural Abundance	Receptivity[i]	Resonance Frequency[ii]	Reference[iii]	Shift Range
½	6.99	12.5	31.55	Neat Me_2Te	~7000ppm

Table 4.1 : NMR spectroscopic properties of ^{125}Te.

^{125}Te has a large chemical shift change for a relatively small change in the electronic environment of the tellurium nucleus. This illustrates how useful ^{125}Te NMR spectroscopy may be in studying relative changes around a tellurium atom in organo-tellurium complexes. This has led some research groups to try to utilize tellurium as a NMR probe in various biological systems where the tellurium atom would act as a reporter capable of giving information regarding its surrounding environment.

Some interesting comparisons.

Intensive efforts have been devoted to studying the bonding of tertiary phosphines to transition metals, and the subtle interplay of steric and electronic factors have been reviewed on a number of occasions.[19] Corresponding factors in neutral group 16 donor ligands have attracted surprisingly little effort, and most of the limited work done is restricted to thioethers. In their review published in 1981, Murray and Hartley[20]

[i] Relative to ^{13}C
[ii] Approximate resonance frequency when ^1H frequency is 100MHz
[iii] Due to the appreciable solvent dependence of the chemical shift, care should be taken to refer data to neat Me_2Te

summarized the relevant data on structures and bonding in metal thio-, seleno- and telluroether complexes, but the data dealing with heavier donor ligands was very limited (e.g. only four X-ray structures had been reported). The past ten years has shown considerable improvement. Nonetheless, it is true that our understanding of the $M-SeR_2$ and $M-TeR_2$ bonding is still very limited, and also partly due to the scattered nature of much of the available data.

Compared with group 15 ligands, steric effects are less important here as a result of the group 16 donor carrying only two R groups. Although telluroethers with very bulky R groups have been reported, their coordination chemistry is largely unexplored. However, a second lone pair may potentially take part in π-donation, or may be a source of π-repulsion. The difficulties in establishing π-acceptor behavior, so familiar in tertiary phosphine complexes, are present in group 16 analogues. The acceptor orbital is usually assumed to be S(Se/Te)nd, but this proposal is open to the same criticism leveled against it in group 15, namely that the nd orbital energy is too high for these orbitals to contribute significantly to the bonding.[21]

Thermodynamic data for a variety of Pd(II) and Pt(II) complexes have been compiled by Mortimer and co-workers.[22, 23] Based upon the kinetics and products of displacements, the effects of various ER_2 groups upon the $\nu(CO)$ stretching frequencies, and the ^{13}C NMR spectroscopic data, the relative stability of the chalcogenether complexes are believed to be $TeR_2>SeR_2>SR_2(>OR_2)$, which may be compared with the usual order of group 15 of $PR_3>AsR_3>SbR_3>NR_3>BiR_3$. The results were also interpreted in terms of the $M-ER_2$ bonding having predominately σ character with little or no π component.
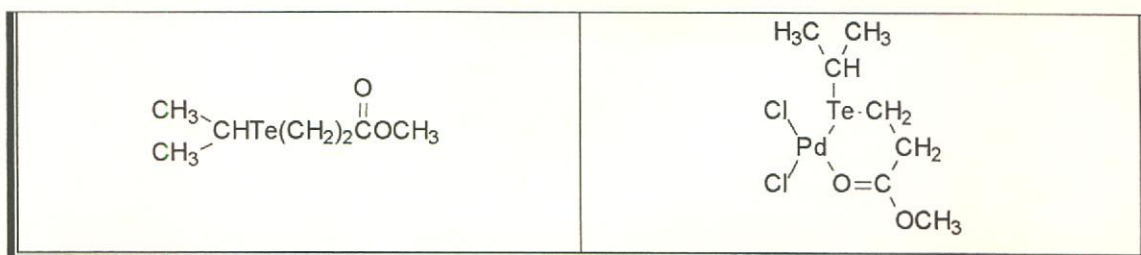
The available X-ray studies of selenoether and telluroether complexes, show that the coordinated chalcogenoethers have pyramidal geometries, and the majority have ER_2 groups coordinated to a single metal center. A small number of examples have been reported where the chalcogenoether behaves

as a four electron-bridging group (μ^2-), utilising both lone pairs.[24, 25] The cautious conclusion has been made that the bond lengths are similar to, or slightly shorter than, those expected for single bonds on the basis of the appropriate radii. This is consistent with the ligands behaving as σ donors, with small or negligible π components.

Finally, the preparation and spectroscopic characterization of several η^3-heteroallyl palladium(II) complexes with ligands of the type R-TeCH$_2$CH$_2$COOCH$_3$, (R = isopropyl, *tert*-butyl ,ethyl) using tellurium(II) and oxygen as the donor atoms within these neutral ligands in a bidentate fashion were investigated. Bis-(η^3-allyl)-di-μ-iodo-dipalladium(II), [(CH$_2$CHCH$_2$)$_2$Pd$_2$I$_2$], was prepared and fully characterised to be used as the starting compound. It was envisioned that the ligands of the type mentioned above would react with the starting compound, bis-(η^3-allyl)-di-μ-iodo-dipalladium(II), thereby cleaving the dimeric palladium starting compound followed by the removable of the remaining iodide from the palladium and chelate ring closure upon treatment of the reaction mixture with silver tetrafluoroborate. The prepared complexes proved to be very unstable. As a result, it was not possible to fully characterise these prepared complexes to conclusively determine whether the target complexes had been prepared. All attempts to obtain crystals suitable for crystal structure determination proved unsuccessful. Table 4.2 below lists both the free ligands as well as the envisioned target complexes that were to be prepared and characterized.

Free Ligand	Target Complex
H₃C–CHTe(CH₂)₂COCH₃ (with H₃C and C=O)	Pd–Te complex with CH(CH₃)₂, Te-CH₂, CH₂, O=C, OCH₃ ⁺BF₄⁻
H₃C–CH₂–Te-CH₂CH₂–C(=O)–OCH₃	Pd–Te complex with CH₃, CH₂, Te-CH₂, CH₂, O=C, OCH₃ ⁺BF₄⁻
CH₃–C(CH₃)(CH₃)–Te(CH₂)₂COCH₃	Pd–Te complex with H₃C–C(CH₃)–CH₃, Te-CH₂, CH₂, O=C, OCH₃ ⁺BF₄⁻
C₆H₅CH₂–Te–CH₂C₆H₅	Pd–Pd dimer with bridging Te(CH₂C₆H₅) groups, 2⁺ (BF₄⁻)₂
Ph–S(CH₂)₂COCH₃	Pd–S complex with Ph, S-CH₂, CH₂, O=C, OCH₃
Ph–CH₂-Te-CH₂-Ph	(CO)₅Cr–Te(CH₂-Ph)(CH₂-Ph)

Table 4.2 : Free ligand and corresponding target complexes attempted.

4.2 Results and Discussion

4.2.1 Complex 8, *bis-(η^3-allyl)-di-μ-iodo-dipalladium(II)* *[(CH$_2$CHCH$_2$)$_2$Pd$_2$I$_2$].*

I) Preparation of complex 8, bis-(η3-allyl)-di-μ-iodo-dipalladium(II)

Bis-(η3-allyl)-di-μ-iodo-dipalladium(II) was synthesised according to scheme 4.1 below based on a literature method used for the synthesis of the analogous methallylpalladium chloride complex[26,27]. The synthesis outlined in scheme 4.1 below includes the changes that were made from the published method to adapt it to allow for the conversion to the allylpalladium iodide analogue of the chloride complex.
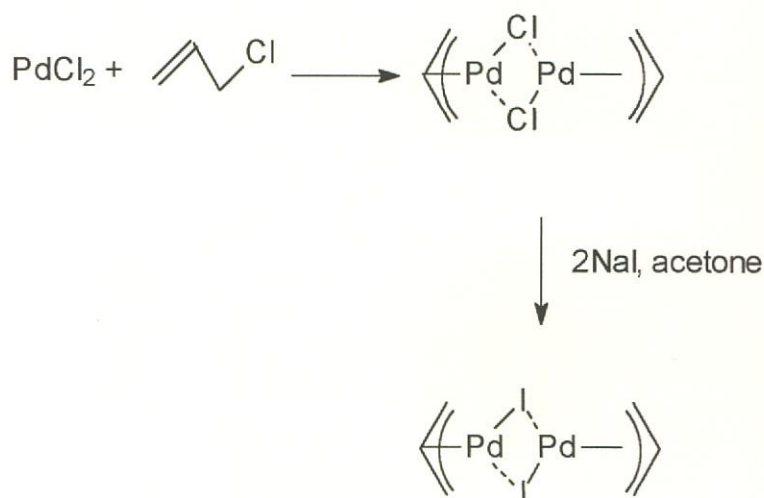
Scheme 4.1 : Preparation of complex 8, bis-(η^3-allyl)-di-μ-iodo-dipalladium(II).

Palladium(II) chloride was reacted with allyl chloride to produce the bis-(η3-allyl)-di-μ-chloro-dipalladium(II) complex which was further reacted with sodium iodide to deliver complex **8**. The bis-(η^3-allyl)-di-μ-iodo-dipalladium(II) prepared above was purified and used as the starting complex for all the other complexes prepared in this chapter. Crystals suitable for crystal structure determination were obtained by layering a concentrated dichloromethane solution of bis-(η^3-allyl)-di-μ-iodo-dipalladium(II) with benzene in a 1:1 ratio.

*II) NMR spectroscopic analysis of complex **8**, bis-(η^3-allyl)-di-μ-iodo-dipalladium(II).*

The ^{1}H and ^{13}C{^{1}H} data of bis-(η^3-allyl)-di-μ-iodo-dipalladium(II) are summarized in Table 4.3 below.

Palladium Starting Complex

Instrument : Varian VXR300	

Spectrum : GB018/I006 *Solvent :* C_6D_6 (TMS as internal standard)	*Spectrum :* GB009/I004 *Solvent :* CD_2Cl_2 (TMS as internal standard)

Proton (δ-values)

$a_{1\text{-anti}}$:	2.43 (d, 2H $J_{H\text{-}H}$ 12.3 Hz)[iv,v]	3.08 (d, 2H, $J_{H\text{-}H}$ 11.7Hz)
$a_{2\text{-syn}}$:	3.81 (d, 2H $J_{H\text{-}H}$ 6.8 Hz) [iv,v]	4.37 (d, 2H, $J_{H\text{-}H}$ 6.9 Hz)
b:	4.36 (vt tr, 1H)	5.32 (vt tr, 1H)

Carbon 13 {^{1}H} (δ-values)

a_1:	66.8	68.0
a_2:	66.8	68.0
b:	108.9	110.1

Table 4.3 : ^{1}H and ^{13}C{^{1}H} NMR data for complex **8**.

[iv] There is an observed pair of doublets arising from the pairs of *syn-* and *anti*-hydrogens on the terminal carbons. This illustrates that these hydrogens of the π-allyl group are equivalent.

[v] Coupling constants of the *syn-* and *anti*-hydrogens in the proton spectra are in line with the first NMR data published for the corresponding palladium chloride complex in 1960[v].

*III) Single crystal structure determination of complex **8**.*

Although the crystal structure of the analogous bis-(η^3-allyl)-di-μ-chloro-dipalladium(II)complex has been solved, the crystal structure of bis-(η^3-allyl)-di-μ-iodo-dipalladium(II) is not known.

Selected crystallographic bond lengths and angles are listed in Table 4.4 and Table 4.5 respectively. The crystal structure of complex **8** is illustrated in Figure 4.4 and the unit cell is illustrated in Figure 4.5 below.

| Selected Bond angles(°)			
C2-Pd-C3A	38.5 (6)	I-Pd-I'	92.20 (2)
C2-Pd-C1	66.9 (4)	Pd-I-Pd	87.80 (2)
C3A-Pd-C1	34.2 (5)	C3A-C1-C3B	48.9 (13)
C2-Pd-C3B	35.0 (6)	C3A-C1-Pd	72.8 (8)
C3A-Pd-C3B	29.4 (7)	C3B-C1-Pd	71.7 (7)
C1-Pd-C3B	36.9 (6)	C3B-C2-C3A	47.2 (12)
C2-Pd-I	166.9 (3)	C3B-C2-Pd	72.9 (9)
C3A-Pd-I	129.3 (6)	C3A-C2-Pd	70.9 (7)
C1-Pd-I	100.0 (3)	C1-C3A-C2	124.0 (19)
C3B-Pd-I	132.9 (6)	C1-C3A-Pd	73.0 (8)
C3B-Pd-I	131.3 (6)I	C2-C3A-Pd	70.6 (8)
C2-Pd-I	100.9 (3)	C2-C3B-C1	126.0 (17)
C3A-Pd-I	135.1 (5)	C2-C3B-Pd	72.1 (8)
C1-Pd-I	167.8 (3)	C1-C3B-Pd	71.4 (8)

Table 4.4 : Selected bond lengths (Å) with e.s.d.s. in parenthesis for complex **8**, bis-(η^3-allyl)-di-μ-iodo-dipalladium(II).

Selected bond lengths(Å).			
Pd-C1	2.125 (8)	Pd-I	2.6488 (7)
Pd-C2	2.120 (8)	Pd-I'	2.6542 (6)
Pd-C3A	2.123 (15)	C1-C3A	1.250 (19)
Pd-C3B	2.129 (16)	C1-C3B	1.35 (2)
Pd...Pd'	3.70	C2-C3B	1.28 (2)
I...I'	3.90	C2-C3A	1.40 (2)

Table 4.5 : Selected bond angles (Å) with e.s.d's. in parenthesis for complex **8**, bis-(η^3-allyl)-di-μ-iodo-dipalladium(II).
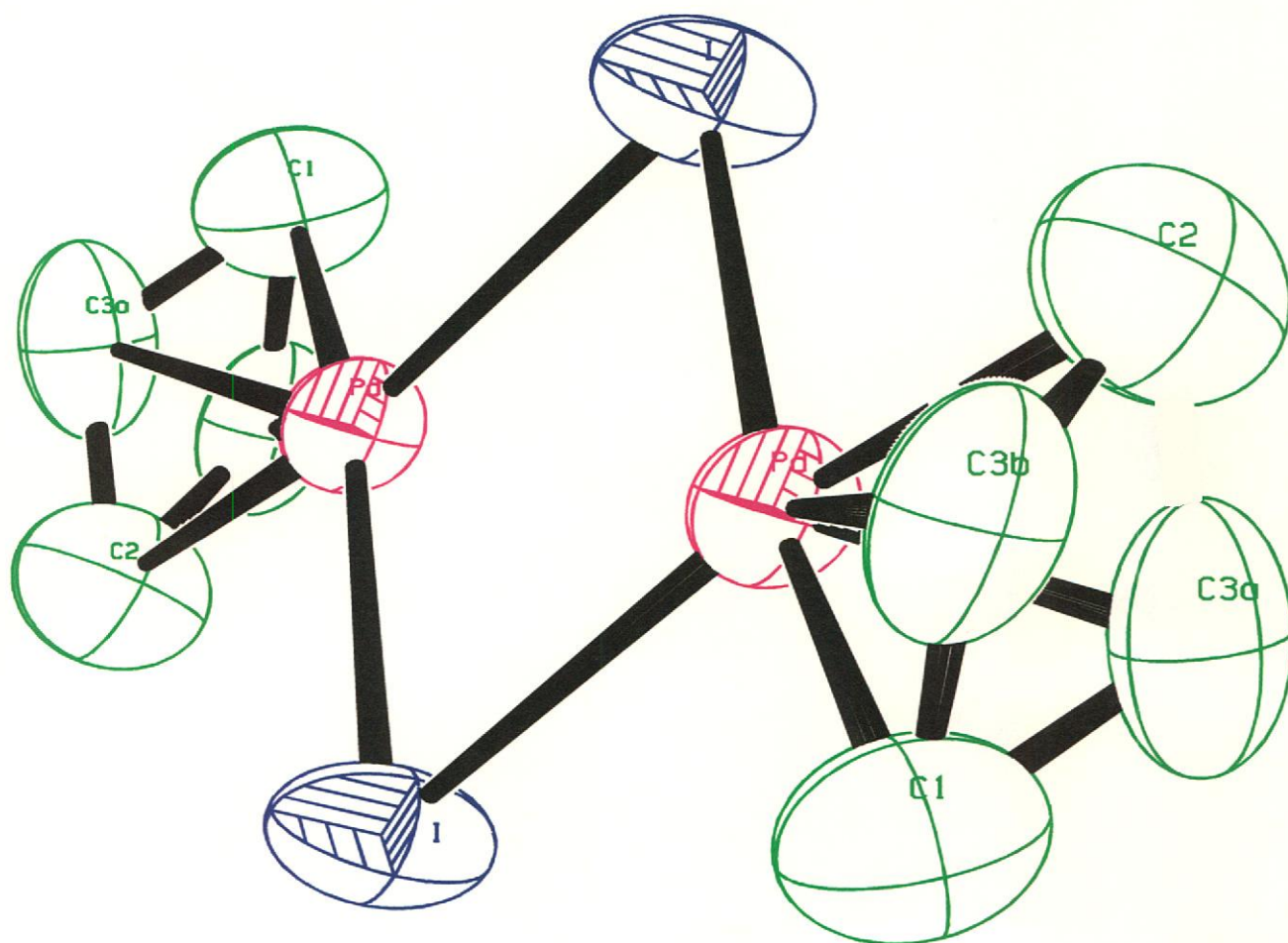
Figure 4.4 : An Ortep3 plot of the molecular structure of *bis*-(η3-allyl)-di-μ-iodo-dipalladium(II) [(CH$_2$CHCH$_2$)$_2$PdI$_2$ at 50% ellipsoid probability showing the numbering scheme used. Hydrogen atoms have been omitted for clarity.
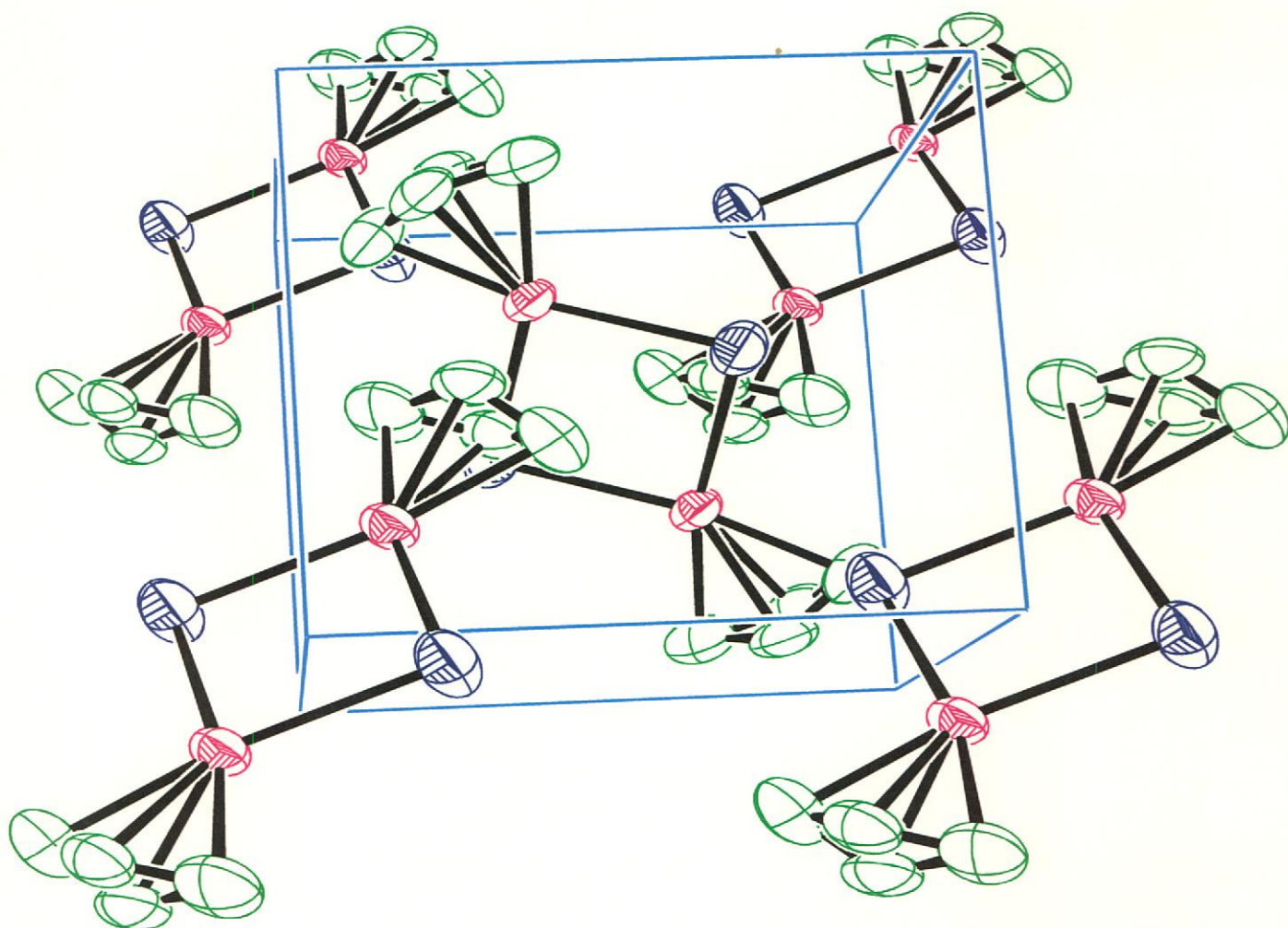
Figure 4.5 : Ortep32 plot of the unit cell of bis-(η3-allyl)-di-μ-iodo-dipalladium(II), $[(CH_2CHCH_2)_2PdI_2$, at 50% ellipsoid probability showing the molecular packing. Hydrogen atoms have been omitted for clarity.

*IV) Discussion of the structure and bonding in complex **8**, bis-(η3-allyl)-di-μ-iodo-dipalladium(II).*

➢ *Previous theories, postulates and background:*

In the past considerable speculation was made concerning the nature of bonding of allylic metal systems. Although the π-allylic-palladium has been considered to be of a non-classical nature,[28] it has also conceptually be viewed from a valence bond picture as involving the usual overlap of two dsp^2 σ-type hybrid orbitals of each palladium with the delocalised π-type orbitals of the allylic group.

As can be seen from Figure 4.4 and Figure 4.5, the allyl group is disordered and occupies two positions at a ration of 1:1. This shows that the difference in energy between the two isomers is very small. This is expected as the orientation of the allyl group is known to flip in solution. This disorder accounts for the high standard deviation coefficient in both the bond angle and bond length data tables given for the central carbon atom of the allyl group (carbon 3a and 3b). This disorder is visualised by the larger ellipsoids of these groups as well as the 3a/3b dual representation of the central carbon of the allyl groups in both the single crystal structure and unit cell diagrams, Figure 4.4 and Figure 4.5 above.

It must also be noted, that apparent configuration change was already reported as early as 1960 for isostructural molecular compounds.[29] This was reported to occur upon dissolution in non-polar organic solvents which was indicated by the relatively high observed dipole moments determined in benzene for $[(C_3H_5)_2Pd_2Cl_2]$[30]. These measurements indicated that, in solution, $[(C_3H_5)_2Pd_2Cl_2]$ and presumably isostructural molecular compounds, undergo considerable deformation from the centrosymmetric configuration in the solid state.

➤ *Discussion of the structure of bis-(η^3-allyl)-di-μ-iodo-dipalladium(II).*

The crystallographic data for this complex reveal that the plane of the three allylic carbons is not perpendicular to the plane of the $(PdI)_2$ bridge system, but intersects at a slight dihedral angel with the central carbon atom being tipped away from the palladium.

The dimeric molecule is linked together by two bridged iodine atoms such that the palladium and iodine atoms form a planar rhombus. The distance from the palladium to the two terminal allylic carbons of each dimer is 2.125(8)Å and 2.120(8)Å, which shows that the palladium, within experimental error, is symmetrically bonded to the allylic system. This is further shown by the fact that that the carbon-carbon (C1-C3, C3-C2) bond lengths of the allyl group, are equivalent, within standard deviation, to each other.

The ^{13}C NMR data alone for complex **8** also supports the conclusion that the two terminal allylic carbons are equivalent and that the allylic group is symmetrically bonded to the palladium in a delocalized fashion (Table 4.3).

The proposed overall molecular configuration based on NMR measurements, with each palladium symmetrically linked to an allyl group, is in agreement with the crystallographic data and the resulting structural configuration deduced therefrom.

The relatively large allylic carbon bond angle, mean 125° (C1-C3a/b-C2), may be a stereochemical consequence of its function as a bidentate group. What would be of interest, but however falls outside the scope of this project, would be the effect of other transition metals with different valences on the geometry of the allylic group.

➢ *Comparison of the crystal structure of complex **8** with the literature known isomorphous palladium chloride complex.*

The Cambridge Crystallographic Database indicates only four articles giving crystallographic data of molecular compounds isostructural to bis-(η^3-allyl)-di-μ-iodo-dipalladium(II). All four refer to the corresponding chloride complex[31, 32, 33, 34] with [34] not having any 3D coordinates available. The crystallographic data published in [32] for this isomorphous palladium chloride complex is listed in Table 4.6 below. A summary of the crystallographic data of complex **8** is listed in Table 4.6 for comparison.

Crystal system	monoclinic
Space group	P2$_1$/n
V/ Å^3	475.9
a/Å	7.46 (2)
b/Å	7.43 (2)
c/Å	8.61 (2)
R$_1$, R$_2$	6.9%, 8.8%

Table 4.6 : Crystallographic data of bis-(η^3-allyl)-di-μ-chloro-dipalladium(II).

Crystal system	monoclinic
Space group	P2$_1$/n
V/ Å^3	553.22 (4)
a/Å	9.3945 (6)
b/Å	7.47604 (18)
c/Å	7.8770 (2)
R$_1$, R$_2$	3.06%, 7.53%

Table 4.7 : Crystallographic data of bis-(η^3-allyl)-di-μ-iodo-dipalladium(II).

The following tables (Table 4.8 and Table 4.9) list selected bond lengths and selected bond angles, as published by Oberhansli and Dahl [32], to enable comparison with the obtained crystallographic structure data of bis-(η^3-allyl)-di-μ-iodo-dipalladium(II) in Table 4.4 and Table 4.5 above.

Selected bond lengths (Å).			
Pd...Pd'	3.460 (7)	Pd-C3	2.02 (37)
Pd-Cl	2.403 (9)	Pd-C2	2.17 (28)
Pd-Cl'	2.398 (8)	C1-C3	1.35 (45)
Cl...Cl'	3.328 (15)	C3-C2	1.37 (40)
Pd-C1	2.14 (24)		

Table 4.8 : Selected bond lengths (Å) for of bis-(η^3-allyl)-di-μ-chloro-dipalladium(II), [(CH$_2$CHCH$_2$)$_2$PdCl$_2$].

Selected Bond angels(^{o})			
Cl'-Pd-Cl	87.8 (3)	Cl-Pd-C2	103.2 (8)
Pd'-Cl-Pd	92.2 (3)	Pd-C1-C3	66.4 (19)
Cl-Pd-C1	172.4 (7)	Pd-C2-C3	64.9 (19)
Cl'-Pd-C2	168.7 (8)	C1-Pd-C2	69.2 (10)
Cl-Pd-C1	99.8 (7)	C1-C3-C2	128.6 (33)

Table 4.9 : Selected bond angles (^{o}) for of bis-(η^3-allyl)-di-μ-chloro-dipalladium(II), [(CH$_2$CHCH$_2$)$_2$PdCl$_2$].

The unit cell of bis-(η^3-allyl)-di-μ-chloro-dipalladium(II) has two dimeric molecules, with each molecule lying on a crystallographic center of symmetry. The asymmetric unit of one half molecule hence contained one palladium, one chlorine and three carbons.

The two structures being compared here, as can be expected, exhibit many similarities. The crystal systems are the same – that being monoclinic, as well as the space groups, P2$_{1/n}$. The unit cell dimensions are also similar except for side A being much longer in the bis-(η^3-allyl)-di-μ-iodo-dipalladium(II) system, 9.3945(6) Å. As a result, the unit cell volume of the chloride analogue

is considerably smaller (475.9 Å^3) than the volume of the unit cell of the iodide complex (553.22 Å^3)

If the bond lengths of bis-(η^3-allyl)-di-μ-iodo-dipalladium(II), [(CH$_2$CHCH$_2$)$_2$PdI$_2$], and the analogous chloride complex are compared, the following trends can be observed.

- The bond lengths of the allyl group in the iodide complex, as expected, are in the same region as that of the chloride complex. The given standard deviation coefficient for the chloride analogue is rather large in comparison with respect to each analogous bond in the corresponding bond data for the iodide complex as described in Table 4.5.

- The Pd-Pd', I-I' and Pd-I and Pd-I' interactions are considerably longer than the corresponding interactions in the chloride complex. This is as expected with the natural increased atomic radius or atomic size of chlorine versus iodine with chlorine r_{ion}=170 and iodine r_{ion}=212.[vi, 35]

- In the structure of the chlorine analogue, the distance from the palladium to the two terminal carbons of the allyl group was found to be equivalent within experimental error (mean = 2.15 ± 0.02Å). However, the distance to the central carbon of the allyl group was found to be considerably shorter (2.02 ± 0.04Å). This is not the case with the iodine analogue. Here the distance from the palladium to all three carbons of the allyl group was found to be the same within experimental error (mean = 2.124Å).

In summary, the data for this structure is in agreement with the structure given by Oberhansli and Dahl [32]. However, the structure of the iodide analogue, as reported here, has been done with its atomic coordinates being more precisely determined than the structure reported by Oberhansli and Dahl [32] thereby giving this structure much better overall reliability factors.

V) _Thermogravimetric analysis of complex **8**._

Thermal decomposition and the presence of potentially stable intermediates was investigated for complex **8**. In the available literature of similar complexes and ligands, no indication of thermogravimetric analysis was found.

Figure 4.4 below is a graphic representation of the temperature program used to follow the thermal decomposition of complex **8**. The temperature program involved a $0 - 700^{\circ}C$ temperature range with an initial $5^{\circ}C$ min^{-1} increase to $30^{\circ}C$, maintained at $30^{\circ}C$ for 6 minutes, followed by a further $5^{\circ}C$ min^{-1} increase to $700^{\circ}C$.
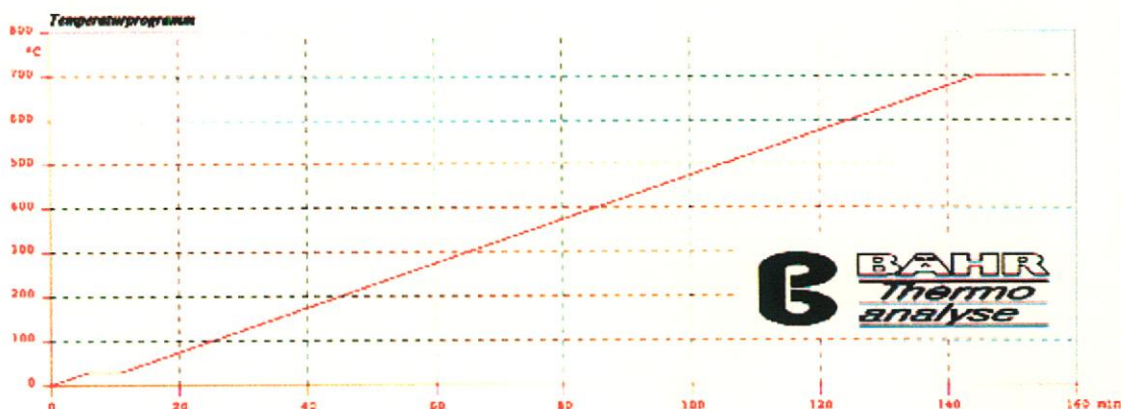
Figure 4.4 : Thermogravimetric analysis temperature program used for complex **8**.

Figure 4.5 below is a plot of TG and dif.TG versus temperature while figure 4.6 is a plot of DTA and TG versus time for the thermogravimetric decomposition analysis of complex **8**.

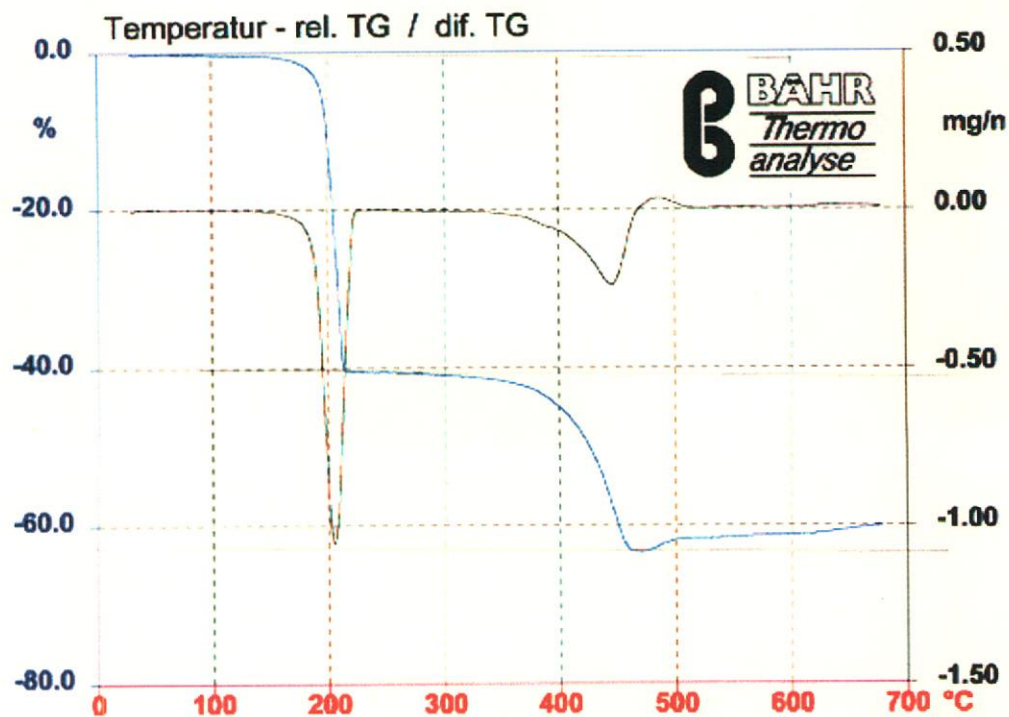vi r_{ion} is the atomic radii of a common ion of the respective element taken from its most typical crystal

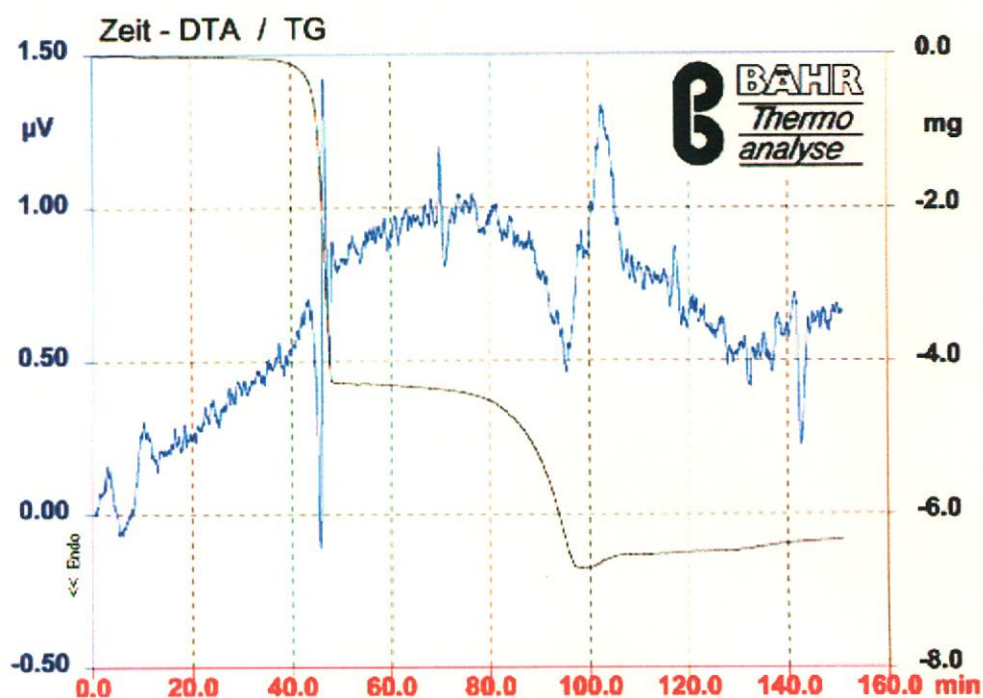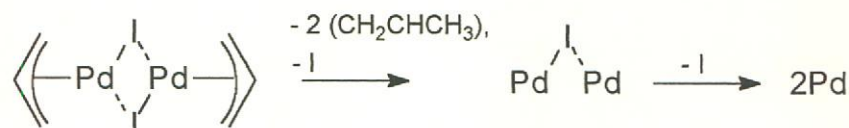**Figure 4.5** : TG and dif.TG versus temperature of the thermogravimetric decomposition analysis of complex **8**.

Figure 4.6 : DTA and TG versus time of the thermogravimetric decomposition analysis of complex **8**.

latice. Radii are given in pm where 100pm = 1Å.

The thermal decomposition of complex **8** is rather simple with only two separate decomposition steps. The decomposiotn can be visualised as illustrated Scheme 4.2 below.

$$\langle\!\langle \text{—Pd} \overset{I}{\underset{I}{\diagup\hspace{-0.3em}\diagdown}} \text{Pd—} \rangle\!\rangle \xrightarrow[\text{- I}]{\text{- 2 (CH}_2\text{CHCH}_3),} \quad \text{Pd} \overset{I}{\diagup\diagdown} \text{Pd} \xrightarrow{\text{- I}} 2\text{Pd}$$

Scheme 4.2 : Thermal decomposition of complex **8**.

Step one of the decomposition above occurs at ~150°C – 225°C and involves the loss of both allyl groups as well as an iodide leaving a thermally stable intermediate up to 350°C. The second decomposition stage occurs over the 350°C–465°C temperature range involving the loss of the remaining iodide.

4.3 Conclusion

I) *Allyl group fluctuation mechanism and the influence thereof on NMR spectral data.*

Fluxionality is characteristic of certain classes of organometallic compounds and is found only sporadically in others. As a result of this fluxionality, there are normally several different carbon and hydrogen atoms that in the absence of this fluxionality would otherwise be equivalent. This can lead to complex NMR spectra. Allyl complexes are characteristically fluxional with several types of mechanisms whereby they can 'flip'[36]. This fluxionality explains the broadness of the signals of the allyl group in the proton NMR spectra of the complexes prepared in this chapter and is possibly a strong contributing factor to the instability of the complexes of this chapter. The applicable mechanisms with respect to the allyl complexes in this series will be discussed in detail here.

The first of these fluctuation processes is the so-called η^3-η^1-η^3 mechanism as shown in scheme 4.19 below[37]. Atomic numbering in the scheme, and in the discussion that follows, is as per the numbering that is used in the crystal structure of bis-(η^3-allyl)-di-μ-iodo-dipalladium(II).
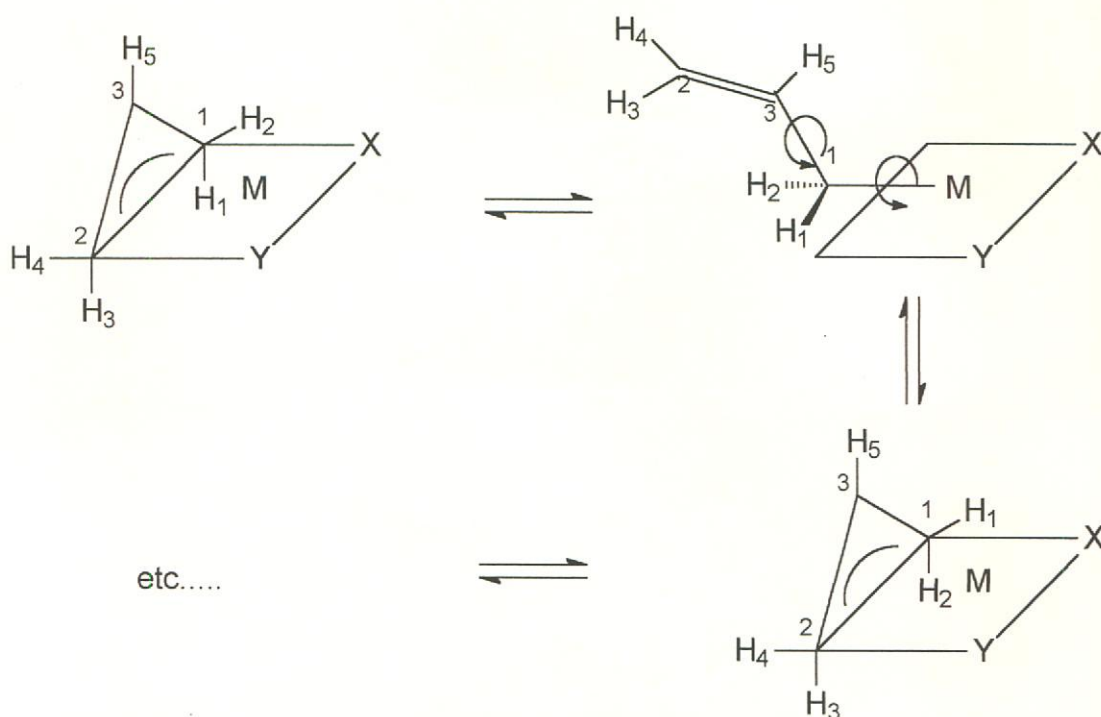
Scheme 4.19 : η^3-η^1-η^3 Fluctuation mechanism.

In this mechanism, fluctuation is enabled when the η^3-coordination is broken and a σ-bond is formed between the palladium and the C1 atoms. As a result, rotation is possible around the C1-C3 bond. The allyl group thus converts from a η^3- to η^1-bonded group and then back to η^3 again. This same mechanism is also possible for the other side of the allyl group allowing for rotation around the C2-C3 bond. While the ligand is in the η^3 form, obviously no rotation is possible around the delocalised π-bond. This rotation route allows the syn- and anti- protons to exchange positions with each other. In a symmetric complex, (X = Y), both the syn- and anti-protons will be equivalent thereby giving a single ^{1}H signal for all four protons in the NMR spectrum at the high temperature limit.

The exchange of carbons C1 and C2 in the allyl group is also possible as a result of this kind of fluctuation because of the nature of how the of η^1-bound intermediate is formed (scheme 4.19 above). It is not known whether this kind of fluctuation exists in unsymmetrical η^3–allyl compounds, (X $\neq$ Y).

If this kind of fluctuation was possible, as with the syn- and anti-protons, there would be a single carbon-13 signal for the C1 and C2 in the carbon-13 NMR spectrum at the high temperature limit. The resulting NMR spectra at the high temperature limit would consist of a single proton signal for all four sin- and anti-protons and a single carbon-13 signal for the C1 and C2 carbons of the allyl group.

If the exchange of carbons C1 and C2 was not possible with unsymmetrical allyl complexes, $(X \neq Y$, as is with this case), two signals would result in the proton spectrum each with the same coupling constant. Two signals would also result in the carbon-13 NMR spectrum, each for C1 and C2 respectively.

This is clearly not the case with the series of synthesised allylpalladium complexes in this chapter. Here, two separate sets of ^{1}H signals for the syn- and anti-protons are evident, each with a different coupling constant, e.g. for complex **8**, the syn-signal is at 4.54ppm with coupling constant of J_{H-H} = 6.6 Hz and the anti-signal is at 3.81ppm with a coupling constant J_{H-H} = 12.6Hz.

If the proton and carbon-13 NMR spectra for the series of synthesised complexes in this chapter are analysed in the light of the previous discussion, the following trends become evident: -

➢ A single carbon-13 signal is evident for C1 and C2 of the allyl group. This could be explained by the mechanism in scheme 4.19 above and the resulting exchange by these carbons.

➢ Two separate signals are evident in the proton spectrum for the syn- and anti-protons of the allyl group, each with a different coupling constant. Therefore, the syn- and anti-protons are not equivalent. Since the two coupling constants aren't equivalent, it affirms that C1 and C2 are not exchanging even though there is a single signal for both carbons in the carbon-13 spectrum.

There is thus an exchange between the syn- and anti-protons of the allyl group, but not between the C1 and C2 carbons of the same group. This exchange is evident by the broad doublets in the proton spectrum. Therefore, the fluxionality that is obviously present is not explained by the mechanism that is illustrated in scheme 4.19.

A second possibility for fluctuation of the η^3-allyl group is based on the possibility of rotation of the η^3-allyl group around the palladium-allyl axis[38]. This method is illustrated in scheme 4.20 below.
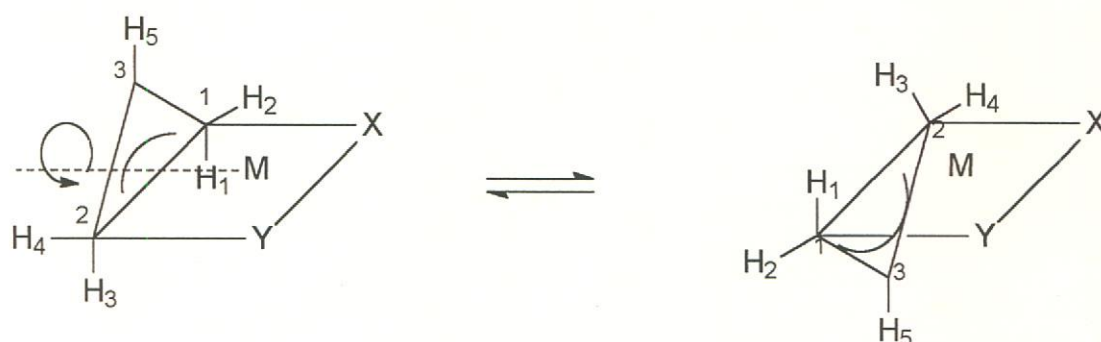
Scheme 4.20 : Palladium-allyl axis fluctuation mechanism.

In the process described above, the syn-protons (2 and 4) and the anti-protons (1 and 3) change positions amongst themselves, but not amongst each other. Syn-protons remain syn-protons and anti-protons remain anti-protons. The expected signal as a result of such a process would be two separate signals for the syn- and anti-protons, each with different coupling constants. This would be the case for both symmetrical (X = Y) and unsymmetrical (X ≠ Y) substituted η^3-allyl complexes at both the fast and slow exchange limits.

This mechanism described in scheme 4.20 above explains the NMR spectra for all the complexes in the series of this chapter. It clearly explains the reason for the two different signals for the syn- and anti-protons, each with different distinct coupling constant.

This mechanism also explains the broad multiplet that is seen for the lone proton (H_5) on C2 of the allyl group at room temperature. In benzene, at lower temperatures, the signal for this proton can be described as a doublet of triplets. This signal is due to the coupling of this proton with two sets of two different protons (2 syn- and 2 anti).

Although it has nothing directly to do with the fluxionality of the complex itself, it must be remembered that there was a definite solvent effect experienced by all the complexes in the series of this chapter. This can be seen when the spectra of the complexes when measured in d_6-benzene are compared to the spectra of those complexes when measured in d_2-dichloromethane. Generally a spectrum with much sharper peaks was obtained when measured in d_2-dichloromethane than in d_6-benzene.

4.4 Experimental.

4.4.1 Materials

Solvents:

High spectroscopic grade solvents were used during synthesis and were pre-dried over 4Å molecular sieves for at least 48 hours prior to use.

Diethyl ether, tetrahydrofuran (THF), benzene and hexane were distilled under nitrogen over sodium with benzophenone as indicator. Dichloromethane was distilled under nitrogen over calcium hydride. All alcohols were distilled under nitrogen from magnesium shavings. Alkyl lithium reagents were standardized by literature methods[39].

All deuterated solvents, dichloromethane (d^2-CD_2Cl_2) and benzene (d^6-C_6D_6), that were used in the spectroscopic investigations for the complexes and ligands in this series were purchased from Aldrich. All deuterated NMR solvents were stored over 4Å molecular sieves under argon in order to keep them free from moisture and oxygen.

4.4.2 Physical Methods.

A. General:

Unless otherwise noted, all reactions and manipulations were carried out under an inert atmosphere with a positive gas flow of argon or nitrogen using standard vacuum line and Schlenk techniques. Solutions were stirred magnetically with Teflon coated stirrer bars. Room temperature refers to about 22-24°C. Clean Glassware was taken from a drying oven at ±120°C, assembled while hot and cooled under vacuum.

B. Instrumentation.

➢ Melting points.

Melting points were determined on a standard Büchi 535 apparatus and are uncorrected.

➤ *Nuclear Magnetic Resonance Spectroscopy*

^{1}H, ^{13}C{^{1}H}, ^{31}P{^{1}H}, ^{125}Te{H} NMR data were recorded on a Varian VXR 300 FT spectrometer. NMR data are expressed as parts per million (ppm) downfield from internal (TMS) or external standard used. The respective nuclei were recorded under the following parameters: -

Nucleus	Frequency	Standard
^{1}H	300 MHz	$(CH_3)_4Si$ as internal standard
^{13}C {^{1}H}	75 MHz	$(CH_3)_4Si$ as internal standard
APT {^{1}H}	75 MHz	$(CH_3)_4Si$ as internal standard
^{31}P {^{1}H}	121 MHz	85% H_3PO_4 as external standard

Table 4.27 : *NMR parameters*

➤ *X-ray crystallography.*

Crystals that were suitable for use in diffraction intensity measurements at room temperature were mounted on a glass fiber using fast adhesive. Crystal structure data collection and correction procedures were carried out on a Phillips PW1100 diffractometer by Prof. G.J. Kruger of the department of Chemistry and Biochemistry, Rand Afrikaans University, Johannesburg, South Africa. All systematic absences were consistent with the space groups assigned in each case. The positions of the hydrogens were calculated by assuming idealized geometries.

C. General preparation of starting materials and ligands:

Several of the starting materials and the ligands were synthesized directly from literature and have been referenced accordingly. However, almost all of the literature methods used have been modified to varying degrees since they refer to similar, but somewhat different products. For this reason, detailed preparative methods are given for all the ligands and starting materials used in this chapter.
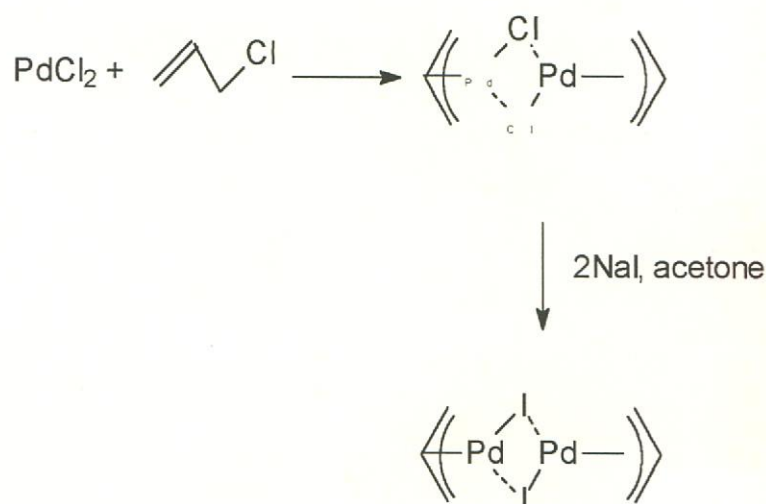
D. *General Preparation of Complexes.*

For the preparation of the n^3-hetero allyl palladium(II) complexes described in this chapter, standard Schlenk techniques were employed throughout and all

manipulations were carried out under an inert atmosphere. All general reagents, unless otherwise stated, were used as received.

4.5.2.1 Preparation of complex 8, bis-(η3-allyl)-di-μ-iodo-dipalladium(II) [(CH$_2$CHCH$_2$)$_2$Pd$_2$I$_2$].

The synthesis of bis-(η3-allyl)-di-μ-iodo-dipalladium(II) was based on a literature method used for the synthesis of the analogous methallylpalladium chloride complex.[40,41] The synthesis is outlined in Scheme 4.21 below and includes the changes that were made from the published method to adapt it to allow for the conversion to the allylpalladium iodide analogue of the chloride complex.

Scheme 4.21 : Preparation of complex **8**, bis-(η3-allyl)-di-μ-iodo-dipalladium(II).

2.256×10^{-2} mol of palladium chloride and 4.517×10^{-2} mol of sodium chloride was dissolved in 8 ml distilled water and stirred for 30 minutes. ~ 50ml of methanol was added to dissolve the suspension and delivered a deep red solution. The solution was stirred for a further 10 minutes.

5.6ml of allyl chloride was added dropwise, followed by the addition of a further 30ml of methanol. CO was allowed to bubble slowly though the

solution. This delivered a precipitate that dissolved when the CO flow was increased along with vigorous stirring.

120ml of distilled water was added and the solution was filtered though a celite packed sinter glass filter. The filtrate was extracted with 5 x 50ml portions of dichloromethane. The combined extracts were dried over anhydrous sodium sulfate and filtered. The dichloromethane was removed under reduced pressure. The product was further dried under high vacuum for 1 hour.

The yellow bis-(η^3-allyl)-di-μ-chloro-dipalladium(II) product was dissolved in 80ml acetone aided by slight heating. While the stirring was continued, 32ml of a saturated sodium iodide solution was added. The solution changes from a yellow to a deep red colour and vigorous stirring was continued for 30 minutes. The acetone was almost totally removed under reduced pressure causing the product to 'fall out' of solution.

The product was re-dissolved in 20ml of distilled water and 80ml of dichloromethane. The solution was extracted with 6 x 20ml portions of dichloromethane. The combined extracts were dried over sodium sulphate, filtered and the solvent removed under reduced pressure. The yellow-brown product was further dried under high vacuum for 1 – 2 hours to yield the desired product bis-(η^3-allyl)-di-μ-iodo-dipalladium(II).

Crystals suitable for X-ray structure determination were obtained by layering a concentrated anhydrous dichloromethane solution of bis-(η^3-allyl)-di-μ-chloro-dipalladium(II) with anhydrous benzene in a 1:1 ratio.

4.5 *Cited References*

[1] H.J. Gysling, *Coord. Chem. Rev.,* 42, **1982**, 133.

[2] E.G. Hope, W. Levason, *Coord. Chem. Rev.,* 122, **1993**, 109.

[3] W. Levason, M. Webster, C.J. Mitchell, *Acta Crystallogr. Sect C*, in press.

[4] H.M.K.K. Pathirana, A.W. Downs, W,R, McWhinnie, P. Granger, *Inorg. Chim. Acta*, 143, **1988**, 161.

[5] A. K. Singh, S. Thomas, *Polyhedron*, 10, **1991,** 2065.

[6] A. K. Singh, S. Thomas B.L. Khandelwal, *Polyhedron,* 10, **1991**, 2693.

[7] A. K. Singh, V. Srivastva, *J.Coord. Chem.*, 21, **1990**, 39.

[8] S. Al-salim and W.R. McWhinnie, *Inorg. Chim. Acta*, 135, **1989**, 213.

[9] A. K. Singh, V. Srivastava, *J. Coord. Chem.,* 21, **1990**, 269.

[10] A. K. Singh, V. Srivastava, *Phosphorus, Sulfur, Silicon. Related Elem.*, 47, **1990**, 471.

[11] A. K. Singh, V. Srivastava, B. L. Khandelwal, *Ployhedron*, 9, **1990**, 495.

[12] A. K. Singh, V. Srivastava, B. L. Khandelwal, *Polyhedron*, 9, **1990**, 39.

[13] 3D Search and Research using the Caimbridge Structural Database. F.H. Allen, O. Kennard, *Chemical Design Automation News*, **1993**, 8, 31 –37 IsoStar: A Library Of Information about Nonbonded Interaction, I.J. Bruno, J.C. Cole, J.P.M. Lommerse, R.S. Rowland, R. Taylor, M. Verdonk, *Jouranal of Computer-Aided Molecular Design*, **1997**, 11-6, 525-537.

[14] T. Kemmitt, W. Levason, M. Webster, R. D. Oldroyd, *Polyhedron,* 11, **1992**, 2165.

[15] T. Kemmitt, W. Levason, M. Webster, *Inorg. Chem.*, 28, **1989**, 692

[16] A. Khalid, B.L. Khandelwal, A.K. Singh, T.P. Singh, B. Padmanabhan, *J. Coord. Chem.*, 31, **1994**, 19.

[17] S. G. Murray, F. R. Hartley, *Chem. Rev.*, 81, **1981**, 265.

[18] A. A. Cheremisin, P. V. Schastnev, *J. Mag. Reson.*, 40, **1980**, 459.

[19] W. Levason, in F. R. Hartley (Ed.), *The Chemistry of Organophosphorus Compounds,* Vol. 1, Wiley, New York, **1990**, Chap. 15.

[20] S. G. Murray F. R. Hartley, *Chem. Rev.*, 81, **1981**, 365.

[21] W. Levason, in F. R. Hartley (Ed.), *The Chemistry of Organophosphorus Compounds,* Vol. 1, Wiley, New York, **1990**, Chap. 15.

[22] A. Evans, C. T. Mortimer, *Thermochim. Acta,* 131, **1988**, 103.

[23] C. T. Mortimer, *Rev. Inorg. Chem.*, 6, **1984**, 233.

[24] A. Belforte, F. Calderazzo, D. Vitali and P.F. Zanazzi, *Gazzetta*, 115, **1985**, 125.

[25] R.K. Chadha, J.E. Drake, *J. Organomet. Chem.*, 286, **1985**, 121.

[26] D.L. Tibbetts, T.L. Brown, *J. Am. Chem. Soc.*, 91, **1969**, 1108.

[27] W.T. Dent, R. Long, A.J. Wilkenson, *J. Chem. Soc.*, 15, **1964**.

[28] S.D. Robinson, B.L. Shaw, *J. Chem. Soc.*, **1963**, 4806

[29] H.C. Dehm, J.C.W. Chien, *J. Am. Chem. Soc.*, 82, **1960**, 4429.

[30] W. E. Oberhansli, L.F. Dahl, *J. Organomet. Chem.*, **1965**, 43.

[31] A.E Smith, *Acta Crystallogr.*, 18, **1965**, 331.

[32] W.E. Oberhansli, L.F. Dahl, *J. Organomet. Chem.*, 3, **1965**, 43.

[33] J.M. Rowe, *Proc. Chem. Soc. London,* **1962**, 66.

[34] V.F. Levdik, M.A. Porai-Koshits, *Zh. Strukt. Khim.*, 3, **1962**, 472.

[35] F.A. Cotton, G. Wilkonson, P.L. Gaus, *Basic Inorganic Chemistry 2nd Ed.*, John Wiley and Sons, **1987**, pg. 60.

F.A. Cotton, G. Wilkonson, *Advanced Inorganic Chemistry*, Wiley-Interscience New York, **1980.**

[36] J.E. Huheey, *Inorganic Chemistry*, 2nd ed., Harper International Edition, **1978**, pg 565 – 566.

[37] F.A. Cotton, G. Wilkenson, *Advanced Inorganic Chemistry*, 5th ed., John Wiley and Sons, New York, **1988**, pg. 1330 - 1333

[38] B. Henc, P.W. Jolly, R. Salz, G. Wike, R. Benn, E.G. Hofman, R. Mynott, G. Schroth, K. Seevogel, J.C. Sekutowski, C. Küger; *J. Organomet. Chem.*, 191, **1980**, 425.

[39] M.F. Lipton, C.M. Soreson, A.C. Sadler, R. H Shapiro, *J. Organomet. Chem., **1980**, 186, 155.*

[40] D.L. Tibbetts, T.L. Brown, *J. Am. Chem. Soc.*, 91, **1969**, 1108.

[41] W.T. Dent, R. Long, A.J. Wilkenson, *J. Chem. Society*, 15, **1964**.